Measuring and Modeling of Atmospheric Deposition on Santa Monica Bay and the Santa Monica Bay Watershed

Keith D. Stolzenbach, Rong Lu, Cheng Xiong, Sheldon Friedlander, Richard Turco
Institute of the Environment
University of California, Los Angeles

Ken Schiff, Liesl Tiefenthaler
Southern California Coastal Water Research Project

FINAL REPORT
to the
Santa Monica Bay Restoration Project

September 2001

Foreword

This project was conducted with the overall support of the Santa Monica Bay Restoration Project (SMBRP) and the Los Angeles County Department of Public Works (LACDPW). This report describes the work done primarily with the funds provided by the SMBRP to UCLA. The chemical data analyses performed using funds provided by the LACDPW to the Southern California Coastal Research Project (SCCWRP) are described in Appendix I of this report. Additional support was provided by the UC Center for Water Resources (Project W-895) and by EPA Grant No. R82-5831, "Integrated Urban Watershed Analysis: The Los Angeles Basin and Coastal Environment."

The authors acknowledge the assistance and patience of Dr. Guangyu Wang of the SMBRP. Additional assistance was provided by Dario Diehl and Dave Tsukada of SCCWRP, the Captain and crew of the *RV Sea World*, and Mel Zeldin and Solomon Teffera of the South Coast Air Quality Management District.

Table of Contents

EXECUTIVE SUMMARY

A review of previous studies indicates clearly that atmospheric deposition may be a significant source of contaminants and nutrients to Santa Monica Bay and other coastal regions and that there is a need for a comprehensive study of this process, particularly as a component of establishing Total Maximum Daily Loads (TMDLs).

This study was designed to answer three research questions:

- *What is the total annual load of toxic contaminants and nutrients to Santa Monica Bay via atmospheric deposition, either directly or indirectly on the Bay's watershed?*
- *What proportion of the annual load of toxic contaminants and nutrients from atmospheric deposition is contributed during specific meteorological events or conditions?*
- *How do atmospheric concentrations of toxic contaminants and nutrients and associated loads vary spatially within the Santa Monica Bay watershed and receiving water and among other regions of Los Angeles?*

The methodology of the study had the following components:

- *Wet deposition on land surfaces was measured directly.*
- *Dry deposition on land surfaces was estimated using measured air concentrations, segregated by aerosol size to the extent possible. The primary source of concentration measurements was regional air quality data collected by the Air Quality Management District (AQMD). Additional measurements at a site on the UCLA campus were used to supplement the AQMD data, providing in particular a measure of concentrations within the Santa Monica Bay watershed. These data were used to calibrate and verify the UCLA SMOG model for defined meteorological conditions. The model was then used to make estimates of dry deposition on land and water surfaces using established algorithms.*
- *The spatial pattern of deposition to the surface of Santa Monica Bay was measured indirectly by collection of water samples from the surface microlayer using a rotating drum system. Bulk water samples were collected at the same time.*
- *Although the measurements conducted by this study included some organic compounds, the primary emphasis was on deposition of trace metals. This emphasis was adopted because of limitations on resources available for data collection and analysis and does not reflect a presumption that trace metals are more important than organic contaminants or nutrients.*

The major findings and conclusions of this study are:

- *The annual rate of atmospheric transport and deposition of trace metals to Santa Monica Bay, defined as the sum of direct and indirect (on the watershed) deposition, is significant relative to other inputs of metals to the Bay.*
- *The annual total of atmospheric deposition of metals on Santa Monica Bay and its watershed is primarily the result of chronic daily dry deposition throughout the year, which far exceeds the estimated annual dry deposition of metals resulting from Santa Ana conditions and the annual wet deposition of metals.*

- *Most of the mass of metals deposited by dry deposition on Santa Monica Bay and its watershed originates as relatively large (bigger than 10 microns) aerosols from area sources (off-road vehicles and small businesses) in the Santa Monica Bay watershed.*

The major implications for environmental management are:

- *At least for metals, atmospheric deposition, primarily chronic daily dry deposition, must be considered as a significant non-point source in establishing TMDLs for Santa Monica Bay and waterbodies in the Bay's watershed.*
- *For some metals, the majority of the metal mass in the urban runoff during the wet season may be material originally associated with aerosols that are transported some distance from their original point of emission into the atmosphere before being deposited in the watershed.*
- *Reductions of non-point source inputs may require a coupling between air quality and water quality regulatory actions and policies. For metals, the most important sources of emission to the atmosphere are non-permitted area sources, which may be relatively difficult to regulate.*
- *For some sources, the deposition may be primarily composed of large aerosols and may occur very locally, perhaps within 100-500 meters of the source. This pattern of deposition will be difficult to monitor on a regional scale and will require a larger number of localized measurements.*

The major needs for additional work are:

- *The source emission database should be used to provide more resolved predictions of deposition associated with particular source categories.*
- *The range of contaminants measured and modeled should be expanded to include toxic organic compounds, such as PAHs and pesticides that are found in runoff, nutrients, such as nitrogen and phosphorous, and metals that exist in the vapor phase, such as mercury. This expansion will require consideration of gas phase transport and deposition as well as transport and deposition of aerosols.*
- *There is a crucial need for data on the concentration of contaminants associated with aerosols greater than 10 microns in size for the purpose of confirming the conclusions of this study with regard to the importance of coarse aerosols in determining the rate and spatial distribution of atmospheric deposition. Sampling of large aerosols will require non-standard sampling techniques.*
- *The hypothesized localized pattern of atmospheric concentration and deposition of large aerosols in the vicinity of contaminant sources should be documented using sampling techniques appropriate for large aerosols.*
- *The relationship between atmospheric deposition during the dry season and runoff during the wet season should be systematically investigated to support or refute the hypothesis developed by this study that for some metals atmospheric deposition is the major contributor to the metal loading in the runoff.*

1. INTRODUCTION

This section contains a discussion of the regional and institutional settings for the study, followed by a statement of the need for the study, the study objectives, and a brief review of related studies in other regions. Finally, the structure and content of the report is summarized.

1.1 BACKGROUND

1.1.1 Santa Monica Bay

Santa Monica Bay is nestled within the regional coastal waterbody known as the Southern California Bight (SCB) (Figure 1). Santa Monica Bay itself has a shoreline length of about 80 km, a surface area of about 1000 sq km, and an average depth of about 55 m. The continental shelf in side the bay is about 20 km wide and is incised by two submarine canyons. The water column is seasonally stratified with mean currents that may flow either to the northwest or southwest, depending upon conditions in the SCB. Tidal currents are weak to moderate, except where internal tides interact with the shelf break (M. Noble, personal communication). The residence time of the bay has not been quantified, but based upon the magnitude of the mean currents (10 cm/sec) is expected to be about a week. The bay (and the adjacent SCB) is home to a wide variety of aquatic species including kelp, fish, and marine birds and mammals. With its many miles of coastline, encompassing some 22 public beaches, Santa Monica Bay is one of Los Angeles' most coveted natural resources. It is estimated that nearly 45 million visitors come to enjoy the bay's mild climate and aesthetic beauty each year; with more than 500,000 visitors per day at the height of summer as residents of the inland empire migrate to take advantage of the dramatically cooler coastal temperatures (www.smbay.org).

Santa Monica Bay is adjacent to metropolitan Los Angeles, home to eight million people, and the shoreline and watersheds draining into the bay are developed almost to saturation. The bay receives discharges from two major sewage treatment plants and a variety of industries including oil refineries and electric power generating stations. At the southern end of the bay there is a federal Superfund site related to a large deposit of DDT and other contaminants in the sediments. Following seasonal rainstorms, large quantities of polluted runoff enter the bay through more than one hundred large or small natural and engineered drainage outlets. Some sources, such as treated wastewater, are well characterized (Raco-Rands 1997) and extensive effort has been spent assessing their impacts to the Bay (Dorsey et al. 1995; Stull 1995). Other sources, however, are virtually unmonitored and the magnitude of their contribution to the Bay's overall pollutant load is unknown. One example of this type of source is atmospheric deposition.

1.1.2 Atmospheric Deposition

Atmospheric deposition has long been recognized as a potentially significant non-point source of contaminants and nutrients to water bodies (Baker 1997). Dry deposition of aerosol-associated contaminants has been studied both theoretically and experimentally (see Pryor and Barthelmie (2000) for a recent review). Many experimental studies have used artificial collection surfaces to measure dry deposition directly and to characterize the deposited material (e.g. Yi et al. 1997a; Yi et al. 1997b; Franz et al. 1998; Paode et al. 1998; Paode et al. 1999; Tai et al. 1999; Shahin et al. 2000). Other studies have also measured the atmospheric concentration of aerosols and contaminants, making possible a computation of an effective deposition velocity (e.g. Holsen et al. 1993; Caffrey et al. 1998; Zufall et al. 1998; Tanner et al. 2001; Yi et al. 2001). Many of these studies concluded that dry deposition was primarily the result of deposition of relatively large aerosols, greater than 10 microns in size, that were present in the atmosphere. Thus, PM 10 data typical of ambient dichotomous measurements are not adequate for estimating dry deposition.

Because of the difficulties involved in collecting the aerosol concentrations and deploying the deposition surfaces, experimental studies have been limited in spatial extent, making the extrapolation of point measurements to regional scales difficult. Collection stations for deposition are generally inadequate to describe atmospheric inputs to urban areas and watersheds, especially over complex terrain (Lovett et al. 1997) and within the large gradients in the pattern of atmospheric deposition commonly found near large cities (e.g. Tai et al. 1999; Lovett et al. 2000). Accordingly, studies of regional deposition have used a combination of measured aerosol-associated concentrations in the atmosphere combined with theoretically derived deposition velocities to compute the rate of dry deposition (e.g. Padro 1996; Ruijgrok et al. 1997; Hillery et al. 1998; Brook et al. 1999; Smith et al. 2000). The effective deposition velocity is computed using theoretical formulations for dry deposition on land (e.g. McRae et al. 1982; Zhang et al. 2001) and water (e.g. Slinn and Slinn 1980; Williams 1982; Lo 1993; Lo et al. 1999) surfaces (see Zufall and Davidson (1997) for a recent review). These deposition relationships are often coupled with regional three-dimensional atmospheric circulation models (e.g. Lu et al. 1997b; Lu et al. 1997a) to determine the spatial distribution and regional loading of atmospheric deposition of contaminants.

The Los Angeles metropolitan area exhibits amongst the worst air quality in the nation. Aerosols in the ambient air of greater Los Angeles are known to contain concentrations of toxic constituents, as well as potentially eutrophying nutrients, for marine ecosystems (Young et al. 1976; Arey et al. 1989). Although the Los Angeles basin has been extensively studied with regard to priority air pollutants and, to a lesser extent, acid rain and fog (e.g. Russell et al. 1993), little information currently exists for assessing the relative risk to the Bay from atmospheric deposition of toxic contaminants and nutrients compared to other, better-characterized sources. There is virtually no monitoring of atmospheric deposition in the basin.

Because of the relatively small annual rainfall in Los Angeles, studies of atmospheric deoposition have focused primarily on dry deposition. The earliest observations of dry deposition in the Los Angeles area were reported by the Southern California Coastal Water Research Project (SCCWRP) (Young et al. 1976; Young and Jan 1977). Kaplan and Lu (1993) estimated the atmospheric deposition of organic and inorganic contaminants onto Santa Monica Bay using observed atmospheric concentrations and assuming that all contaminant mass within a certain distance of the coastline deposits on the Bay. They concluded that atmospheric deposition was significant relative to other discharges to the Bay for nickel, zinc, arsenic, selenium, cadmium, mercury, and lead. Eaganhouse and Venkatesan (1993) used measurements of carbon compounds by Gray et al. (Gray et al. 1986) and assumed deposition velocities to compute the deposition of carbon compounds throughout the region.

Much of the work on airborne contaminants (other than the priority pollutants) in Los Angeles has focused on trace metals. Trace metal measurements have been used to characterize urban aerosols (Milford and Davidson 1985; Davidson and Osborn 1986), identify source-receptor relationships with chemical mass balance methods (e.g. Cass and McRea 1986; Lyons et al. 1993). Davidson (1977) made measurement of dry deposition of trace metals, Pb, Zn and Cd, on flat Teflon plates and simultaneous measured airborne mass size distributions with a cascade impactor. He found that the sedimentation of large aerosols accounted for about 70% of the total mass deposition over flat surface at Caltech in Pasadena, California. On vegetation surfaces Davidson and Friedlander (1978) found that impaction controls the dry deposition of these trace metals and about 90% of the deposited lead, and even greater fraction for Zn and Cd, comes from the impaction of aerosols larger than 10μm. Huntzicker et al. (1975) estimated that of a total 17.9 metric tons/day of lead emitted by mobile sources, 9.5 tons deposited on the street near the source and 2.0 tons deposited regionally by dry deposition. The coastal waters received 0.43 tons/day in runoff from streets, 0.3 tons by regional dry deposition, and 0.09 tons by regional wet deposition. This total of 0.81 tons/day reaching the coastal waters exceeded the 0.64 tons/day estimated as the contribution from sewage discharges. In an update to this study Lankey et al. (1998) estimated that although the total quantity of lead emitted was greatly reduced (0.6 metric tons/day), the relative quantities of local (street) deposition, regional deposition, and removal by wind were approximately the same as in the earlier study.

1.2 OBJECTIVES AND APPROACH

1.2.1 Need for the Study

As indicated in the previous sections, Santa Monica Bay and other coastal regions adjacent to metropolitan Los Angeles contain valuable natural and human resources that may be affected by urban contaminants, some of which may reach the water by atmospheric transport and deposition. Although other pathways for contaminants, such as industrial, sewage, and stormwater discharges have been the focus of previous research and monitoring studies, atmospheric deposition of contaminants has not been systematically investigated in the Los Angeles region. This study was motivated by the clear need for such information.

Although there are several regulatory structures that govern the quality of coastal waters, the most immediate specific institutional need to understand the contribution of atmospheric transport and deposition to coastal waters resides in the EPA's Total Maximum Daily Load (TMDL) Program under section 303(d) of the Clean Water Act (CWA). There are still waters in the nation that do not meet the CWA national goal of "fishable, swimmable" despite the fact that nationally required levels of pollution control technology have been implemented by many pollution sources. CWA section 303(d) addresses these waters that are not "fishable, swimmable" by requiring states to identify the waters and to develop total maximum daily loads (TMDLs) for them, with oversight from the U.S. Environmental Protection Agency. A TMDL is a quantitative assessment of water quality problems, contributing sources, and load reductions or control actions needed to restore and protect bodies of water (http://www.epa.gov/region09/water/tmdl/index.html).

Santa Monica Bay is among the water bodies designated by EPA and the State of California as impaired, and a schedule for the establishment of TMDLs for a number of contaminants, including metals, hydrocarbons, and nutrients, has been promulgated (http://www.epa.gov/iwi/303d/18070104_303d.html). A specific requirement of the TMDL process is the identification of non-point sources of these contaminants that may contribute to the overall stress on and impairment of the water body and thus must be taken into account in establishing TMDLs. This study is designed to contribute to understanding the role of atmospheric transport and deposition in the TMDL program.

1.2.2 Objectives of the Study

Understanding the transport and deposition of toxic contaminants and nutrients to Santa Monica Bay is a large and very complex proposition and needs a phased approach. In the first (initial) phase, the following three research questions have been identified:

- *What is the total annual load of toxic contaminants and nutrients to Santa Monica Bay via atmospheric deposition, either directly or indirectly on the Bay's watershed?*

  Answering this question will make it possible to compare the inputs from atmospheric deposition to current inputs from other sources. This will provide resource managers charged with protecting the Bay the necessary information to evaluate the relative environmental risk from atmospheric deposition as a source of contaminants. If atmospheric deposition contributes a large portion of the total load for a specific pollutant, then greater efforts may need to be expended in order to control this source. If the contribution of that pollutant from atmospheric deposition is small, then less effort should be spent on atmospheric as a source of contamination and management efforts may be more efficiently directed elsewhere. Finally, if a management decision is made to reduce pollutants inputs from atmospheric deposition, the total annual load estimates generated during this study will provide the benchmark for assessing whether the management actions implemented were effective at reducing loads of pollutants to the Bay.

- *What proportion of the annual load of toxic contaminants and nutrients from atmospheric deposition is contributed during specific meteorological events or conditions?*

  Answering this question will determine if the annual load from atmospheric sources are primarily large, but episodic in nature, or if they are a low level, but chronic contributor of pollutants to the Bay. Studies in southern California and other areas around the nation indicate that episodic events such Santa Ana winds, fire storms, and rain storms can increase deposition rates significantly and may be extremely important components of the total annual load (Young and Jan 1977; Offenberg and Baker 1997). However, this assessment has not been accomplished within the Santa Monica Bay watershed. This understanding of when the greatest degree of inputs occurs is crucial to focusing future work including biological effect studies, source reduction strategies, or design of transport and deposition models.

- *How do atmospheric concentrations of toxic contaminants and nutrients and associated loads vary spatially within the Santa Monica Bay watershed and receiving water and among other regions of Los Angeles?*

  Answering this question will enable us compare the concentrations in Santa Monica Bay to the greater Los Angeles region, providing the larger spatial scale and adding context to the toxic contaminant loads being delivered by atmospheric deposition. This question also recognizes that there are two distinct mechanisms in which loads from atmospheric deposition may get transported into the Bay. The first is direct deposition, whereby atmospheric fallout is directly to Bay water surfaces. The second is indirect, whereby atmospheric fallout is onto land surfaces within the Bay's watershed only to be washed into the ocean during the next rain event. These distinctly different mechanisms will have a profound impact on how resource managers may approach control measures or implement management or regulatory actions for other sources, most notably urban runoff. This question will also entail investigations into the distribution patterns and net deposition of aerosols, contaminants, and nutrients to assess what proportion of source emissions deposit locally rather than regionally. It may be that the deposition observed in the Bay may be largely from contaminants generated outside of the watershed and are transported westward towards the Bay. However, there may also be significant contributors within the watershed that play a fundamental role in local deposition.

1.2.3 Research Approach

For this study the major technical issue is how to measure atmospheric deposition to land and water surfaces. As discussed in section 1.1.2, for both types of surfaces there are two general methods:

- *Direct measurement using deposition plates (for dry deposition) or rainwater collectors (for wet deposition).*

- *Indirect measurement in which a measured concentration in the air is multiplied by a theoretical "deposition velocity" which is a function of the local meteorology and the type of surface.*

Both of these techniques have been used in previous studies of atmospheric deposition to water bodies. There is general agreement that collection of rainwater is a feasible method of measuring wet deposition and relatively standard methods have been developed for this purpose. In contrast, the direct measurement of dry deposition is more difficult because of the lack of geometric and fluid dynamic similitude between artificial collector surfaces and actual land and water surfaces. Measurements of deposition at a limited number of locations are difficult to extrapolate to regional scales. Measurement of deposition over water surfaces presents special problems. Fixed platforms are rarely available for obtaining long-term measurements of either deposition or atmospheric concentration. The use of boats to make these measurements over shorter periods must be done in a way that avoids contamination by exhaust gases.

On the basis of these considerations the following combination of methodologies were selected:

- *Wet deposition on land surfaces will be measured directly.*

- *Dry deposition on land surfaces was estimated using measured air concentrations, segregated by aerosol size to the extent possible. The primary source of concentration measurements was regional air quality data collected by the Air Quality Management District (AQMD). Additional measurements at a site on the UCLA campus was be used to supplement the AQMD data, providing in particular a measure of concentrations within the Santa Monica Bay watershed. These data was be used to calibrate and verify the UCLA SMOG model for defined meteorological conditions. The model was then used to make estimates of dry deposition on land and water surfaces using established algorithms.*

- *The spatial pattern of deposition to the surface of Santa Monica Bay was measured indirectly by collection of water samples from the surface microlayer using SCCWRP's rotating drum system. Bulk water samples were collected at the same time.*

- *Although the motivation for this study encompassed nutrient deposition and the measurements conducted by this study included some organic compounds, the primary emphasis was on deposition of trace metals. This emphasis was adopted because of limitations on resources available for data collection and analysis and does not reflect a presumption that trace metals are more important than organic contaminants or nutrients.*

1.3 SUMMARY OF REPORT

The purpose of this report is to present a comprehensive picture of the methods, results, and conclusions of this study. Accordingly, Section 2 discusses in detail the methodologies and results of the data collection and modeling efforts. Section 3 then discusses the results in terms of the objectives outlined earlier in this section. Finally , Section 4 summarizes the major conclusions of the study, the implications for management options, and the needs for additional research.

2. METHODS AND RESULTS

This section first summarizes the methodologies used in obtaining data related to atmospheric concentrations, wet and dry deposition rates of toxic contaminants, bulk and surface microlayer water concentrations, and toxic source emission inventories. Following that, the details of the modeling of atmospheric deposition are discussed.

2.1 DATA

Four types of data were utilized in this study: atmospheric concentrations of aerosol-associated toxic contaminants, wet and dry deposition rates of toxic contaminants, bulk and surface microlayer concentrations of toxic contaminants, and toxic contaminant source emission inventories. Methodologies and results for these measurements are discussed separately in the sections below. It should be noted that many of the details of the measurement program for this study are contained in a data report "Atmospheric Transport and Deposition of Toxic Contaminants to Santa Monica Bay, CA" (SCCWRP 2000), which appears in Appendix I of this report. Additional climatological and geographical data used in the modeling are discussed in the next section on modeling. All data collected by this project may be obtained in MS Access database format or ASCII table format from the SCCWRP web site (www.sqqwrp.org).

2.1.1 Atmospheric Concentrations

Measurements of atmospheric concentrations of aerosol-associated toxic contaminants were obtained from three sources: the Technical Enhancement Program for the 2000 Air Quality Management Program (TEP 2000) conducted by the Air Quality Management District (AQMD); the Multiple Air Toxics Exposure Study (MATES II) conducted by the AQMD; and, measurements made specifically for this study at a site on the campus of the University of California, Los Angeles (UCLA).

TEP 2000

During the period August 1998 through July 1999 the AQMD made 24-hour average measurements of ion, carbon, trace metal, and total mass concentrations for PM2.5 and PM10 every six days at 8 sites in the AQMD region (see Figure 2).

MATES II

MATES II is an urban toxics monitoring and evaluation study (AQMD, 2000) in which a network of 10 fixed sites was monitored for toxic air contaminants once every six days for an entire year (from April 1998 through March 1999). Also, during the period three mobile platforms were used to sample at 14 additional sites for one or two months each (see Figure 3). Instead of PM 10, total suspended particles (TSP) were collected in MATES II.

UCLA

The UCLA measurement site was located on a rooftop on the main UCLA campus in Westwood (see Figures 2 and 3). This site has a long historical record of meteorological conditions (wind speed and direction, precipitation, barometric pressure, and humidity). The building is four stories above ground level (approx. 12 m) where airflow is not impeded by any nearby structure; the surrounding area is comprised of parking lots, trees and shrubs, and other buildings.

Two types of air samplers were used. The first was a dichotomous air sampler that collects two size fractions: particulate matter less than 10 microns (PM_{10}) and particulate matter less than 2.5 microns ($PM_{2.5}$) in size. In addition, a Multi-Orifice Uniform Diameter Impacter (MOUDI) sampler was used to collect aerosols in 12 different size fractions from >18 to < 0.06 microns (Marple et al. 1991). Dichotomous samples were collected every six days during winter (Jan-Feb, 1999), summer (Jul-Aug 1999) and fall (Sep-Oct 1999). MOUDI samples were collected once per month during these same index periods. Details of the aerosol sampling program at the UCLA site can be found in SCCRP (2000).

All aerosol samples were analyzed for total aerosol mass and for trace metals. Aerosol filter samples for trace metal analysis were prepared by strong acid digestion. Inductively coupled plasma-mass spectroscopy (ICP-MS) was used to determine concentrations of aluminum, antimony, arsenic, beryllium, cadmium, chromium, copper, iron, lead, mercury, nickel, selenium, silver, and zinc. Selected MOUDI samples were analyzed by Gas chromatography-Mass Spectroscopy (CGMS) to determine concentrations of chlorinated hydrocarbon constituents (isomers and metabolites of DDT, 41 PCB congeners) and polynuclear aromatic hydrocarbon constituents (28 PAH).

The relative values of metal mass in samples of aerosols at the UCLA site were consistent with typical levels in the LA urban airshed by the MATES II study (see Figure 4), although this comparison is qualitative because the UCLA measurements are of PM10 and the MATES II measurements are of total suspended particulates (TSP). Seasonal changes in observed metal concentrations were modest (see Figure 5). Typical size distributions in samples obtained by the MOUDI sampler are shown in Figure 6. The mass collected by the MOUDI sampler was not sufficient to detect organic compounds in the samples.

2.1.2 Dry Deposition

An aerodynamic surrogate surface developed by others (Zufall and Davidson 1997; Zufall et al. 1998) was deployed at our master site at UCLA. The surrogate surface was deployed simultaneously with the MOUDI sampler. The surface was designed to minimize turbulence and maintain laminar flow across its length to achieve consistent deposition results. The surrogate surface was covered with a Teflon filter and coated with oleic acid to minimize aerosol bounce. Dry deposition samples were analyzed for metals and organics (see section 2.1.1).

Dry deposition fluxes of metals to surrogate surfaces varied by constituent and time of year (Table 1). The greatest flux was for zinc and the least was nickel. The greatest flux for nearly all metals was observed during Fall (October). Concentrations of organic constituents were mostly non-detectable, except for a few PAHs.

2.1.3 Wet Deposition

Wet deposition was sampled directly using rainwater collectors developed by the National Atmospheric Deposition Program (NADP 1997). This technique utilizes a rain sensor that uncovers the sampler when precipitation is occurring, then covers the sampler when precipitation ceases to reduce evaporation and dry deposition contamination. All sampleable storms were targeted between January and May 1999. Wet deposition samples were analyzed for metals only (see section 2.1.1).

Concentrations of metals in wet deposition samples were weighted by the total rainfall collected in each sample to obtain an average value representative of the cumulative deposition during individual sampling periods (Table 2). As a check on the consistency of these values, a "scavenging ratio" was computed for each metal as the ratio of the average wet deposition concentration to the average concentration in the aerosol phase measured at the UCLA site (see Table 8). For all metals except zinc, the computed scavenging ratio is on the order of 10^5, which is consistent with values reported in the literature (Pekar 1996). The ratio for zinc was an order of magnitude higher as a result of one anomalously high sample value. The scavenging ratio for zinc with this value removed was consistent with the other metals (Table 2). Based on this analysis the wet deposition rate for zinc will be computed without the anomalous value.

The rain-weighted wet deposition concentrations were used to compute the total metal loadings to Santa Monica Bay and the Santa Monica Bay watershed (Table 2) corresponding to the total rainfall during the 1998/99 wet season (10.8 in). This loading will of course be different in drier and wetter years.

2.1.4 Microlayer and Bulk Water Concentrations

Nine sampling sites were located in Santa Monica Bay for seasurface microlayer measurements (see Figure 7). These sites were designed in a grid fashion for assessing gradients in deposition rates across Bay water surfaces.

A Teflon-coated rotating drum was used to collect samples of the seasurface microlayer (Cross et al. 1987). Microlayer depths of approximately 50 microns are sampled using this system; the rotating drum is towed at slow speeds (1/4 knot) alongside a vessel with a non-contaminating hull and uses a zero emission electric motor. For comparison purposes, bulk seawater samples were collected at depths of 1 m using a peristaltic pump. Microlayer samples were analyzed for metals and organic compounds, but the sample size precluded meaningful identification of organic constituents. Details of the surface microlayer sampling program can be found in SCCRP (2000).

Microlayer metal concentrations were analyzed in two ways. Enrichment factors were defined as the ratio of the microlayer to bulk concentration and were plotted as a function of location within the bay (see Figure 8). Concentrations were normalized to unit area defined using the measured length and width of the sea-surface sampled in order to accommodate variations in seasurface microlayer thickness and surface tensions (Table 3).

2.1.5 Emission Inventories

The emission inventories used in these studies are from the 1998 emission inventory compiled by the Southern California Air Quality Management District (SCAQMD). The inventory consists of on-road mobile sources, off-road mobile and area sources, and major point sources. On-road mobile sources include cars, trucks, buses and motorcycles. Emission inventory for the on-road mobile source is a product of the CARB EMFAC7G model with emissions factors for 1998. Area and off-road sources represent numerous distributed sources of emissions. For example, area sources include dry cleaners, gasoline stations, auto body shops, and chrome platers; and off-road sources include construction equipment, motor boats and airplanes. Stationary point sources consist of industrial facilities that discharge pollutants into the atmosphere.

The 1998 emission inventory provided emission rates of CO, NO_x, SO_x, VOC, and particulate matter (PM) for all source categories identified by the Source Classification Codes (SCC's) on a 5 km × 5 km spatial grid covering the South Coast Air Basin. The 1998 emission inventory for these compounds is summarized in Table 4. Temporal variations of emission rates are specified with detailed diurnal, weekday, and monthly profiles. Emission inventories for individual volatile organic compounds and particulate matter components are obtained by applying the latest CARB VOC and PM speciation profiles to the VOC and PM emissions for each source categories. The on-road mobile PM emissions are assigned as 40.6% for diesel exhaust, 9.1% for gasoline exhaust and 50.3% for tire and brake wear for 1998, based on studies for the Los Angeles county (Xinqiu Zhang, personal Comm.). With PM size fraction and species profiles, the PM inventory is segregated to four size fractions for each chemical composition, i.e., diameters < 1 μm, < 2.5 μm, < 10 μm and Total. Due to some inconsistencies between the PM size fraction profiles and chemical species profiles, small negative mass fractions may occur on the size ranges 1-2.5 μm, 2.5-10 μm and > 10 μm. A correction scheme has been developed to eliminate those negative mass fractions by adjust the chemical species fractions for the diameters < 1 μm, < 2.5 μm and < 10 μm. The total chemical species fractions are conserved. An example of PM emission rates for a weekday of August is shown in Table 5. A typical distribution of metal mass among the different sizes and sources is shown in Figure 9.

Emission rates for particulate metals were used in the modeling of metal deposition by allocating the sizes reported in the emission inventory to appropriate size bins in the model simulation. See section 2.2.3 below for more details of the use of the source inventory in the modeling portion of the study.

2.1.6 Summary of Data

The following table summarizes the data collection and applications presented in the foregoing sections:

Data ID	**Source**	**Data Profile**	**Application**
TEP 2000	AQMD	Air concentration, 24 h average/6 days, PM2.5 and PM10	Reviewed but not used because it contains unexplained high values.
MATES II	AQMD	Air concentration, 24 h average/6 days, TSP	Primary measurement data used to calibrate the model
UCLA-Dry Air	UCLA/ SCCWRP	Air concentration, 24 h average/6 days, 12 size fraction from >18 to <0.06 microns	Provide measurement in western LA airshed to supplement MATES data. Used to check agreement of the measurement with model prediction.
UCLA-Wet	UCLA/ SCCWRP	Rain-weighted deposition concentration	Provide deposition estimate during rain events.
UCLA-Dry Plate	UCLA/ SCCWRP	Mass deposited/area	Did not use because of possible experimental bias.
Microlayer	UCLA/ SCCWRP	Concentration/unit sea surface area	Used to show similarity in sea surface concentration and model-predicted deposition pattern
Emission Inventory	AQMD/ARB	Emission (MT)/day, 4 size fractions (<1um, <2.5um, 2.5um-10um, total)	Used to calculate dry deposition (mt/yr.) after being adjusted by MATES data-based model estimates

2.2 MODELING

This section discusses the application of the UCLA SMOG model to predict atmospheric deposition. As mentioned at the end of Section 1, the modeling was focused on trace metals, in spite of the fact that the data collected included some organic compounds. There were two major reasons for this. First, the organic compounds represented in the source database were mainly volatile and semi-volatile organics, and there was no information on most of the organic compounds of interest in the context of water quality standards such as DDT, PCB, and the high molecular weight PAHs. Second, although selected samples taken as a part of this study were analyzed for organic compounds, the analysis indicated non-detectable levels in almost all cases, in part because of insufficient mass of the compound was obtained (see section 2.1).

The results of the modeling, including comparison with data, are presented for five metals (chromium, copper, lead, nickel, and zinc), all considered highly conservative and highly aerosol associated, so that transformations between the aerosol and vapor phases did not have to be considered. Although there is much interest in the contribution of atmospheric mercury, this metal was not modeled because of the complexity of its potential to be present in the vapor phase.

2.2.1 The UCLA SMOG Modeling System

The Surface Meteorology and Ozone Generation (SMOG) air pollution model (Lu et al. 1997a) is used to calculate the concentration and deposition of air pollutants, including ozone, nitrates and trace metals, in the basin. The model includes detailed treatments of meteorology, tracer transport and dispersion, chemical and aerosol microphysical transformations, and solar and terrestrial radiation transfer. With these important atmospheric processes, the model has been a powerful tool to study many scientific problems and policy strategies related to urban and regional air pollution. The performance of the air pollution modeling system has been evaluated by comparing with the intensive measurement data collected during the Southern California Air Quality Study (SCAQS) (Lu et al. 1997b). The agreements between predictions and observations indicated that the air pollution modeling system is able to reproduce the main features of mesoscale meteorology, pollutant dispersion and transformations in the atmosphere.

The model domain for these simulations covers the entire southern California with a configurable inner domain used for air quality calculations and predictions (Figures 10 and 11). The grid spacing is 0.05° longitude × 0.045° latitude (about 5×5 km) uniformly for both grids. Variable grid spacing is used in the vertical direction with higher resolution in the boundary layer. Meteorological parameters, including three-dimensional winds, temperature, pressure and relative humidity, are predicted over the larger domain with 85×55×20 grid cells. Details of the model structure are described by Lu et al. (1997a). The inner domain covers the Los Angeles basin and vicinity for normal summer and winter conditions, and extends to a much larger area over the ocean surface during Santa Ana conditions when pollutants emitted in the basin are transported offshore. Subregions defined within the domain include Santa Monica Bay, the Santa Monica Bay watershed, and Los Angeles County.

2.2.2 Atmospheric Conditions Simulated

The local climate in southern California is primarily controlled by the large-scale pressure systems, including the semi-permanent high-pressure system over the North Pacific Ocean

(DeMarrais et al. 1965) and the local thermally-forced wind flows, such as sea-land breeze and mountain-valley flows, as well as terrain channeling effects (Lu and Turco 1994; Lu and Turco 1995). The strength and relative positions of the Pacific High to the west of southern California and a thermal Low to the east determine the pressure gradient over the area throughout most of the year. During the summer months, southern California is under the eastern edge of the Pacific High. Light synoptic winds, clear sky and intensive sunshine are the normal weather conditions associated with the high-pressure system. Elevated temperature inversion is present almost continuously, day and night, during the warm half of the year over the southern California. During the winter months the Pacific High moves to a southwest position, allowing storms to move down to Southern California. The most frequent synoptic regime in winter is an additional high-pressure cell at the surface centered to the northeast of the southern California over the Great Basin. The clear skies accompanies the Basin High during the long winter nights readily allow cooling of the surface layer of air by radiation and the formation of a ground-based inversion.

In this study the averaged conditions for the summer and winter are used to simulate the concentration and deposition of trace metals in the Los Angeles basin. The composite up-air soundings from three meteorological stations surrounding the Los Angeles basin, DRA, KBX and VBG, averaged over periods July 1 – August 31, 1998 and November 1, 1998 – January 31, 1999 are used to initialize the summer and winter cases respectively. These two cases represent the most frequently occurred conditions for the summer and winter. Other individual events, such as storms and Santa Ana conditions are significantly different from the averaged cases but occur in much lower frequency and are expected to make only small changes to the annual deposition loading. Similar to observed winds, the predominant daytime flow in the summer is the southwesterly from western coast to the eastern basin (Figure 12). The daytime sea breeze regime moves pollutants from the major emission sources in the western LA to the San Fernando valley, up the mountain ranges and to the eastern LA basin. Onshore flow over the coastal region improves the air quality over the coastal region and offshore. The winds during the night and in the early morning are light and unorganized in the basin. In the coastal region land breeze is not obvious at summer night in the simulation or the routine AQMD measurements.

The daytime sea-breeze regime in the winter has a flow pattern similar to the summer one, but in a much weaker intensity. The radiative cooling of the land surface during the long winter night produces down-slope flow and land breeze, leading to a general easterly and northeasterly surface flow in the basin (Figure 13). Offshore land breeze is developed near the coast and extended to the warmer ocean surface, which carries pollutants offshore over the coastal ocean.

During Santa Ana events, the predominant winds are offshore. Deposition of contaminants on the ocean surface is extended to a much larger area offshore and has larger impact on the ocean atmospheric input. Santa Ana conditions occur on about 40 days of the year, mostly during the period between September and May with the highest frequency in December and January (Ventura County 1998). We simulate the Santa Ana event on December 16, 1998 as an example of typical transport and deposition pattern during a Santa Ana event (Figure 14).

2.2.3 Representation of Particulate Sources

The size-distributions of particulates are modeled using discrete size bins. Twelve aerosol size bins are used to resolve aerosol sizes range from 0.01 um to 40 um diameters. One internally-mixed aerosol type with many volume fractions of aerosol components, including Cr, Cu, Ni, Pb, Zn, as well as nitrates, sulfates, sea salt components, organic and elemental carbon, water and others, is used to represent the simplified mixture of urban particulate. The fixed 12 model size bins are the dry aerosol sizes that consist of all the volatile and non-volatile components except water. The model predicts the number concentration and composition for each size bin in each model grid cell in three-dimensions. The aerosol water content changes with ambient relative humidity and the resulting wet aerosol sizes are used for coagulation, sedimentation and deposition calculations. Gas-phase photochemistry, as used by Lu et al, (1997a), is carried out in the simulation.

With PM size fraction and species profiles, the PM inventory is segregated to four size fractions for each chemical composition, i.e., diameters < 1 um, < 2.5 um, < 10 um and Total. The emission rates for size ranges with diameters < 1um, 1-2.5 um, 2.5-10 um and > 10 um are calculated and then interpolated into 12 model size bins used in the model simulation (Table 6). Emissions from the three larger size ranges are evenly distributed into their corresponding model size bins directly because they each cover two or less model size bins. Log-normal distributions are assumed for aerosols smaller than 1 um where the nuclei mode and accumulation mode reside. Automobiles and trucks in the Los Angeles basin are the largest and strongest source of nuclei mode aerosols. We assume that emissions from these sources have been dispersed to the area of the model grid cell (5 km X 4.5 km) and during the dispersion aerosols in the nuclei mode have been scavenged significantly. Therefore, the emissions for aerosols less than 1 um are placed in the accumulation mode in this study. This assumption is consistent with aerosol measurement at urban sites in the basin that the volume of nuclei mode is small (less than a few percent) compared with the volume of the accumulation mode (Whitby and Sverdrup 1980). Based on Whitby and Sverdrup (1980), the geometric volume mean size of 0.32 um and geometric standard deviation of 2.16 for urban average accumulation mode are used to distribute emissions in the sub-micron size range for chemical components except for trace metals studied here.

Many measurements of size distributions of trace metal containing aerosols can be found in literature, mostly measured using cascade impactors. (Milford and Davidson 1985) and (Davidson and Osborn 1986) have summarized the size distributions of trace metals measured before early 1980's. They found that trace elements with aerodynamic mass median diameter less than 2um, including Cr, Cu, Ni, Zn and Pb, generally have bimodal distribution: a dominant peak in the range 0.5-1 um and a smaller peak at about 3-5 um. Lyons et al. (1993) presented the size distributions of several trace metals measured at two locations in the Los Angeles area. Their size distributions for Cu, Pb and Zn exhibited three modes in the 0.075-0.26, 0.5-1 and 2-4 um size ranges. The mode in 0.075-0.26 may be the result of fresh emissions from vehicles near the sites. The mode in 0.5-1 um appeared to be either primary emission or the growth from smaller aerosols. The size distributions of Ni were bimodal with broad peaks below 0.5 um and peaks in the 2-4 um range. We place sub-micron emissions of Cu, Pb and Zn in a log-normal distribution with geometric volume mean size of 0.7 um and geometric standard deviation of 1.8 to represented the measured peak in the 0.5-1 um size range. The broader lognormal distribution used for the accumulation mode of other species is used for the sub-micron Ni emissions. Like

Zn, Cr arises from small contributions from a large number of industrial and fugitive sources. The sub-micron emission sizes for Cr is set the same as used for Zn. A cutoff at 1 um is used for these log-normal distributions to ensure that all sub-micron emissions are distributed in sub-micron portion of the model size bins.

2.2.4 Calculation of Dry Deposition

The dry deposition fluxes *F* of gases and aerosols are assumed to be proportional to the concentration *C* and deposition velocity v_d at a reference height (the middle of the model's lowest layer, about 20 m, is used in this study):

$$F = v_d C \tag{1}$$

A resistance dry deposition model is used to calculate deposition velocity, in which the transport of pollutants from the atmosphere to the surface is expressed in terms of an electrical resistance analog. The deposition velocity for gases at the reference height is defined as the inverse of the total resistance to pollutant deposition:

$$v_d = \frac{1}{r_t} = \frac{1}{r_a + r_b + r_s} \tag{2}$$

The total resistance is the sum of the resistance to deposition due to turbulent transport through the atmosphere to a thin layer near the surface (r_a); the resistance due to molecular scale diffusive transport through the thin viscous sub-layer near the surface (r_b); and the resistance due to the chemical interaction between the surface and the pollutant of interest once the gas molecules have reached the surface (r_s). The surface resistance r_s for gases is a function of surface type and pollutant of interest.

Dry deposition for aerosols includes the effects of Brownian diffusion, inertial impaction and aerosol gravitational sedimentation. Assuming that aerosols adhere to the surface upon contact without re-suspension, i.e., $r_s = 0$, dry deposition velocity for aerosols can be written as (Seinfeld 1997):

$$v_d = \frac{1}{r_a + r_b + r_a r_b v_g} + v_g \tag{3}$$

The turbulent resistance r_a is determined by atmospheric stability and calculated based on the similarity theory. The viscous sub-layer resistance r_b depends on molecular diffusivity for gases through the Schmit number (Wesely et al. 1977), $r_b = \frac{2}{\kappa u_*} Sc^{2/3}$, and for aerosols r_b depends on the effects of both Brownian diffusion and inertial impaction, $r_b = \frac{\kappa U}{u_*^2 (Sc^{-2/3} + 10^{-3/St})}$. The dimensionless Schmidt number is $Sc = \upsilon / D$ and the Stokes number is $St = v_g u_*^2 / g\upsilon$, where υ is the kinematic viscosity of air and D is the diffusivity of trace gas molecular or aerosol of interest. The aerosol gravitational settling velocity is calculated following the approach used by Toon et al. (1989).

Over water surface dry deposition velocity for aerosols is calculated based on the model of Williams (1982), which takes into account the effects of wave breaking and spray formation in high winds and aerosol growth in the humid sub-layer near the air/water interface. Based on the electrical resistance approach, the model includes two parallel deposition paths in addition to gravitational settling. Across the turbulent layer and viscous sub-layer, one path controls the deposition to the smooth water surfaces and the other path to the fraction of water surface that is broken with the formation of spray and bubbles. Another resistance, r_m, is used to represent the horizontal transfer between the smooth and broken areas. The gravitational settling in the viscous sub-layer is adjusted for aerosol growth due to the high relative humidity near water surface. Over fresh water, the relative humidity may approach to 100%, while it is limited to about 98.3% over ocean surface because of the dissolved salts (Williams 1982). In this study, wet aerosol diameters in the viscous sub-layer is estimated using the formula of (Fitzgerald 1975) with relative humidity of 98% over ocean surface. The fraction of surface area, α, that has broken surface is a function of wind speed:

$$\alpha = 1.7 \times 10^{-6} U_{10}^{3.75} \tag{4}$$

The turbulent resistances and the sub-layer resistance over smooth water surface are evaluated the same way as over land surfaces. The lateral resistances between the smooth and broken areas are set to the same value as the turbulent resistance over smooth water surface. Little is known about the sub-layer resistance for the broken surfaces. A tentative value of 0.1 s cm^{-1} is used in the current study. By setting the resistance value to that of smooth surface, the model is essentially reduced to the model of Slinn and Slinn (Slinn and Slinn 1980) without the effect of the slip of water surface.

A key parameter to determine the aerodynamic state of surface is the surface roughness height. A surface roughness data set from the Southern California Air Quality Management District is used for land surfaces. The surface of open oceans can be considered aerodynamically smooth at low wind speeds ($U_{10} < 3$ m/s, where U_{10} is the wind speed at a reference height above the surface of 10 m) and fully rough at high wind speeds ($U_{10} > 7$ m/s), with a transition region in between (Wu 1969; Garratt 1977). Following Garratt (1977) and Giorgi (1986), we estimate the value of aerodynamic roughness height on ocean surface using the formula of Charnock (1955):

$$z_0 = \alpha \frac{u_*^2}{g} \tag{5}$$

where $\alpha = 0.0144$ and $g = 9.81\,\mathrm{m\ s^{-2}}$. The formula has been found to give good agreement with observational data for $U_{10} < 25$ m/s. The friction velocity $u_* = {C_{DN}}^{1/2} U \approx 0.023 {U_{10}}^{1.23}$ for the ranges $4 < V < 21$ m s^{-1} (Garratt 1977).

$$z_0 = 0.0144 \frac{C_{DN} {U_{10}}^2}{9.81} = 0.0144 \frac{5.1 \times 10^{-4} {U_{10}}^{2.46}}{9.81} = 7.5 \times 10^{-7} {U_{10}}^{2.46} \tag{6}$$

Here U_{10} is in m/s and z_0 is in meter. The roughness height is assumed to be limited at the high wind speed by the value 0.024 m.

2.2.5 Model Calibration

By comparing with various data sets we found that the TEP 2000 data contains some trace metal measurements with exceptional large values. Hence the MATES II data are used in this study to calibrate and validate trace metal simulations. The TSP measurements in MATES II are more useful for the trace metal deposition study due to the fact that a major portion of PM mass in atmospheric dry deposition is contributed by aerosols larger than 10 μm diameter, as shown in direct deposition observations (e.g. Tai et al. 1999).

Large uncertainties in model simulations are usually associated with the emission inventories that are used as model inputs. Excessive or inadequate emissions in the inventories cause bias in model predictions in comparison with measurements. To reduce the uncertainties in emissions we use the MATES measurement data to calibrate the model simulation by adjusting the emission inventories. For trace metals that do not undergo significant physical and chemical transformations the predicted concentrations change approximately linearly with emission intensity. A calibration factor derived from predicted concentration is used to adjust the emission inventories uniformly over the model domain. First we calculate the normalized bias in the temporally and spatially paired comparison between the model prediction and measurements. The normalized bias (B_n) is defined as:

$$B_n = \frac{1}{N}\sum_{i=1}^{N}\frac{p_i - o_i}{o_i} \tag{7}$$

where N is the number of stations; p_i and o_i are the model predicted and observed concentrations at the ith station. In order to eliminate the normalized bias in the model calculation we introduce a calibration factor, α_n, for each trace metal component. The calibration factor is an adjustment factor required for the model-predicted concentrations to match with measurements:

$$\sum_{i=1}^{N}\frac{\alpha_n p_i - o_i}{o_i} = 0\,, \tag{8}$$

That is

$$\alpha_n = \frac{N}{\sum_{i=1}^{N}\frac{p_i}{o_i}}\,. \tag{9}$$

By scaling the emissions of trace metals in the inventory with corresponding calibration factors the overall bias with respect to the MATES measurements are minimized.

The adjustment factors and the gross and RMS errors of modeled concentration after adjustment are given in Table 5 for the summer case. Before adjustment the normalized gross errors for most of the metals, except Fe, Mn and Ni, come from the normalized biases. Uncertainties in the emission estimates and in the systematic biases of measurements could lead to these biases in comparison. Assuming that the MATES II measurement data is more reliable than emission estimates, we applied an adjustment factor to emission rates of each trace metal to eliminating the normalized bias. After the adjustment the normalized gross errors have been reduced considerably.

The model predicted 24-hour average concentrations in general agree reasonably well with the MATES II 24h measurement averaged over the corresponding period. For example, comparisons of observed and model predicted 24-hour average concentration and spatial distribution of Zn and Pb are shown in Figure 15. The model predicted the high concentration areas in both the east and west Los Angeles basin, as well as the gradient near the coast. However, the high Zn peaks at Wilmington and Fontana are under-predicted probably because the local sources has been smoothed out by model grid cells. The agreement is demonstrated further in the correlation between measurement and model predictions (Figure 16 for Pb and Zn). Despite of large variability in the measured trace metal concentrations, the model predicted concentrations correlate well with the average measured concentrations at measurement sites in the basin. The modeled trace metal PM 2.5 and PM 10 concentrations at UCLA have been compared with measured concentrations in Table 8. In the table the measured concentrations at UCLA are annual average of 24-hour measurements for PM 2.5 and PM 10, whereas the modeled concentrations are 24-hour mean concentrations averaged for the summer and winter cases. The modeled PM 10 and PM2.5 concentrations are in good agreement with UCLA measurements.

2.2.6 Trace Metal Concentration and Deposition

The fundamental output of the model is concentration and deposition as a function of time and spatial location throughout the modeled period. Model simulations are conducted for 2 to 3 consecutive days with the same averaged meteorological conditions. The spin-up processes are noticed in the first day of simulation. The differences of the surface concentration and deposition amount between the second and third day are quite small. Hence we use the results of the second day for analysis. All the simulation results show here are from second day run. For purposes of analysis this large data set has been reduced by appropriate selection of times and locations and by the generation of meaningful averages. In particular, a daily average concentration and deposition value was obtained by averaging the last day of the simulation, for which it was assumed that steady state had been reached.

Appendix II contains spatial plots of average concentration and deposition of all five metals analyzed during summer and winter and for the Santa Ana condition. Additional spatial plots showing particular phenomena such as diurnal differences, aerosol size, etc. are presented and discussed in Section 3.

2.2.7 Deposition Loadings

Daily average deposition loads (kg/day) for the five metals analyzed were computed for each season and for the Santa Ana condition (Table 9). An annual load (metric ton/year) was computed by averaging the summer and winter results. Daily and annual loads were also subdivided by the location of deposition (entire domain, total land, Santa Monica Bay watershed, total water, and Santa Monica Bay) and the location of the source (entire domain, LA County, and Santa Monica Bay Watershed). These results are discussed in detail in Section 3.

3. DISCUSSION

This section discusses the results of the measurement and modeling applications presented in Section 2, including model calibration, spatial and temporal distributions of concentration and deposition, deposition loadings, and comparisons with other sources.

3.1 MODEL CALIBRATION

This study is based on deposition rates predicted from modeled distributions of aerosol constituents. Accordingly, the model is calibrated to reproduce measured aerosol concentrations rather than observed deposition rates. The primary source of observed atmospheric concentrations was the MATES database, which, as discussed in the previous section, was used to adjust source rates for individual metals according to an objective statistical analysis. The results of this calibration, as presented in Table 7 and Figures 15 and 16, indicate that the model is reproducing the regional pattern of constituent concentrations.

Emission inventory and air quality measurements are sometimes compared for consistency. For example, Cass and McRea (1986) compared the relative abundance of trace metals in their fine aerosol emissions inventory to the relative abundance of elements in long-term average ambient monitoring data, and analyzed the agreement and mismatch between them. We compared the relative abundance of unadjusted and adjusted trace metal emissions with the averaged trace metal abundance of MATES II measurements for the winter and summer periods. The comparisons for the summer case are shown in Figure 17. The adjustment increases the agreement between the emission inventory and the measurements. This calibration process represents a crude adjustment of the model simulation to fit measurement data without any spatial and aerosol size discrimination. By applying the calibration factors to the emission inventory we made calibrated model predictions that represent the overall loading measured in MATES. The simulations are used for the analysis of trace metal concentrations and deposition discussed here.

As the primary motivation for this study is constituent transport to Santa Monica Bay, it is of considerable importance that the model accurately predict the concentrations over Santa Monica Bay and its watershed. The measurement site at UCLA was established because the MATES database (indeed all AQMD databases) has relatively few measurement sites in the western portion of the LA airshed where the gradients in concentration are quite high. The generally good agreement between the predicted and measured annual average concentration of metals at the UCLA site gives credibility to the estimates of deposition relevant to Santa Monica Bay (Table 8).

A more indirect set of indicators of the model's ability to replicate deposition patterns on the Bay and its watershed are the measurements of metal concentrations in the sea surface microlayer measurements in Santa Monica Bay. Concentrations of chromium, copper, lead, iron, and zinc were all uniformly higher near the shoreline. Concentrations of copper and iron increased as much as 10-fold while concentrations of lead and zinc increased as much as 5-fold moving from offshore towards near shore. Both the enrichment over bulk seawater (Figure 8) and the increase in concentration per unit area (Table 3) were consistent with spatial pattern of atmospheric deposition predicted by the UCLA SMOG model, particularly during periods of diurnal offshore winds (see section 3.2.2 below).

Attempts were made to compare the dry deposition on surrogate surfaces with the predicted dry deposition (see Table 1). Except for zinc, the flux rates measured using surrogate surfaces were much lower for all metals evaluated relative to modeled estimates at the UCLA site. The reasons for the differences in flux rates between the two methods are unknown, but could be the result of bias in the surrogate surface sampling method, including surface area, length of deployment, and/or concentration of large particulates. Surrogate surface sampling technology has great potential, but the bias in sampling and analysis needs to be assessed before this methodology can be used with complete confidence.

3.2 SPATIAL AND TEMPORAL DISTRIBUTION

The following sections discuss the geographic and temporal patterns of trace metal concentration and deposition predicted by the model. For brevity, zinc (Zn) and sometimes lead (Pb) are used to represent the typical patterns observed in all the trace metals analyzed.

3.2.1 Summer and Winter

The simulated 24-hour averaged Zn and Pb summer concentrations in the lowest model layer are shown in Figs. 15a, b. Large spatial variability is found in the region. High 24-hour concentrations occur in the basin that is bounded by mountain ranges and the Pacific Ocean. Large gradient can be seen near the coast as Zn and Pb are mostly emitted over land. Peak concentrations are centered at the areas of emission sources and near the San Gabriel and San Bernardino mountain ranges. The 24-hour Zn and Pb summer deposition patterns are similar to those for the near-surface air concentrations (Figs. 18a, b). These results are consistent with measurements made by Lovett (2000) that the concentrations and deposition fluxes of most ions and metals decline significantly with distance from the New York city within about 45 km of the city. As a result of the high degree of spatial variability in an urban area and its vicinity, a single sampling point is unlikely to be representative for the region. Measurements within the urban area may not accurately represent adjacent suburban areas because of the gradients near urban boundaries.

During the winter the surface trace metal concentrations are higher than those during the summer. The spatial patterns of surface concentration and dry deposition resemble to the summer patterns (Figs. 19a, b for Zn), except that the areas of winter high concentration and deposition fluxes are shifted slightly to the coast, which enhances the dry deposition over the coastal ocean surfaces.

3.2.2 Diurnal Variations

Significant diurnal variation of trace metal concentrations can be found in the simulations, which reflects the diurnal changes of the local winds and the depth and mixing in the atmospheric boundary layer, as well as the emission rates. Unlike ozone that is generated in the polluted boundary layer under sunshine, trace metal concentrations are increased due to primary emissions and decreased due to the vertical mixing in the daytime mixed layer and deposition processes. As an example Figures 20a, b show the Zn concentration and deposition rates in the summer afternoon. The typical wind flows during the summer months has been discussed by Lu and Turco (1995). The simulated summer afternoon winds are shown in Figure 12. From the mid-morning to late-afternoon onshore and inland winds move fine aerosols from the western coast to the north and east of the basin. High peaks of Zn total mass concentration are found near the southern slope of the San Gabriel and San Bernardino mountain ranges. Trace metals in fine particulate modes (< 2.5μm) can move away from the basin through mountain passes, such as the transport through Cajon and Newhall passes to the high desert region in the simulation, as well as be lofted to the free troposphere by mountains and convergence zones. These fine aerosols are subject to long-range transport. Coarse aerosols (>2.5 μm) have the atmospheric lifetime of minutes to days and contribute to the dry deposition of trace metals within the basin. The afternoon Zn deposition pattern shown in Figure 20b are the results of dry deposition of coarse aerosols a few to tens of kilometers downwind of various of emission sources. Large deposition rates are bounded within the basin, with high peaks just east of central Los Angeles and near Fontana. Under the normal onshore sea-breeze regime, the deposition of tracer metals from the basin to the coastal ocean surface is not significant.

At the summer night the boundary layer changes from neutral in the evening to stable due to the nighttime surface cooling. The surface winds are usually stagnant at night and in the early morning without significant land breeze developed near the coast. Trace metal components tend to drift around the emission sources, leading to dry deposition near the sources (Figure 21a, b). Although most of the nighttime emissions from transportation and industry are much smaller, the reduced mixing and dispersion in the stable boundary layer leads to much higher trace metal concentrations near the surface at night, especially for fine aerosols. However, the deposition rates are smaller at night and in the early morning than in the daytime because of the reduced deposition velocity in the stable boundary layer and the reduced emissions of coarse aerosols. Deposition of trace metals near the coast can be seen at night.

During the winter season, the afternoon onshore sea breeze is developed similar to, but weaker than, those found in the summer. However, in contrast to the stagnant conditions in the summer night, land breeze can be developed frequently during the winter nights near the coast (e.g., Figure 13). The offshore land breeze moves particulate matters offshore near the coast, leading to the enhanced dry deposition over the coast ocean surface. As shown in Figure 22a and b, an area of high Zn concentrations move close to the western coast and extended to the Santa Monica bay in the early morning, causing deposition in the Santa Monica bay. Similar deposition patterns have been found in the measurements of surface microlayer enrichment over bulk seawater conducted in the Santa Monica bay deposition project (Xiong 1999). Atmosperic dry deposition is the main factor for the enrichment of contaminant concentration in the surface microlayer with respect to the bulk water. The patterns of atmospheric deposition indicated in the measured surface microlayer enrichment in the Santa Monica bay for a similar period (e.g., Zn shown in Figure 8) are consistent with model simulations. The diurnal variations are also consistent with aerosol samples made by Xiong (1999) on the Santa Monica Pier. Xiong found that the dominant species, particularly iron and aluminum as well as fine aerosols, increased dramatically during the early morning sampling period (2 to 10 a.m.), during which the winds shifted from sea breeze to land breeze.

3.2.3 Santa Ana Event

Santa Ana winds in Southern California are generally referred to as the strong and widespread foehn winds that blow from the east or northeast offshore. Santa Ana winds develop when a cold surface high pressure builds over the Great Basin. Clockwise circulation around the center of this high-pressure area forces air downslope from the high plateau, resulting in strong warm and dry northeasterly winds over most of Southern California.

Santa Ana conditions make pronounced changes in the flow pattern in Southern California. We simulate the Santa Ana event on December 16, 1998 as an example of typical transport and deposition pattern during a Santa Ana event. The northeasterly Santa Ana winds increases during the morning and reach maximum intensity in the afternoon. Simultaneously, the onshore sea breeze is developed near the coast and penetrates inland. The simulated winds at 1600 PST are shown in Figure 14a. Very strong northeast winds predominate over most inland area. However, there is sea breeze shown in the coastal region of the Los Angeles basin. The sea breeze and Santa Ana winds meet and converge in the coastal plain. Another sharp zone of convergence extends from the Orange County to the eastern Los Angeles basin. The Santa Ana winds at night and in the early morning are not well organized and the strong northeast flow does not prevail all over the region (Figure 14b). Winds are light and variable inside the Los Angeles basin. However a general offshore flow extends from the coast to the ocean surface. The offshore winds move the pollutants emitted in the Los Angeles basin to the ocean surface.

Figure 23 shows the 24-hour averaged Zn surface concentration and deposition fluxes during the Santa Ana event. Compared to those under normal meteorological conditions, the peak concentrations have been moved to the coastal region and a tongue of high concentrations extended to southwest over the ocean surface under the Santa Ana conditions. Deposition of contaminants on the ocean surface covers a much larger area offshore and has larger impact on the ocean atmospheric input.

3.3 DEPOSITION LOADING IN THE LA BASIN

This section presents the model results in terms of total trace metal deposition loadings (mass/time), and discuses the major mode of deposition (dry vs. wet, seasonal vs. Santa Ana, small vs. large aerosols) and the location of the sources. Details of all model deposition results are found in Tables 9-14.

3.3.1 Seasonal Dry vs. Wet and Santa Ana Deposition

As discussed in the previous sections, atmospheric deposition can occur as seasonal dry deposition throughout the summer and winter, as dry deposition during a Santa Ana event, and as wet deposition. To compare the deposition rates by these different mechanisms and to compute a total annual deposition for Santa Monica Bay and its watershed it was assumed that the summer dry deposition occurs half the days of the year, the winter condition occurs for half the days minus forty days, and the Santa Ana condition occurs for forty days (all values taken from Table 9). Total dry deposition loadings to the Bay and its watershed computed in this way were added to the measured wet deposition loadings in Table 2. The results of this comparison are shown in Table 10 and Figure 24. It is clear that for all the metals studied the seasonal non-Santa Ana dry deposition is the largest component, ranging from 50% to 70% of the total. Dry deposition during Santa Ana conditions is characterized by daily deposition rates of the same order as the seasonal dry deposition, but the reduced frequency of this event limits its contribution to the total loading to about 10% at most. Wet deposition can contribute as much as about 45% (Ni) and as little as 25% (Pb and Cr).

3.3.2 The Effect of Aerosol Size

Dry deposition of aerosols is strongly size-dependant. Brownian diffusion governs the transport of small aerosols (< 0.05 μm diameter) across the quasi-laminar surface sub-layer.

Aerosols in the size range of 2 to 20 µm diameters can be effectively transported across the surface sub-layer by inertial impaction. The gravitational settling enhances and controls the dry-deposition of large aerosols. A characteristic minimum in deposition velocity resides in the accumulation size range of 0.1 to 1 µm diameters due to a lack of effective transport mechanisms across the laminar sub-layer. In this study we have assumed in the emission inventory that the nucleation mode has been scavenged significantly during the dispersion from emission source to the model grid. Two modes are typically simulated in the near surface trace metal concentrations. An example of 24-hour Zn size distribution in sources and averaged concentrations in the basin is shown in Figure 25. The accumulation mode, between 0.2 and 1 µm, coincides with the one commonly observed in Los Angeles (e.g. Lyons et al. 1993). Industrial petroleum gas heaters, stationary liquid fuel internal combustion engine, jet aircraft and timber and brush fires are among the major contributors to Zn emission in the sub-micron range. Various types of dust from paved road, tire wear, unpaved road, construction, as well as windblown dust are the major source of Zn in the coarse aerosol mode. These emission sources are also the main contributors of Pb in the fine and coarse size ranges, respectively.

The size distribution of 24-hour Zn deposition fluxes averaged in the basin is shown in Figure 25. About 80 % of the Zn deposition flux was due to aerosols larger than 10 µm. The deposition flux for aerosols less than 2.5 µm is small due to the small deposition velocity in the accumulation mode size range. The results are consistent with trace metal deposition measurement studies (e.g. Davidson 1977; Paode et al. 1998; Tai et al. 1999).

About 35 to 45 percent of the emissions in the model domain are deposited locally in the simulated area (see Table 11). The rest of the trace metal emissions are dispersed to regional and larger scales through long-range transport. Local deposition of these trace metals in the basin is almost exclusively composed of coarse aerosols. Aerosols less than 10 µm in diameter contribute only about 20 percent of the trace metal deposition in the basin. Fine aerosols can be exported out of the basin because of their relatively long atmospheric lifetime (days to weeks), especially after PBL ventilation and turbulent mixing have lofted them in elevated layers.

It should be noted that the above conclusions regarding the effects of aerosol size, particularly the conclusion that most of the deposition in the LA basin consists of coarse aerosols, is entirely dependent on the aerosol size information in the source database. Although the MOUDI aerosol samples taken at the UCLA site do confirm the presence of significant aerosols greater than 10 µm in size (see Figure 6), these samples are too limited in extent to confirm or deny the general predominance of coarse aerosols in the regional atmospheric deposition process. For this reason, one of the major priorities for future work relates to obtaining better information on the coarse aerosol fraction (see Section 4).

3.3.3 Geographic Distribution of Deposition and Sources

The source database used in the modeling of dry deposition specifies a total rate at which each metal is discharged into the atmosphere. It is of some interest to note the ultimate fate of this material in terms of whether it is advected out of the model domain by air movement, deposited on land, or deposited on water. Model predicted annual deposition rates of chemical species have been used to calculate the amount of atmospheric deposition on various sub regions of the model domain, including the Los Angeles, Orange, Riverside and San Bernardino counties, the Santa Monica Bay watershed, and Santa Monica Bay itself (Table 11). Because of the large amount of emissions in the Los Angeles County it receives about 40 percent of the total deposited trace metals in the simulation. The deposition in the Orange County is also significant with respect to its smaller area. Another 35 to 40 percent are deposited in the San Bernardino and Riverside counties in the eastern part of the basin due to both local emission and downwind transport. The peak deposition rates are usually found just south of San Gabriel and San Bernardino mountain ranges in the Los Angeles and San Bernardino counties. A significant fraction of the material, mostly fine aerosols, as discussed above, is carried out of the model domain.

Since the southeasterly is the predominant winds in the basin, dry deposition of most trace metals on the Pacific Ocean is only about 2 percent of the total deposited in the model domain. However, under typical meteorological conditions, the dry deposition of trace metals from the basin on ocean surface is concentrated near the coast and decreases rapidly offshore. The atmospheric input from dry deposition can still have significant impacts on the coastal ocean environment. Larger amount of dry deposition over much broader areas over the coastal Pacific Ocean can occur during offshore events, such Santa Ana conditions.

Table 12 summarizes the amount of particulate-born trace metals entering the SMB and SMB watersheds from atmospheric dry deposition from a few of source areas. Since the Santa Monica Bay is in the upwind direction of the Los Angeles basin trace metal deposition fluxes are much smaller than those in the heavily polluted Los Angeles municipal area. However these amounts of trace metal dry deposition are still significant in the Santa Monica watershed and Santa Monica Bay.

Among the total direct dry deposition in the SMB, about 70 to 80 percent come from the emissions in the SMB watersheds and about 95 percent come from the emission sources in the Los Angeles County. Therefore emission sources from adjacent land areas contribute majority of the trace metal deposition in the bay. As for the SMB watersheds, about 70 percent of the dry deposition come from emission sources within the watersheds and about 84 percent of the deposition come from all the emission sources in the Los Angeles County. Long-range transport from other regions outside of the LA air basin, which could potentially increase the atmospheric deposition in the SMB and SMB watershed, has not been considered in the simulations conducted here.

3.4 COMPARISON WITH OTHER SOURCES

It is clearly of interest to determine if the atmospheric deposition rates for metals predicted by this study are comparable to other inputs of metals to Santa Monica Bay. Annual metal loadings were obtained from a variety of relatively recent studies of point and non-point sources and are shown in Table 13. Also included in this table is the estimated total dry and wet deposition on Santa Monica Bay and on the Santa Monica Bay watershed (see section 3.3.1).

This comparison with other sources must take into account the possibility that non-point source stormwater runoff may contain material originating in the atmosphere. In this regard, the values in Table 13 support the notion that for the metals studied the estimated dry deposition on the watershed is the same order of magnitude as the metal loading in the runoff and thus that the runoff loading may be largely due to atmospheric deposition.

The annual dry and wet deposition may now be compared with other sources to Santa Monica Bay, assuming exclusion of runoff loading to avoid double counting of metal mass (see

Table 14). These results indicate that atmospheric sources are a significant contributor to metal loadings to the Bay, particularly for lead (99%), chromium (50%), and zinc (43%).

4. CONCLUSIONS AND RECOMMENDATIONS

This section contains a summary of the major conclusions of the study of atmospheric transport and deposition of contaminants to Santa Monica Bay and its watershed. Also presented are recommendations for continuing research on this problem.

4.1 CONCLUSIONS

On the basis of the methodologies, results, and discussion presented in the earlier sections of this report, the major conclusions of this study are:

- *The annual rate of atmospheric transport and deposition of trace metals to Santa Monica Bay, defined as the sum of direct and indirect (on the watershed) deposition, is significant relative to other inputs of metals to the Bay.*

  The contribution of atmospheric to total metal loading to the Bay for the five metals studied varies from 13% to 99% (see Table 14). These percentages are computed assuming that the indirect deposition on the watershed, which is larger than the direct deposition for all the metals studied, also reaches the Bay as runoff during the wet season. This hypothesis is supported by the fact that the predicted indirect deposition on the watershed is the same order of magnitude as the measured metal loading in the runoff. It should also be noted that the accuracy of the atmospheric percentages calculated are affected by uncertainties in the estimates of other sources of metals to the Bay.

- *The annual total of atmospheric deposition of metals on Santa Monica Bay and its watershed is primarily the result of chronic daily dry deposition throughout the year, which exceeds the estimated annual dry deposition of metals resulting from Santa Ana conditions and the annual wet deposition of metals.*

  Dry deposition of metals on Santa Monica Bay and its watershed occurs throughout the year, with the deposition during the summer season being only slightly higher than during the winter (see Table 9). Chronic dry deposition of metals on the water surface in Santa Monica Bay is significantly enhanced by the presence of a diurnal offshore wind and results in an onshore-offshore gradient of deposition over the scale of the Bay (see Figure 22) that is evident in the samples of trace metals taken in the sea surface microlayer of the Bay (see Figure 8). The daily quantities of metals deposited on Santa Monica Bay and its watershed during Santa Ana and rainfall events are comparable to the chronic daily deposition (see Table 9), but the frequency of Santa Ana events and the total rainfall in Los Angeles are not high enough to result in an annual total deposition that is comparable to the chronic annual deposition (see Table 10).

- *Most of the mass of metals deposited by dry deposition on Santa Monica Bay and its watershed originates as relatively large aerosols from widespread "area sources" in the Santa Monica Bay watershed.*

  The breakdown of metal emissions by size and source category in the 1988 SCAQMD emission inventory indicates that for all of the metals studied the largest mass is typically in the larger aerosol size fractions, particularly those greater than 10 microns, and originates from area sources (small businesses and off-road vehicles such as construction vehicles, boats, planes, etc.). The presence and predominance of larger aerosols in the source data base and in limited samples taken at the UCLA site suggest that aerosols greater than 10 microns in size (see Table 9) account for most of the deposition and most deposition occurs relatively close to the emission source (see Table 12). The confirmation of this conclusion should be a major priority in future work (see below).

4.2 IMPLICATIONS FOR MANAGEMENT OPTIONS

The conclusions summarized in the preceding section have several implications for the management of non-point sources in the Santa Monica Bay watershed, and in other coastal watersheds exposed to urban air pollution:

- *At least for metals, atmospheric deposition, primarily chronic daily dry deposition, must be considered as a significant non-point source in establishing TMDLs for Santa Monica Bay.*

- *For some metals the majority of the metal mass in the urban runoff during the wet season may be material originally associated with aerosols that are transported some distance from their original point of emission into the atmosphere before being deposited in the watershed.*

- *Reductions of non-point source inputs may require a coupling between air quality and water quality regulatory actions and policies. For metals, the most important sources of emission to the atmosphere appear to be non-permitted area sources, which may be relatively difficult to regulate.*

- *For some sources, the deposition may be primarily composed of large aerosols and may occur very locally, perhaps within 100-500 meters of the source. This pattern of deposition will be difficult to monitor on a regional scale and will require a larger number of localized measurements.*

4.3 NEEDS FOR ADDITIONAL STUDIES

Although this study has largely achieved the objectives outlined in Section 1, there is a clear need for additional work on atmospheric transport and deposition in the Los Angeles region:

- *The source emission database should be used to provide more resolved predictions of deposition associated with particular source categories.*

- *The range of contaminants measured and modeled should be expanded to include toxic organic compounds, such as PAHs and pesticides that are found in runoff, nutrients, such as nitrogen and phosphorous, and metals that exist in the vapor phase, such as mercury. This expansion will require consideration of gas phase transport and deposition as well as transport and deposition of aerosols.*

- *There is a crucial need for data on the concentration of contaminants associated with aerosols greater than 10 microns in size for the purpose of confirming the conclusions of this study with regard to the importance of coarse aerosols in determining the rate and spatial* *distribution of atmospheric deposition. Sampling of large aerosols will require non-standard sampling techniques.*

- *The hypothesized localized pattern of atmospheric concentration and deposition of large aerosols in the vicinity of contaminant sources should be documented using sampling techniques appropriate for large aerosols.*

- *The relationship between atmospheric deposition during the dry season and runoff during the wet season should be systematically investigated to support or refute the hypothesis developed by this study that for some metals atmospheric deposition is the major contributor to the metal loading in the runoff.*

5. REFERENCES CITED

Arey, J. R., R. Atkinson, B. Zielinska and P. McElroy (1989). "Diurnal concentrations of volatile polycyclic aromatic hydrocarbons and nitroarenes during a photochemical air pollution episode in Glendora, CA." Environmental Science and Technology **23**: 321-327.

Baker, J. E., Ed. (1997). Atmospheric Deposition of Contaminants to the Great Lakes and Coastal Waters. Pensacola, FL, SETAC Press.

Brook, J. R., L. M. Zhang, F. Di-Giovanni and J. Padro (1999). "Description and evaluation of a model of dry deposition velocities for routine estimates of air pollutant dry deposition over North America. Part I: model development." Atmospheric Environment **33**: 5037-5051.

Caffrey, P. F., J. M. Ondov, M. J. Zufall and C. I. Davidson (1998). "Determination of size-dependent dry particle deposition velocities with multiple intrinsic elemental tracers." Environmental Science & Technology **32**(11): 1615-1622.

Cass, G. R. and G. J. McRea (1986). Emissions and air quality relationships for atmospheric trace metals. Toxic Metals in the Atmosphere. J. O. Nriagu and C. I. Davidson. New York, John Wiley & Sons**:** 145-171.

Charnock, H. (1955). "Wind stress on a water surface." Q. J. Meteorol. Soc. **81**: 639-640.

Cross, J., J. Hardy, G. Hose, L. Hershelman, R. Antrium, R. Gossett and E. Crecilius (1987). "Contaminant concentrations and toxicity of sea-surface microlayer near Los Angeles, California." Marine Environmental Research **23**: 307-323.

Davidson, C. I. (1977). "Deposition of Trace Metal-Containing Particles in Los-Angeles Area." Powder Technology **18**(1): 117-126.

Davidson, C. I. and S. K. Friedlander (1978). "Filtration Model for Aerosol Dry Deposition - Application to Trace-Metal Deposition from Atmosphere." Journal of Geophysical Research-Oceans and Atmospheres **83**(C5): 2343-2352.

Davidson, C. I. and J. F. Osborn (1986). The sizes of airborne trace metal containing particles. Toxic Metals in the Atmosphere. J. O. Nriagu and C. I. Davidson. New York, Wiley**:** 355-390.

DeMarrais, G. A., G. C. Holzworth and C. R. Hosler (1965). Meteorological summaries pertinent to atmospheric transport and dispersion over southern California, Weather Bureau, U.S. Department of Commerce**:** 86 p.

Dorsey, J., C. Phillips, A. Dalkey and G. Deets (1995). "Changes in assemblages of infaunal organisms around wastewater outfalls in Santa Monica Bay, CA." Bulletin Southern California Academy of Sciences **94**: 46-64.

Eganhouse, R. P. and M. I. Venkatesan (1993). Chemical Oceanography and Geochemistry. Ecology of the Southern California Bight. M. D. Dailey, D. J. Reish and J. W. Anderson. Berkeley, University of California Press.

Fitzgerald, J. W. (1975). "Approximation formulas for the equilibrium size of an aerosol particle as a function of its dry size and composition and the ambient relative humidity." Journal of Applied Meteorology **14**(6): 1044-9.

Franz, T. P., S. J. Eisenreich and T. M. Holsen (1998). “Dry deposition of particulate polychlorinated biphenyls and polycyclic aromatic hydrocarbons to Lake Michigan.” Environmental Science and Technology **32**(23): 3681-3688.

Garratt, J. R. (1977). “Drag Coefficients over Oceans and Continents.” Monthly Weather Review **105**(7): 915-929.

Giorgi, F. (1986). “A particle dry-deposition parameterization scheme for use in tracer transport models.” Journal of Geophysical Research **91**(D9): 9794-806.

Gray, H. A., G. R. Cass, J. J. Huntzicker, E. K. Heyerdahl and J. A. Rau (1986). “Characteristics of atmospheric organic and elemental carbon particle concentrations in Los Angeles.” Environmental Science and Technology **20**(6): 580-588.

Hillery, B. R., M. F. Simcik, I. Basu, R. M. Hoff, W. M. Strachan, D. Burniston, C. H. Chan, K. A. Brice, C. W. Sweet and R. A. Hites (1998). “Atmospheric deposition of toxic pollutants to the Great Lakes as measured by the Integrated Atmospheric Deposition Network.” Environmental Science and Technology **32**(15): 2216-2221.

Holsen, T. M., K. E. Noll, G. C. Fang, W. J. Lee, J. M. Lin and G. J. Keeler (1993). “Dry Deposition and Particle-Size Distributions Measured During the Lake-Michigan Urban Air Toxics Study.” Environmental Science & Technology **27**(7): 1327-1333.

Huntzicker, J. J., S. K. Friedlander and C. I. Davidson (1975). “Material balance for automobile-emitted lead in Los Angeles basin.” Environmental Science and Technology **9**: 448-457.

Kaplan, I. and S. T. Lu (1993). Contribution of Atmospheric Contaminants to the Southern California Bight Water Column, Report to the Southern California Coastal Water Research Project.

Lankey, R. L., C. I. Davidson and F. C. McMichael (1998). “Mass balance for lead in the California south coast air basin.” Environmental Research **78**: 86-93.

Lo, A. K. F. (1993). “The direct calculation of fluxes and profiles in the maring surface layer using measurements from a single atmospheric level.” Journal of Applied Meteorology **32**: 1893-1900.

Lo, A. K. F., L. M. Zhang and H. Sievering (1999). “The effect of humidity and state of water surfaces on deposition of aerosol particles onto a water surface.” Atmospheric Environment **33**(28): 4727-4737.

Lovett, G. M., J. J. Bowser and E. S. Edgerton (1997). “Atmospheric deposition to watersheds in complex terrain.” Hydrological Processes **11**(7): 645-654.

Lovett, G. M., M. M. Traynor, R. V. Pouyat, M. M. Carreiro, W. X. Zhu and J. W. Baxter (2000). “Atmospheric deposition to oak forests along an urban-rural gradient.” Environmental Science & Technology **34**(20): 4294-4300.

Lu, R. and R. P. Turco (1994). “Air Pollutant Transport in a Coastal Environment .1. 2-Dimensional Simulations of Sea-Breeze and Mountain Effects.” Journal of the Atmospheric Sciences **51**(15): 2285-2308.

Lu, R. and R. P. Turco (1995). "Air Pollutant Transport in a Coastal Environment .2. 3-Dimensional Simulations over Los-Angeles Basin." Atmospheric Environment **29**(13): 1499-1518.

Lu, R., R. P. Turco and M. Z. Jacobson (1997a). "An integrated air pollution modeling system for urban and regional scales .1. Structure and performance." Journal of Geophysical Research-Atmospheres **102**(D5): 6063-6079.

Lu, R., R. P. Turco and M. Z. Jacobson (1997b). "An integrated air pollution modeling system for urban and regional scales .2. Simulations for SCAQS 1987." Journal of Geophysical Research-Atmospheres **102**(D5): 6081-6098.

Lyons, J. M., C. Venkataraman, H. H. Main and S. K. Friedlander (1993). "Size Distributions of Trace-Metals in the Los-Angeles Atmosphere." Atmospheric Environment Part B-Urban Atmosphere **27**(2): 237-249.

Marple, V. A., K. L. Rubow and S. M. Behm (1991). "A microorifice uniform deposit impactor (MOUDI): description, calibration, and use." Aerosol Science and Technology **14**: 434-446.

McRae, G. J., W. R. Goodin and J. H. Seinfeld (1982). "Development of a second-generation mathematical model for urban air pollution - I. Model formulation." Atmospheric Environment **16**(4): 679-696.

Milford, J. B. and C. I. Davidson (1985). "The Sizes of Particulate Trace-Elements in the Atmosphere - a Review." Journal of the Air Pollution Control Association **35**(12): 1249-1260.

NADP (1997). National Atmospheric Deposition Program/National Trends Network wet deposition in the United States 1996. Champaign, IL, Illinois State Water Survey.

Offenberg, J. H. and J. E. Baker (1997). "Polychlorinated biphenyls in Chicago precipitation: Enhanced wet deposition to near-shore Lake Michigan." Environmental Science and Technology **31**: 1534-1538.

Padro, J. (1996). "Summary of ozone dry deposition velocity measurements and model estimates over vineyard, cotton, grass and deciduous forest in summer." Atmospheric Environment **30**(13): 2363-2369.

Paode, R. D., U. M. Shahin, J. Sivadechathep, T. M. Holsen and W. J. Franek (1999). "Source apportionment of dry deposited and airborne coarse particles collected in the Chicago area." Aerosol Science and Technology **31**(6): 473-486.

Paode, R. D., S. C. Sofuoglu, J. Sivadechathep, K. E. Noll, T. M. Holsen and G. J. Keeler (1998). "Dry deposition fluxes and mass size distributions of Pb, Cu, and Zn measured in Southern Lake Michigan during AEOLOS." Environmental Science & Technology **32**(11): 1629-1635.

Pekar, M. (1996). Regional Models LPMOD and ASIMD. Algorithms, Parameterization and Results of Application to Pb and Cd in Europe Scale for 1990. Moscow, EMEP Meteorological Synthesizing Center - East.

Pryor, S. C. and R. J. Barthelmie (2000). "Particle dry deposition to water surfaces: processes and consequences." Marine Pollution Bulletin **41**: 220-331.

Raco-Rands, V. (1997). Characteristics of effluents from large municipal wastewater facilities in 1995. Southern California Coastal Water Research Project Annual Report 1995. S. B. Weisberg. Westminster, CA, Southern California Coastal Water Research Project**:** 3-16.

Ruijgrok, W., H. Tieben and P. Eisinga (1997). "The dry deposition of particles to a forest canopy: a comparison of model and experimental results." Atmospheric Environment **31**(3): 399-415.

Russell, A. G., D. A. Winner, R. A. Harley, K. F. McCue and G. R. Cass (1993). "Mathematical modeling and control of dry deposition flux of nitrogen-containing air pollutants." Environmental Science and Technology **27**: 2772-2782.

SCCWRP (2000). Atmospheric Transport and Deposition of Toxic Contaminants to Santa Monica Bay, CA - Data Report. Westminster, CA, Southern California Coastal Water Research Project.

Seinfeld, J. H., S. N. Pandis (1997). Atmospheric chemistry and physics: From air pollution to climate change. New York, Wiley.

Shahin, U. M., S. M. Yi, R. D. Paode and T. M. Holsen (2000). "Long-term elemental dry deposition fluxes measured around lake Michigan with an automated dry deposition sampler." Environmental Science and Technology **34**(10): 1887-1892.

Slinn, S. A. and W. G. N. Slinn (1980). "Predictions for particle deposition on natural waters." Atmospheric Environment **14**(9): 1013-16.

Smith, R. I., D. Fowler, M. A. Sutton, C. Flechard and M. Coyle (2000). "Regional estimation of pollutant gas dry deposition in the UK: model description, sensitivity analysis, and outputs." Atmospheric Environment **34**: 3757-3777.

Stull, J. (1995). "Two decades of maring biological monitoring, Palos Verdes, CA." Bulletin Southern California Academy of Sciences **94**: 21-45.

Tai, H. S., J. J. Lin and K. E. Noll (1999). "Characterization of atmospheric dry deposited particles at urban and non-urban locations." Journal of Aerosol Science **30**(8): 1057-1068.

Tanner, P. A., P. T. Law and W. F. Tam (2001). "Comparison of aerosol and dry deposition sampled at two sites in Southern China." Journal of Aerosol Science **32**: 461-472.

Toon, O. B., R. P. Turco, J. Jordan, J. Goodman and G. Ferry (1989). "Physical processes in polar stratospheric ice clouds." Journal of Geophysical Research **94**(D9): 11359-80.

Ventura County (1998). PM10 Monitoring Network Plan, Ventura County Air Pollution Control District.

Wesely, M. L., B. B. Hicks, W. P. Dannevik, S. Frisella and R. B. Husar (1977). "An eddy-correlation measurement of particulate deposition from the atmosphere." Atmospheric Environment **11**(6): 561-3.

Whitby, K. T. and G. M. Sverdrup (1980). California aerosols: their physical and chemical characteristics. The character and origins of Smog aerosols: a digest of results from the California aerosol characterization experiments (ACHEX). G. M. Hidy, P. K. Mueller, D. Grosjean, B. R. Appel and J. J. Wesolowski. New York, Wiley**:** 477-517.

Williams, R. M. (1982). “A model for the dry deposition of particles to natural water surfaces.” Atmospheric Environment **16**(8): 1933-8.

Wu, J. (1969). “Wind stress ans surface roughness at air-sea interface.” J. Geophys. Res. **74**: 444-455.

Xiong, C. (1999). Chemical and Morphological Studies of Marine and Urban Aerosols. Department of Chemical Engineering. Los Angeles, University of California.

Yi, S. M., T. M. Holsen and K. E. Noll (1997a). “Comparison of dry deposition predicted from models and measured with a water surface sampler.” Environmental Science & Technology **31**(1): 272-278.

Yi, S. M., T. M. Holsen, X. Zhu and K. E. Noll (1997b). “Sulfate dry deposition measured with a water surface sampler: A comparison to modeled results.” Journal of Geophysical Research-Atmospheres **102**(D16): 19695-19705.

Yi, S. M., U. M. Shahin, J. Sivadechathep, S. C. Sofuoglu and T. M. Holsen (2001). “Overall elemental dry deposition velocities measured around Lake Michigan.” Atmospheric Environment **35**: 1133-1140.

Young, D. and T. K. Jan (1977). “Fire fallout of metals off California.” Marine Pollution Bulletin **8**: 109-112.

Young, D., D. J. McDermott and T. Heesen (1976). “Aerial Fallout of DDT in Southern California.” Bulletin of Environmental Contamination and Toxicology **16**: 604-611.

Zhang, L. M., S. Gong, J. Padro and L. Barrie (2001). “A size-segregated particle dry deposition scheme for an atmospheric aerosol module.” Atmospheric Environment **35**: 549-560.

Zufall, M. J. and C. I. Davidson (1997). Dry deposition of particles to water surfaces. Atmospheric Deposition of Contaminants to the Great Lakes and Coastal Waters. J. E. Baker. Pensacola, FL, SETAC Press.

Zufall, M. J., C. I. Davidson, P. F. Caffrey and J. M. Ondov (1998). “Airborne concentrations and dry deposition fluxes of particulate species to surrogate surfaces deployed in southern Lake Michigan.” Environmental Science and Technology **32**(11): 1623-1628.

Table 1: Dry deposition flux measured at the UCLA site using a surrogate surface. The last column contains the annual average predicted deposition flux at the UCLA site. All values are in units of ug/m^2-day.

Metal	Feb-Mar 1999	Jul-Aug 1999	Oct 1999	Nov-Dec 1999	Entire Year	Model prediction
Cr	0.11	0.00	0.83	0.00	0.24	1.8
Cu	0.44	0.03	0.66	0.03	0.29	11.6
Pb	0.26	0.01	0.35	0.02	0.16	10.5
Ni	0.01	0.03	0.00	0.02	0.02	1.2
Zn	0.77	56.33	134.05	23.13	53.57	41.7

Table 2: Measurements of trace metals in wet deposition at the UCLA site during the 1998/99 storm season

Metal	Rain weighted mean concentration in wet sample (ug/L)	Annual average concentration on aerosols (ng/m3)	Scavenging ratio	Total load to Santa Monica Bay and watershed (mt/year)
Cr	0.28	5.8	4.8E+04	0.16
Cu	2.16	16.1	1.3E+05	1.2
Pb	1.47	12.3	1.2E+05	0.84
Ni	0.55	2.1	2.6E+05	0.31
Zn	53.5	20.2	2.6E+06	31
Zn*	8.70	20.2	4.3E+05	5.0

* excluding anomalous high value of zinc concentration

Table 3: Average concentration (ug/m^2) of trace metals in the seasurface microlayer as a function of alongshore and cross shore position

Parameter	Cross Shore (km from beach)	Along Shore (km North from King Harbor) 0	10	20
Cadmium	1	0.01	0.01	0.01
	3	0.03	0.01	0.01
	5	0.01	0.01	0.02
Chromium	1	0.07	0.02	0.03
	3	0.04	0.02	0.02
	5	0.02	0.01	0.03
Copper	1	0.13	0.10	0.07
	3	0.11	0.01	0.02
	5	0.05	0.01	0.01
Iron	1	7.31	0.87	4.44
	3	2.82	0.71	1.30
	5	0.96	0.49	0.50
Lead	1	0.08	0.02	0.02
	3	0.06	0.01	0.02
	5	0.01	0.01	0.01
Nickel	1	0.05	0.02	0.02
	3	0.04	0.01	0.02
	5	0.01	0.01	0.03
Zinc	1	0.99	1.10	0.62
	3	0.65	0.87	0.93
	5	0.33	0.28	0.35

Table 4: Emission inventory for 1998 (mt/day)

	On-Road Mobile	Off-Road and Area	Point	TOTAL
CO	3426.65	1440.17	141.60	5008.42
NOx	588.16	365.40	134.11	1087.66
SOx	14.21	43.27	22.84	80.32
VOC	448.09	1020.18	218.37	1686.63
PM	26.34	1392.04	22.61	1441.00
TOTAL	4503.45	4261.06	539.52	9304.03

Table 5: PM Emission rates (kg/day) for an August weekday.

Elements	PM Size	On-Road Mobile	Area and Off-road Mobile	Point	All Sources
Al	Total	3.34	73685.38	8.35	73697.05
	<10um	1.81	47281.54	2.59	47285.95
	<2.5um	0.03	8852.69	1.67	8854.39
	<1um	0.03	2483.62	1.06	2484.7
As	Total	0.04	20.51	11.54	32.09
	<10um	0.04	14.64	10.42	25.11
	<2.5um	0.04	6.96	10.26	17.26
	<1um	0.04	5.2	10.13	15.37
Cd	Total	0.72	23.38	3.18	27.28
	<10um	0.55	18.74	3.04	22.33
	<2.5um	0.55	5.4	2.51	8.45
	<1um	0.13	4.27	2.43	6.82
Cr	Total	1.31	244.09	30.53	275.92
	<10um	1.3	139.2	28.96	169.45
	<2.5um	1.2	75.49	27.85	104.54
	<1um	1.19	14.53	27.22	42.94
Cu	Total	1.52	134.19	4.95	140.67
	<10um	1.45	84.97	3.83	90.25
	<2.5um	1.31	19.5	2.76	23.57
	<1um	1.29	8.28	2.54	12.11
Fe	Total	12.08	50341.32	145.31	50498.71
	<10um	6.6	29772.04	116.14	29894.78
	<2.5um	2.49	5700.79	97.76	5801.04
	<1um	2.38	2302.31	90.29	2394.98
Mn	Total	1.44	965.96	5.88	973.28
	<10um	1.44	573.15	5.6	580.19
	<2.5um	1.36	112.98	4.82	119.16
	<1um	1.27	46.49	4.6	52.37
Ni	Total	1.37	71.43	35.27	108.07
	<10um	1.36	43.3	27.47	72.13
	<2.5um	1.25	10.45	25.15	36.85
	<1um	1.24	4.96	23.77	29.98
Pb	Total	0.32	774.54	11.6	786.46
	<10um	0.32	490.57	10.7	501.59
	<2.5um	0.11	112.29	10.01	122.41
	<1um	0.11	47.9	9.81	57.82
Zn	Total	270.43	789.91	35.05	1095.38
	<10um	111.45	516.45	28.41	656.31
	<2.5um	88.71	170.2	26.66	285.57
	<1um	56.82	102.2	25.65	184.67

Table 6: Model aerosol size bins.

Bin #	Mean Diameter (μm)	Low Edge (μm)	High Edge (μm)
1	0.017	0.010	0.020
2	0.033	0.020	0.040
3	0.066	0.040	0.080
4	0.131	0.080	0.158
5	0.261	0.158	0.316
6	0.520	0.316	0.630
7	1.038	0.630	1.257
8	2.069	1.257	2.506
9	4.126	2.506	4.997
10	8.228	4.997	9.964
11	16.41	9.964	19.871
12	32.72	19.871	39.625

Table 7: Prediction error and adjustment factors (Summer case)

		Before Adjustment				After Adjustment	
	$\bar{o}$	$\bar{p}$	E_n (%)	B_n (%)	α	$\bar{p}$	E_n (%)
Al	1.302	2.503	113.3	112.5	0.4705	1.178	30.95
Cr	0.008	0.017	136.1	136.1	0.4235	0.007	34.04
Cu	0.037	0.007	77.4	-77.4	4.4150	0.030	38.56
Fe	1.753	1.627	25.7	-0.1	1.0014	1.629	25.74
Pb	0.031	0.037	49.0	39.8	0.7153	0.026	29.20
Mn	0.032	0.032	40.3	17.9	0.8481	0.027	29.09
Ni	0.010	0.010	46.9	8.9	0.9184	0.010	46.21
Zn	0.088	0.056	35.3	-32.5	1.4823	0.083	21.90

$\bar{o}$:	Observed concentration averaged over all MATES II sites (mg m^{-3}).
$\bar{p}$:	Model predicted concentration averaged over all MATES II sites (mg m^{-3}).
E_n:	Normalized gross error (%).
B_n:	Normalized bias (%).
α:	Adjustment factor derived by eliminating normalized bias.

Table 8: Comparisons of modeled and measured concentrations at UCLA

	PM 10 (ng m^{-3})		PM 2.5 (ng m^{-3})	
	Measured	Modeled	Measured	Modeled
Cr	5.8 ± 8.9	2.4	2.7 ± 4.4	2.0
Cu	16.1 ± 12.6	16.1	5.4 ± 9.6	4.2
Ni	2.1 ± 1.3	2.3	1.4 ± 1.0	1.3
Pb	12.3 ± 31.9	13.8	8.3 ± 26	3.2
Zn	20.2 ± 10.2	43.6	11.3 ± 7.2	17.6

Table 9: Summary of deposition calculation results

		Total Domain		Total Land		Total Water		SM Bay		SMB Watershed		Bay & Watershed	
		(45902 km^2)		(34684 km^2)		(11218 km^2)		(751 km^2)		(1335 km^2)		Combined	
Summer Emissions (July, 1 - Aug. 31, 98) [kg/day]													
	Emissions (tons/yr)	TSP	PM10	TSP	PM10	TSP	PM10	TSP	PM10	TSP	PM10	TSP	PM10
Zn	1400.03	605.83	122.19	597.66	121.00	8.21	1.19	2.61	0.40	35.34	5.65	37.95	6.05
Ni	84.49	29.88	6.47	27.96	6.33	1.93	0.14	0.21	0.04	1.31	0.28	1.52	0.32
Pb	455.29	195.83	57.22	194.04	56.79	1.79	0.43	0.79	0.16	11.19	2.66	11.97	2.83
Cu	508.61	210.77	61.19	208.79	60.71	1.99	0.49	0.86	0.18	11.57	2.74	12.42	2.92
Cr	95.46	33.64	4.39	33.32	4.35	0.31	0.04	0.16	0.02	1.75	0.16	1.91	0.18
Winter Deposition (Nov, 1, 98 - Jan. 31, 99) [kg/day]													
	Emissions (tons/yr)	TSP	PM10	TSP	PM10	TSP	PM10	TSP	PM10	TSP	PM10	TSP	PM10
Zn	928.39	415.10	65.51	397.80	59.87	17.28	5.64	4.85	1.52	26.42	3.29	31.27	4.81
Ni	45.26	16.42	2.88	14.65	2.56	1.77	0.33	0.27	0.08	0.83	0.14	1.10	0.22
Pb	187.68	81.82	19.21	78.25	17.66	3.57	1.55	1.14	0.43	5.21	0.97	6.35	1.40
Cu	262.32	113.12	26.28	108.13	24.13	5.02	2.18	1.61	0.59	7.15	1.31	8.76	1.90
Cr	50.43	19.19	1.95	18.48	1.78	0.71	0.16	0.25	0.05	1.19	0.08	1.44	0.13
Annual Deposition (Summer+Winter)/2 * 365/1000 [tons/Year]													
	Emissions (tons/yr)	TSP	PM10	TSP	PM10	TSP	PM10	TSP	PM10	TSP	PM10	TSP	PM10
Zn	424.94	186.32	34.25	181.67	33.01	4.65	1.24	1.36	0.35	11.27	1.63	12.63	1.98
Ni	23.68	8.45	1.71	7.78	1.62	0.68	0.08	0.09	0.02	0.39	0.08	0.48	0.10
Pb	117.34	50.67	13.95	49.69	13.59	0.98	0.36	0.35	0.11	2.99	0.66	3.34	0.77
Cu	140.69	59.11	15.96	57.84	15.48	1.28	0.49	0.45	0.14	3.42	0.74	3.87	0.88
Cr	26.62	9.64	1.16	9.45	1.12	0.19	0.04	0.07	0.01	0.54	0.04	0.61	0.06
Santa Ana Deposition: Calibrated with winter factors [kg/day]													
	Emissions (tons/yr)	TSP	PM10	TSP	PM10	TSP	PM10	TSP	PM10	TSP	PM10	TSP	PM10
Zn	928.39	361.19	75.53	263.39	40.25	97.82	35.29	7.58	1.55	25.51	4.10	33.09	5.65
Ni	45.26	15.53	3.74	10.24	1.91	5.30	1.85	0.35	0.09	0.81	0.17	1.16	0.26
Pb	187.68	74.49	21.68	53.37	12.32	21.12	9.35	1.49	0.41	5.10	1.24	6.59	1.65
Cu	262.32	104.59	30.20	74.65	17.04	29.95	13.17	2.07	0.57	6.84	1.63	8.91	2.20
Cr	50.43	17.24	2.79	12.72	1.46	4.52	1.33	0.36	0.06	1.14	0.11	1.50	0.17

Table 10: Comparison of estimated annual loading of metals to Santa Monica Bay and the Santa Monica Bay watershed by dry deposition during non-Santa Ana (SA) conditions, dry deposition during Santa Ana conditions, and wet deposition (mt/year)

Metal	Dry non-SA	Dry SA	Wet	Total
Cr	0.55	0.06	0.16	0.77
Cu	3.51	0.36	1.24	5.11
Pb	3.09	0.26	0.84	4.19
Ni	0.43	0.05	0.31	0.80
Zn*	11.38	1.32	5.0	17.69

* excluding anomalous high value of zinc concentration in wet deposition samples

Table 11: The amount of emission and dry deposition of some trace metals in the Los Angeles basin (mt/year)

	Total Emissions	Model Domain	Ocean Surface	Los Angeles County	Orange County	Riverside County	San Bernardino County
Cr	26.62	9.96	0.19	3.94	1.18	1.78	2.14
Cu	140.69	60.29	1.28	24.03	7.81	9.27	13.17
Pb	117.34	51.76	0.98	21.96	6.85	7.19	10.85
Ni	23.68	8.61	0.68	3.40	1.06	1.14	1.62
Zn	424.94	189.17	4.65	79.51	26.21	27.99	39.08

Table 12: Dry deposition of trace metals in the Santa Monica Bay (SMB) and the SMB watershed (SMBW) from sources in the basin, in Los Angeles County, and in the SMB watershed. (mt/year). Note that the values are inclusive, i.e. the Basin Source values includes the LA County values , which include the SMBW values.

	Deposition to the Santa Monica Bay			Deposition to the SMB watersheds		
	Basin Source	LA Source	SMBW Source	Basin Source	LA Source	SMBW Source
Cr	0.067	0.064	0.051	0.527	0.442	0.370
Cu	0.399	0.377	0.275	3.300	2.732	2.227
Pb	0.314	0.298	0.222	2.901	2.419	1.999
Ni	0.078	0.076	0.064	0.382	0.320	0.268
Zn	1.215	1.160	0.872	10.945	9.492	7.890

Table 13: Comparison of combined dry and wet deposition of metals with other trace metal inputs to Santa Monica Bay (mt/year)

	Deposition on SM Bay	Deposition on watershed	Runoff[1]	Hyperion[2]	Chevron[2]	Power Plants[2]
Chromium	0.14	0.64	0.040	0.6	0.021	0.14
Copper	0.92	4.20	1.0	16.0	0.032	0.010
Lead	0.67	3.53	1.1	0.0	0.015	0.0
Nickel	0.20	0.59	0.0	5.1	0.13	0.006
Zinc	3.27	14.43	10.2	21.0	0.16	2.40

Notes: [1] Los Angeles County Department of Public Works Wet Season Report 1994-95 (1996)
[2] Southern California Coastal Water Research Project Annual Report 1994-95 (1996)

Table 14: Comparison of atmospheric and non-atmospheric trace metal inputs to Santa Monica Bay (mt/year)

	Atmospheric Input	Non-Atmospheric Input	Percent Atmospheric
Chromium	0.77	0.76	50%
Copper	5.1	16.0	24%
Lead	4.2	0.02	99%
Nickel	0.79	5.24	13%
Zinc	17.7	23.6	43%

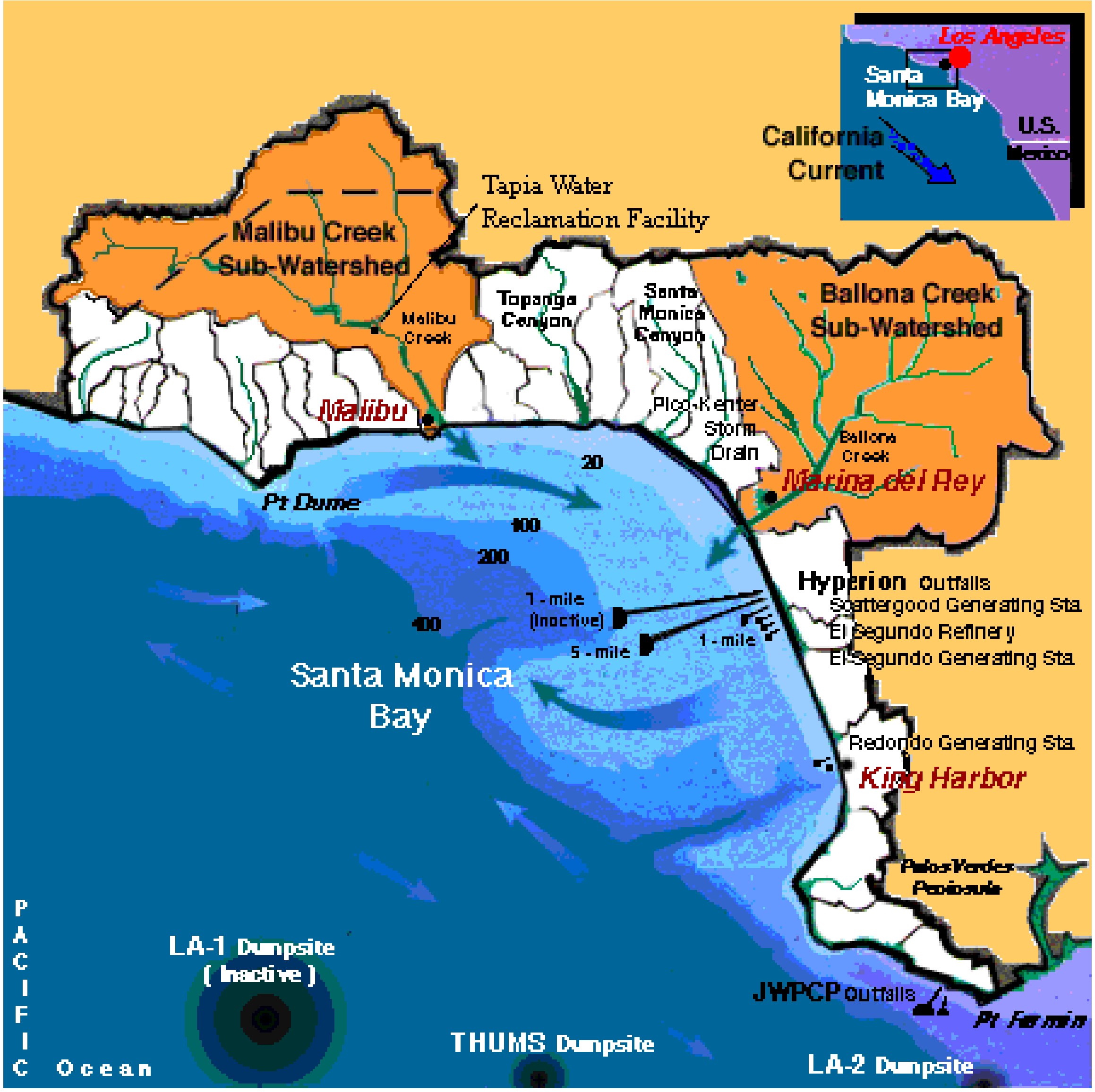

Figure 1: Schematic view of Santa Monica Bay
(courtesy of the SBMRP)

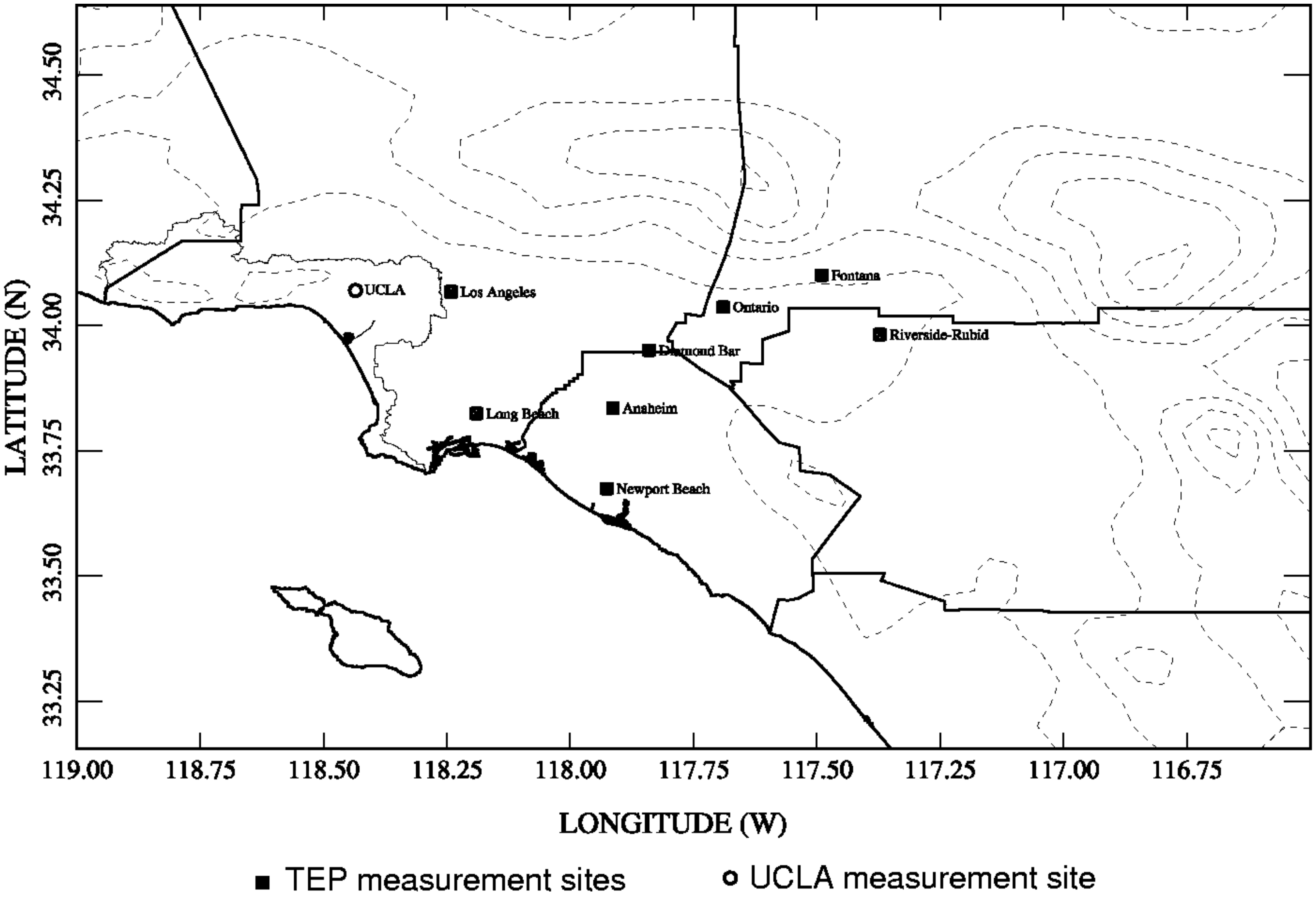

Figure 2: Location of the TEP and UCLA sites

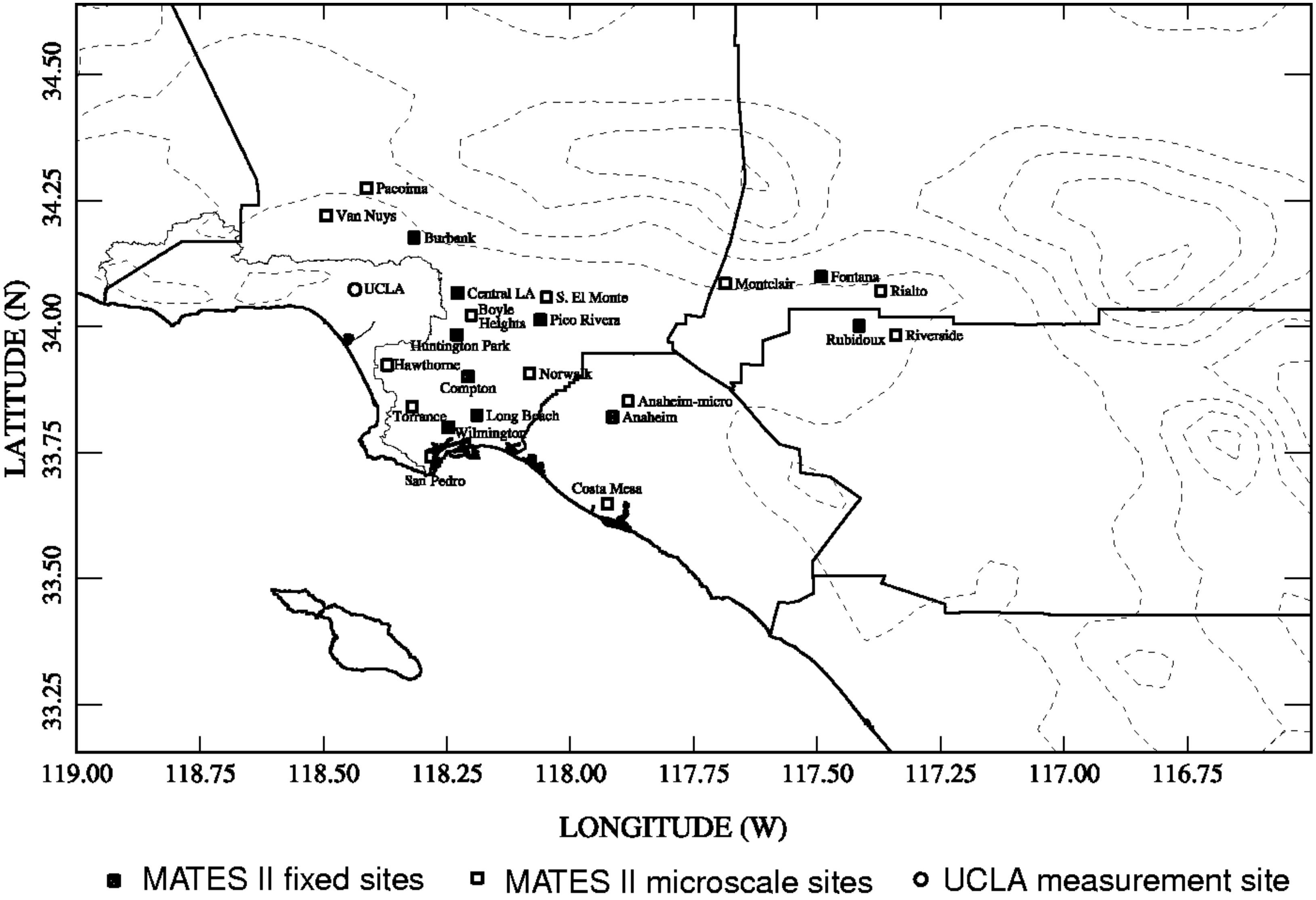

Figure 3: Location of the MATES II sites

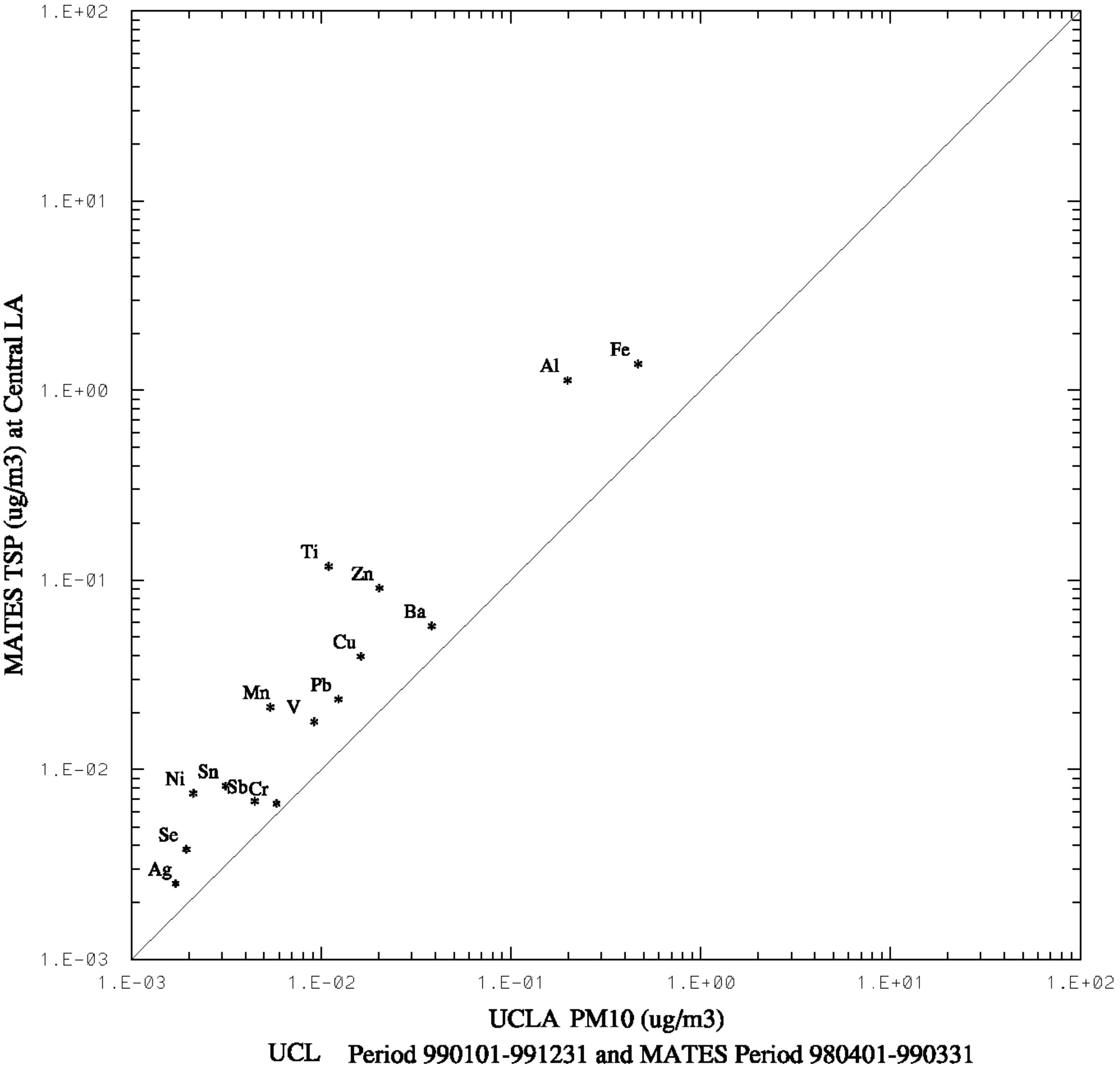

Figure 4: Comparison of metal concentrations measured at the UCLA and LA MATES II sites. Note that the UCLA data is based on a sample of PM10 and the MATES on TSP

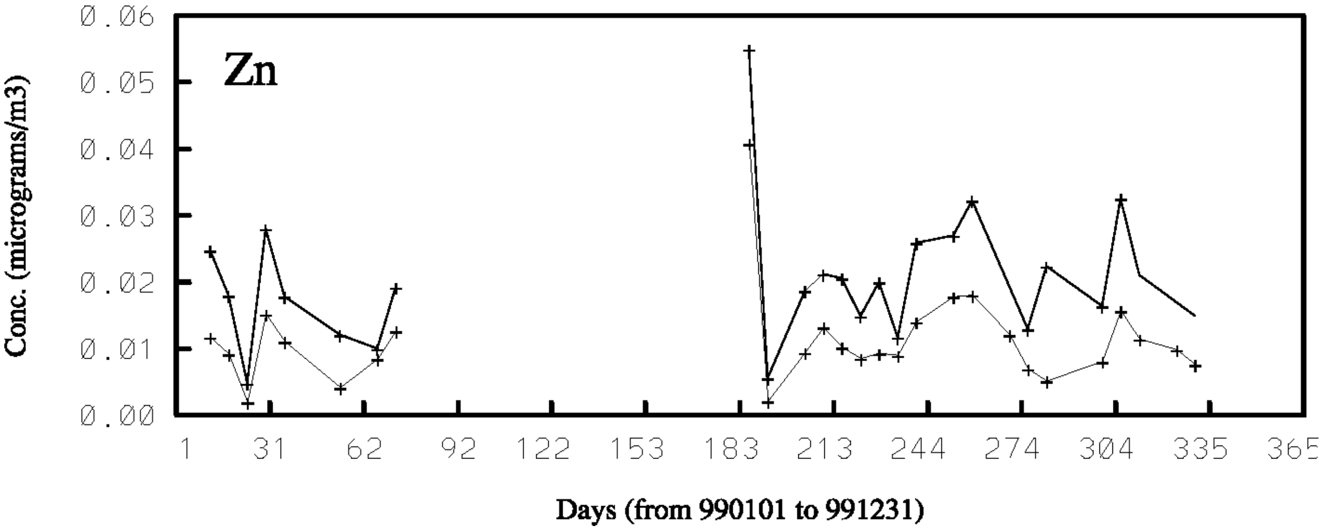

Figure 5: Seasonal variation in zinc concentrations measured at the UCLA site

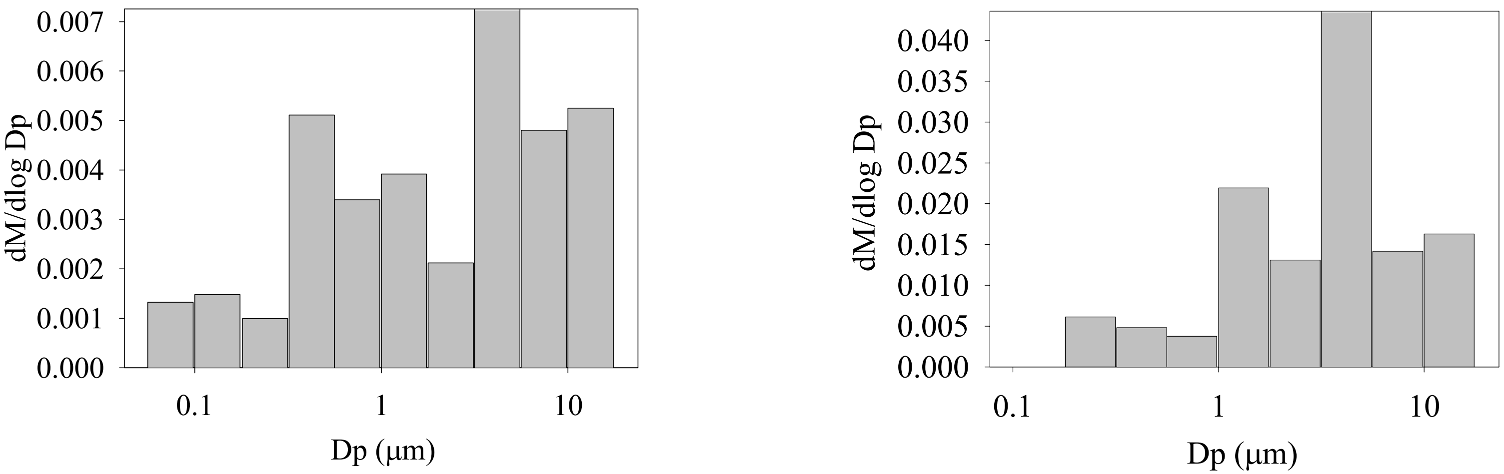

(a) Pb

(c) Cu

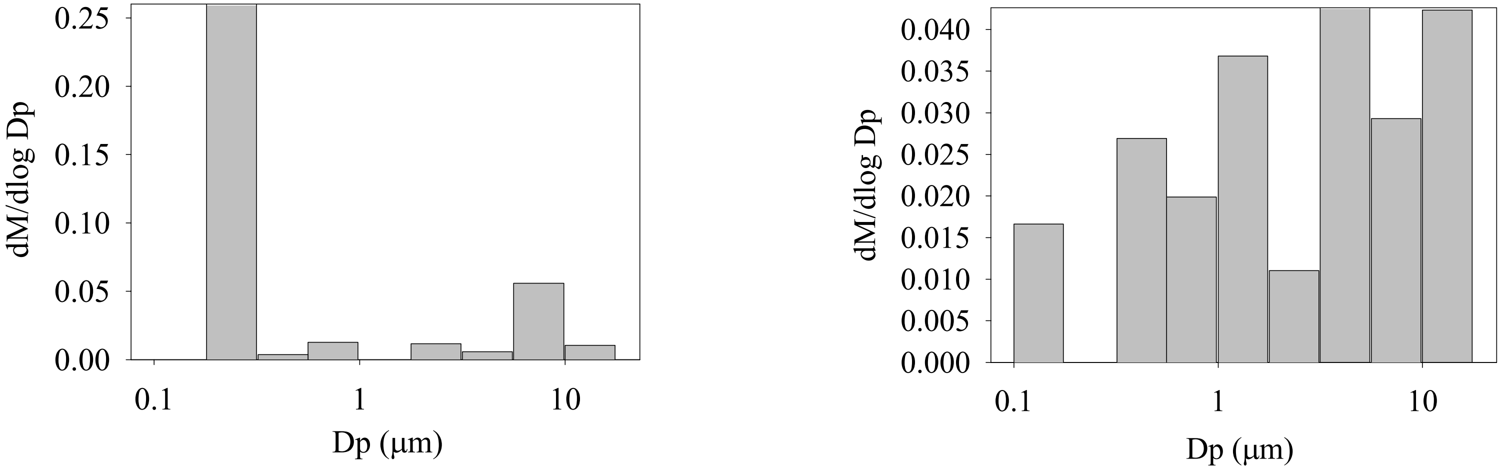

(b) Cr

(d) Zn

Figure 6: 24-hour averaged size distributions of metal concentrations collected with the MOUDI sampler at the UCLA site: a) Pb on October 20, 1998; b) Cr collected on October 21, 1998; c) Cu on October 21, 1998; d) Zn on October 21, 1998

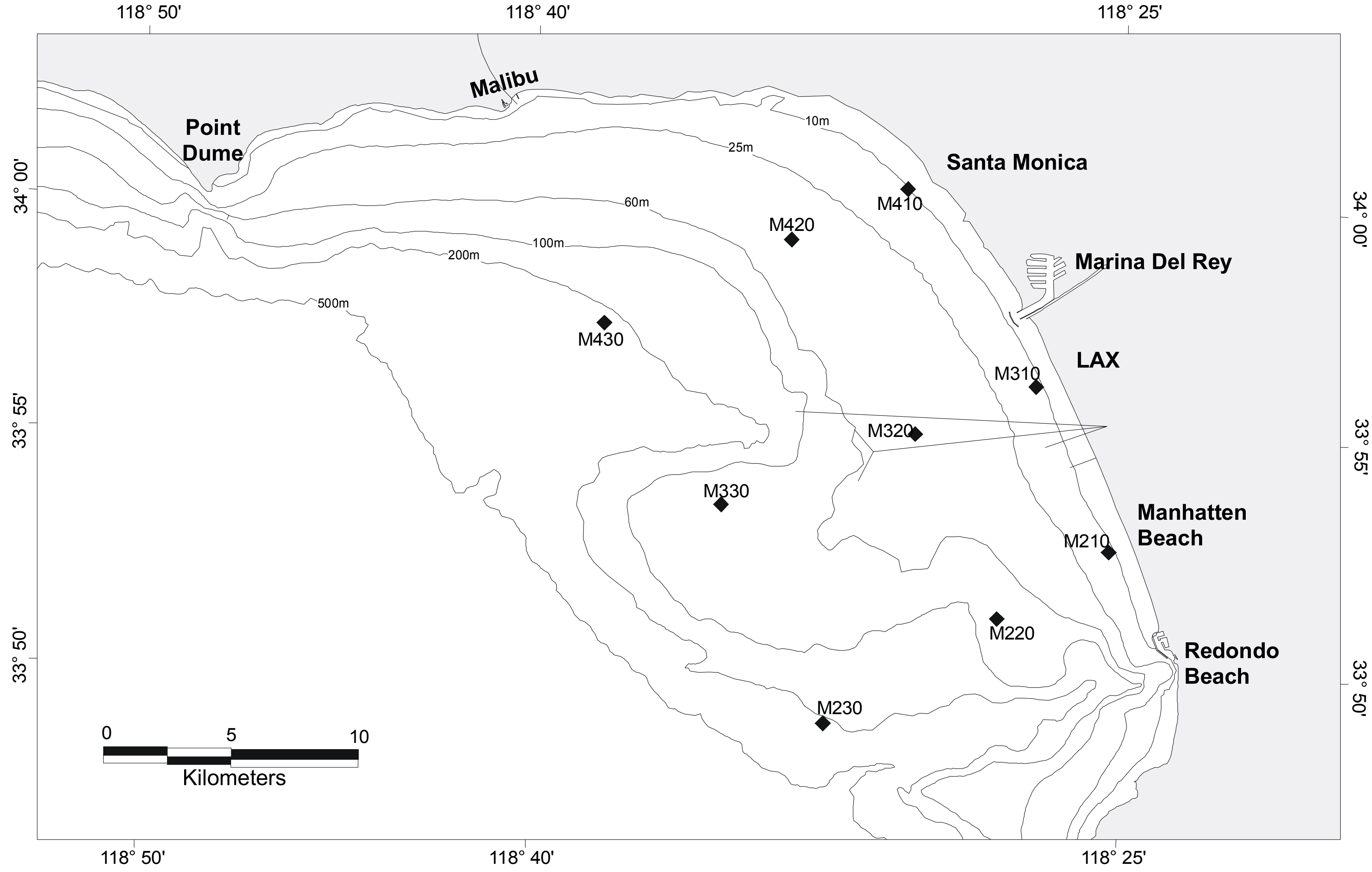

Figure 7: Sites of the microlayer measurements in Santa Monica Bay

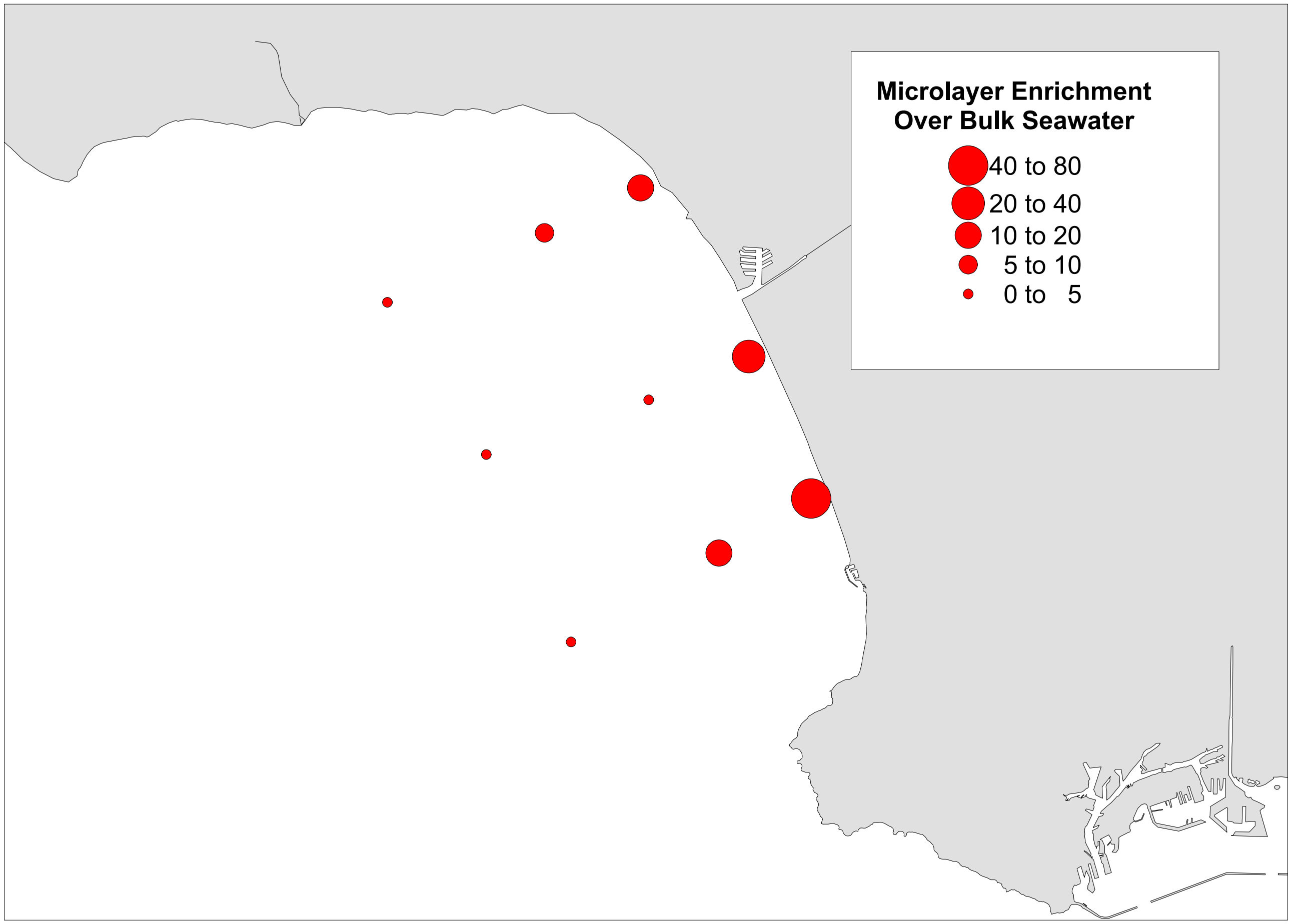

Figure 8: An example of the spatial distribution of zinc enrichment measured in the sea surface microlayer (ratio of the zinc concentration in the microlayer to the zinc concentration in the bulk water)

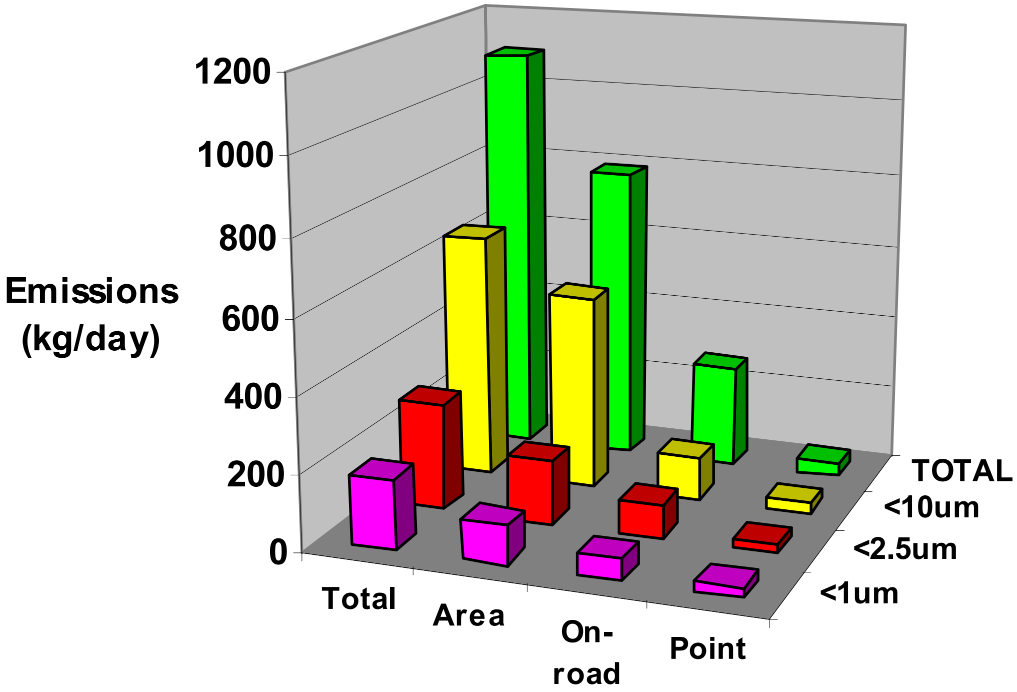

Figure 9: Emission rates for zinc as a function of source and aerosol size

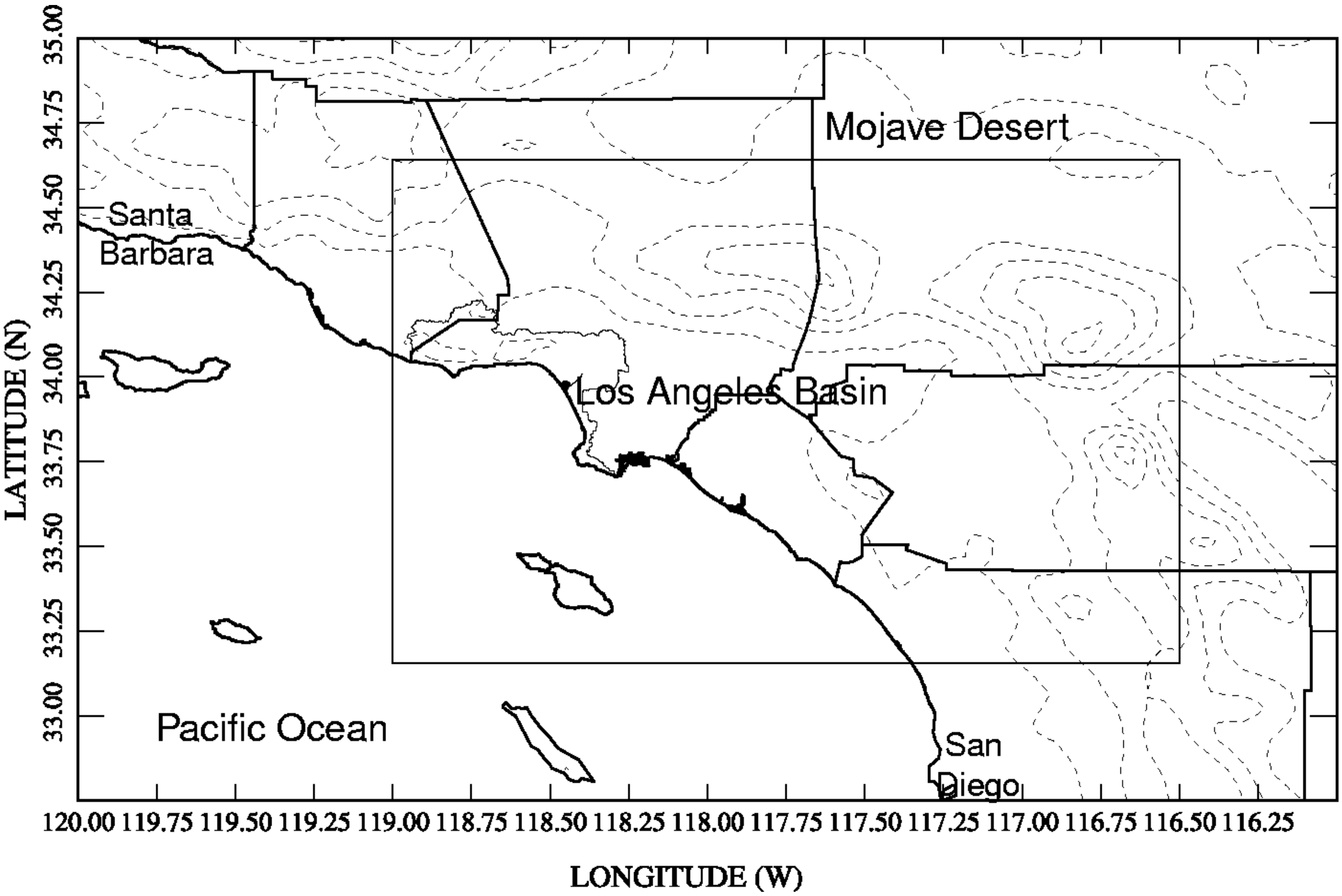

Figure 10: The outer model domain

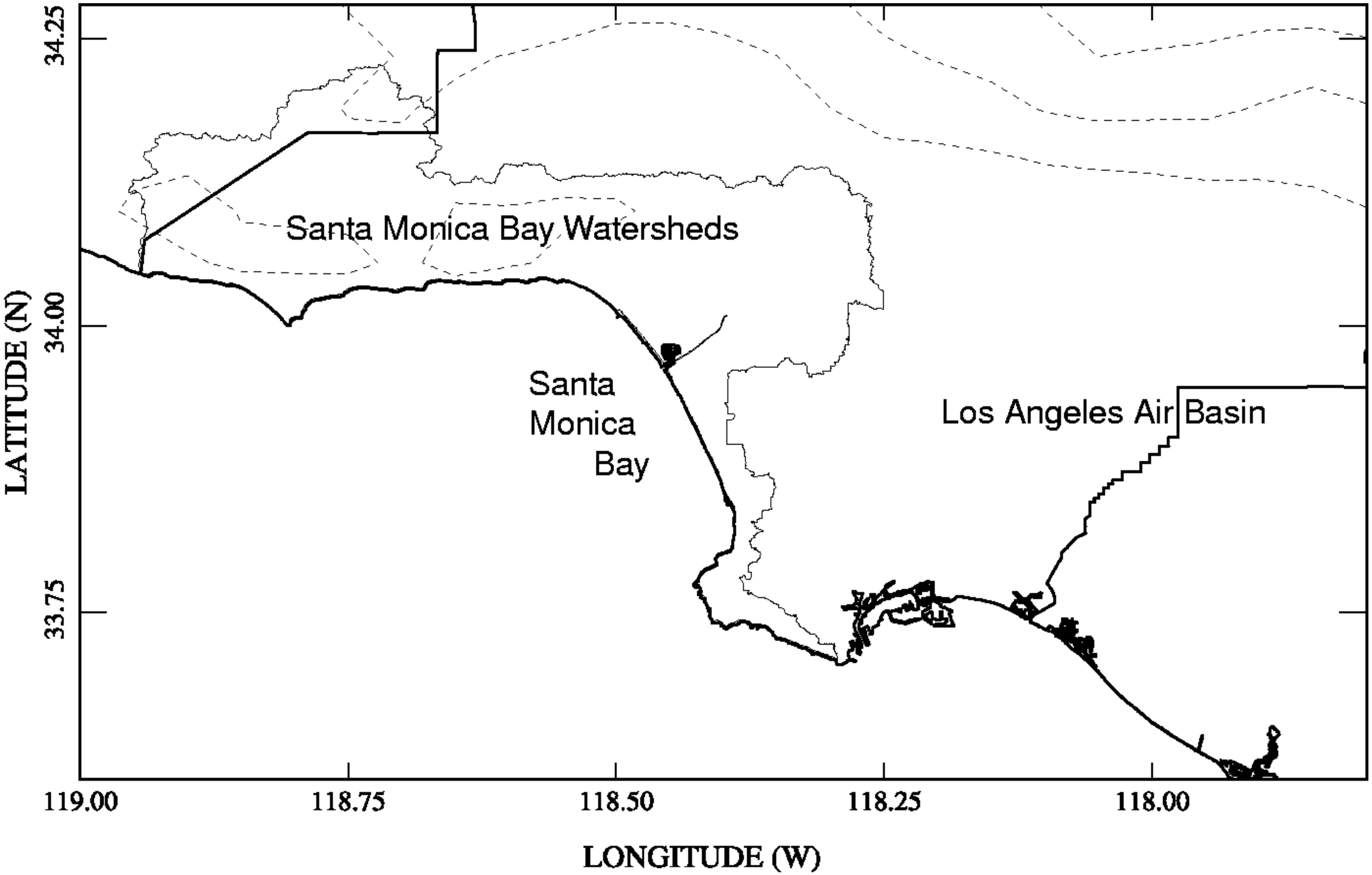

Figure 11: The inner model domain

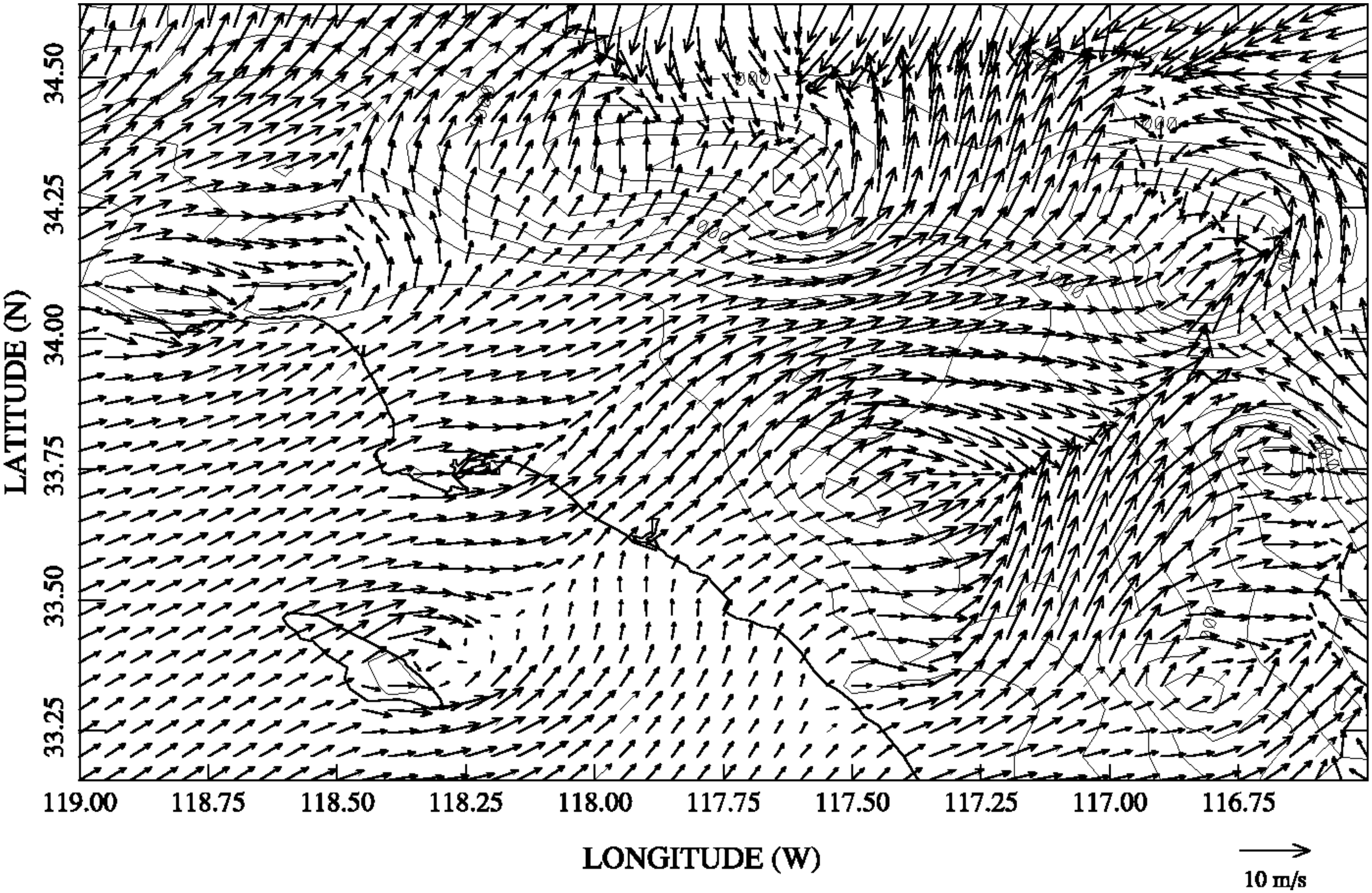

Figure 12: Simulated surface winds in the summer afternoon (1600 PST)

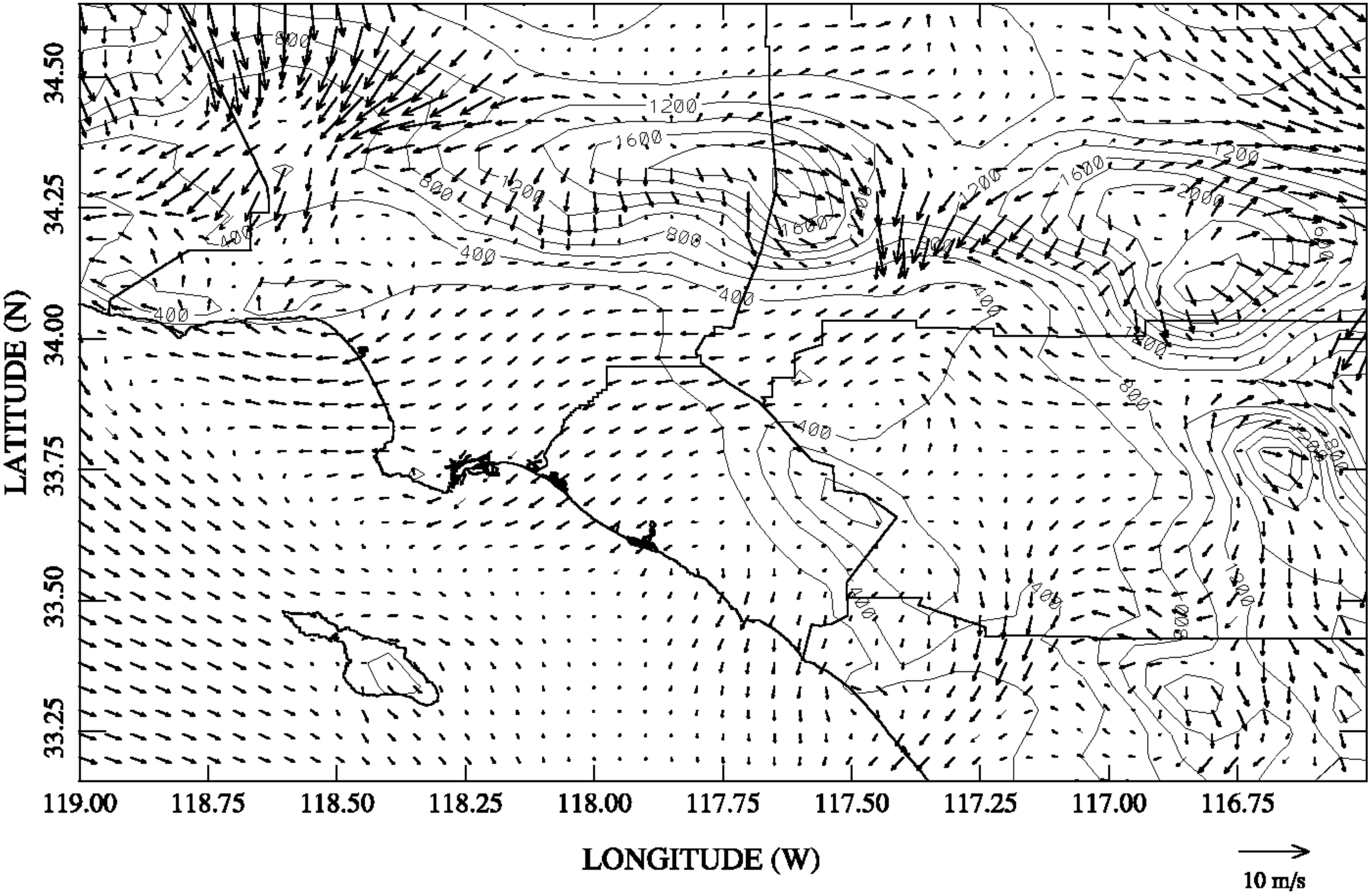

Figure 13: Simulated surface winds in the winter night (0400 PST)

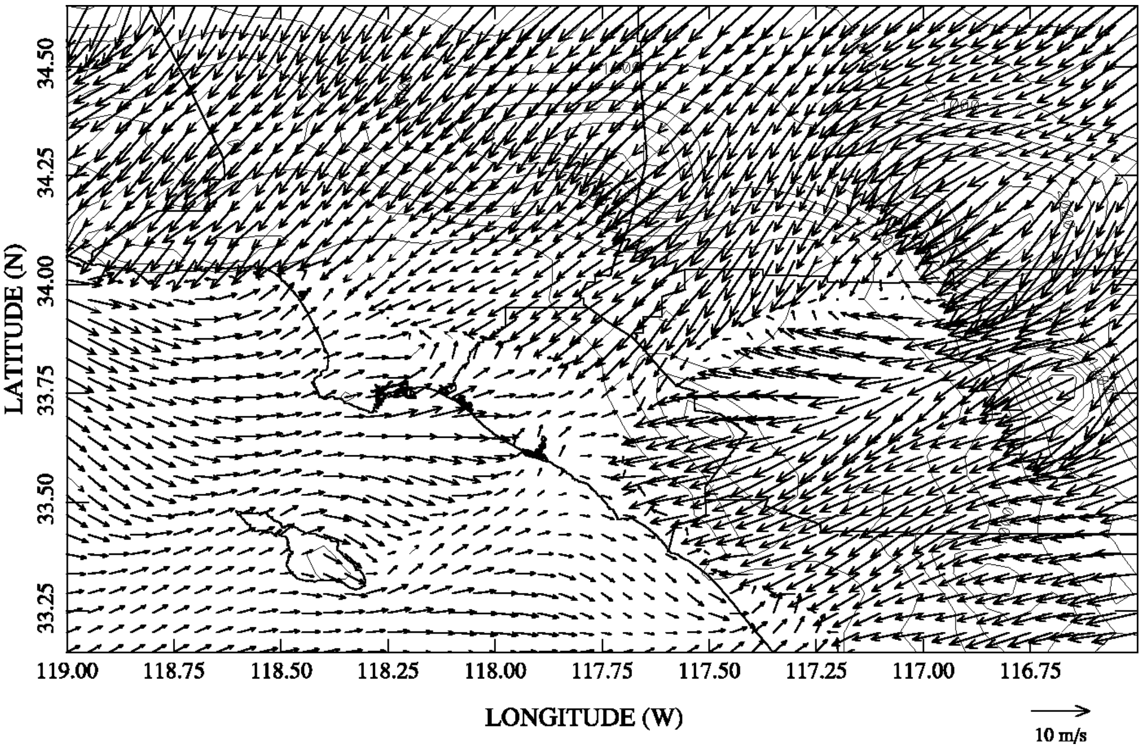

Figure 14a: Simulated surface winds in the afternoon (1600 PST) during a Santa Ana event.

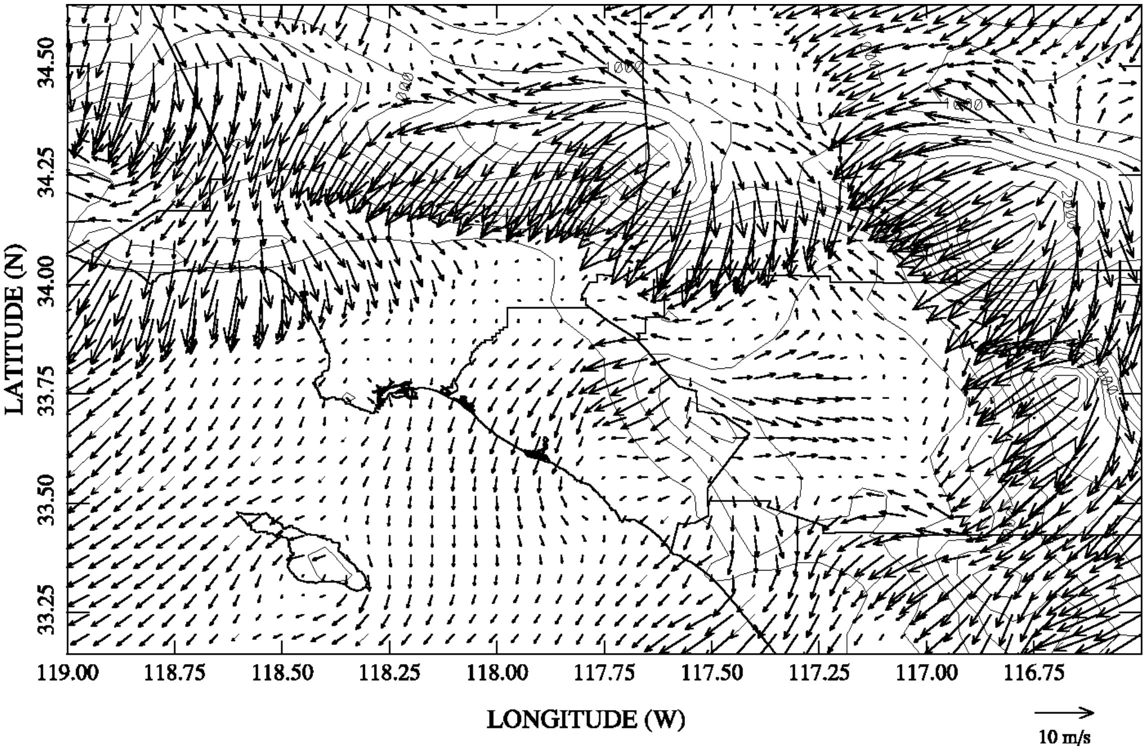

Figure 14b: Simulated surface winds in the early morning (0400 PST) during a Santa Ana event.

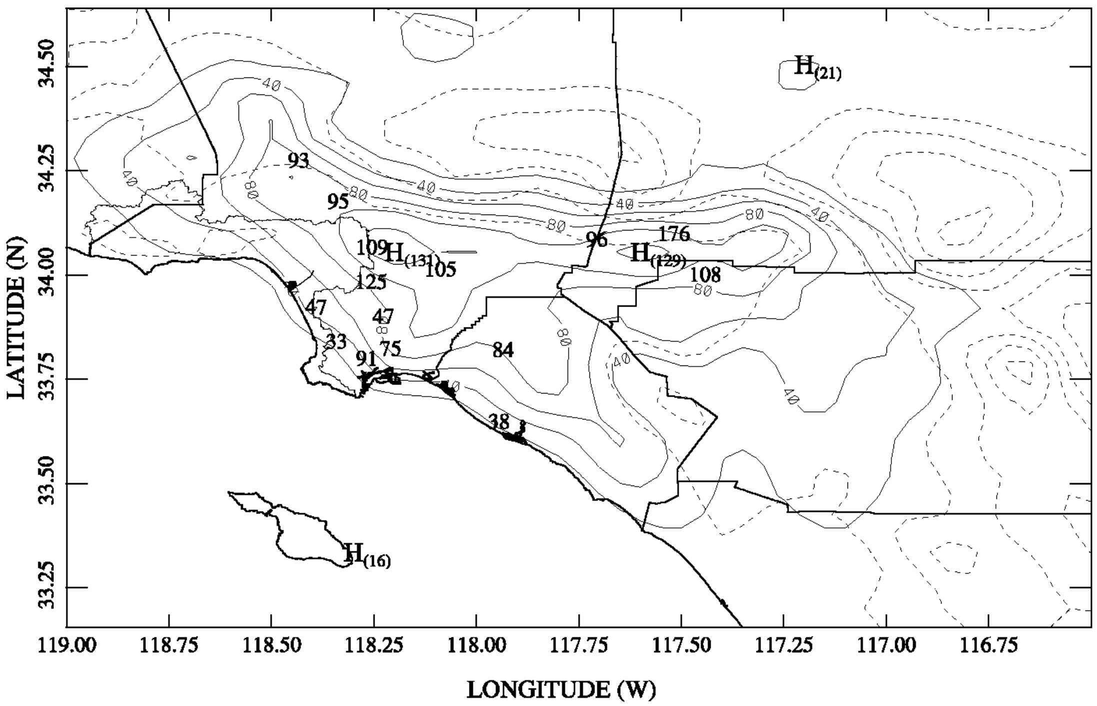

Figure 15a: Comparison of modeled and measured 24-hour average Zn concentrations for the summer case (ug/m^3)

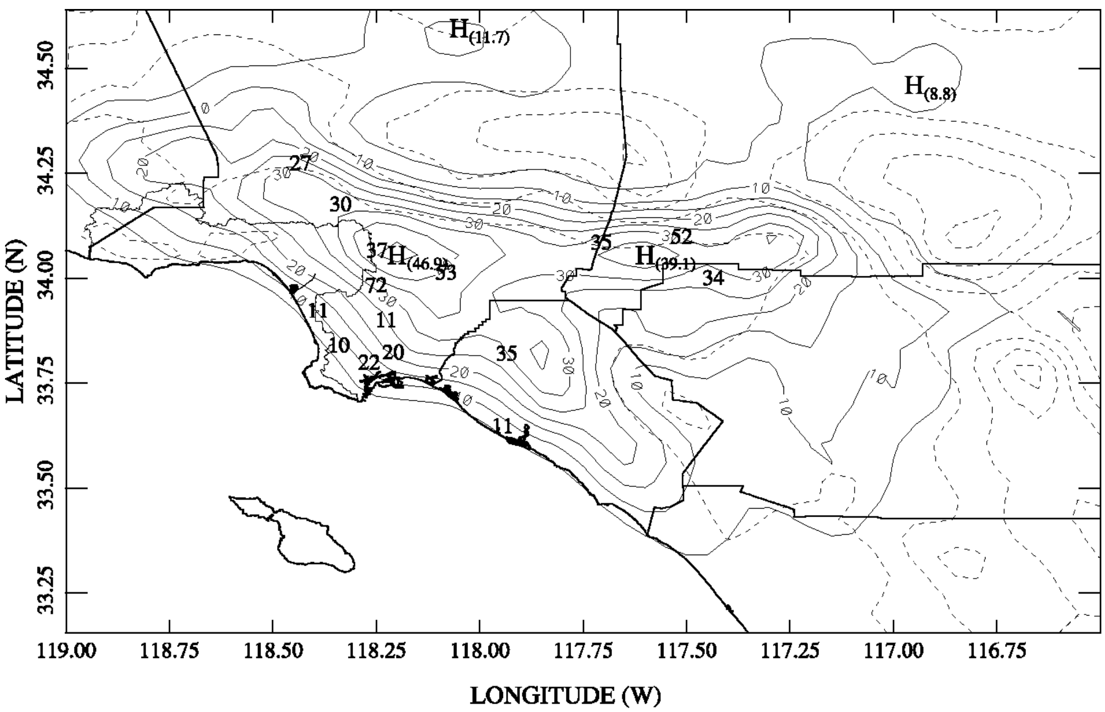

Figure 15b: Comparison of modeled and measured 24-hour average Pb concentrations for the summer case (ug/m^3)

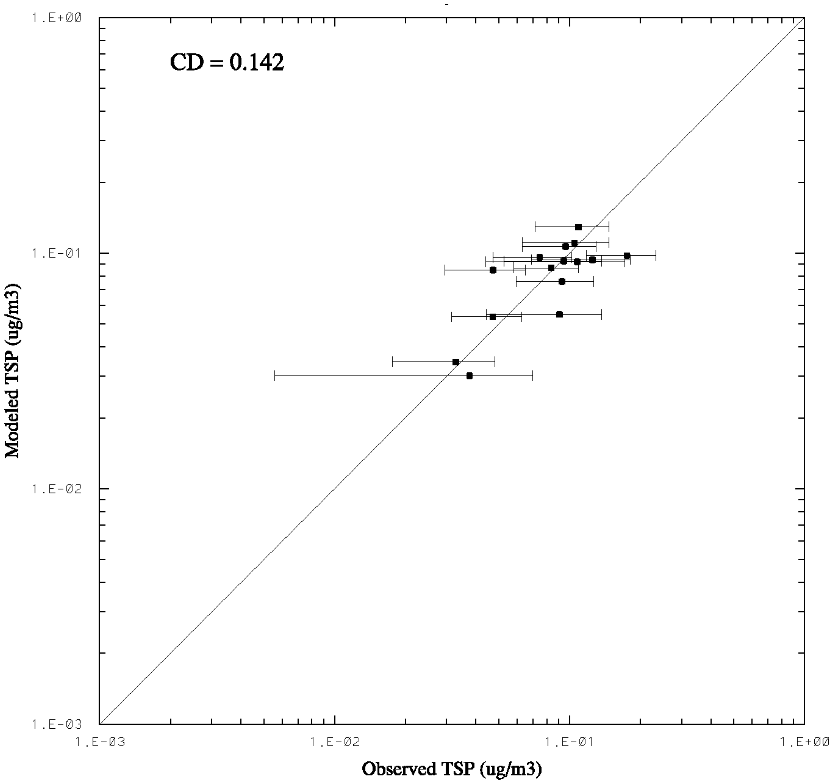

Figure 16a: Correlation between modeled and measured zinc concentrations for the summer case

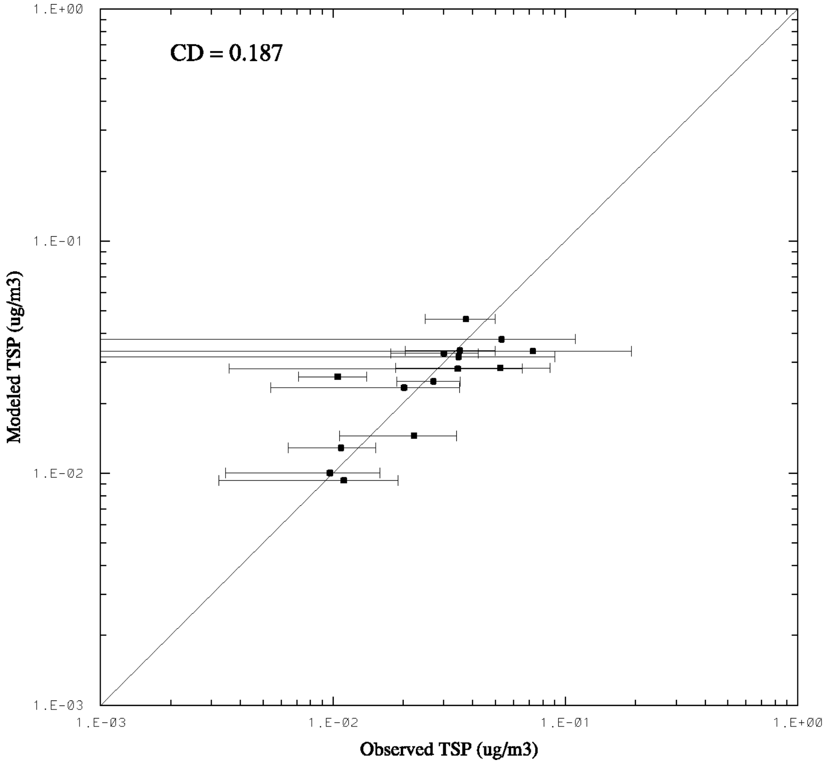

Figure 16b: Correlation between modeled and measured lead concentrations for the summer case

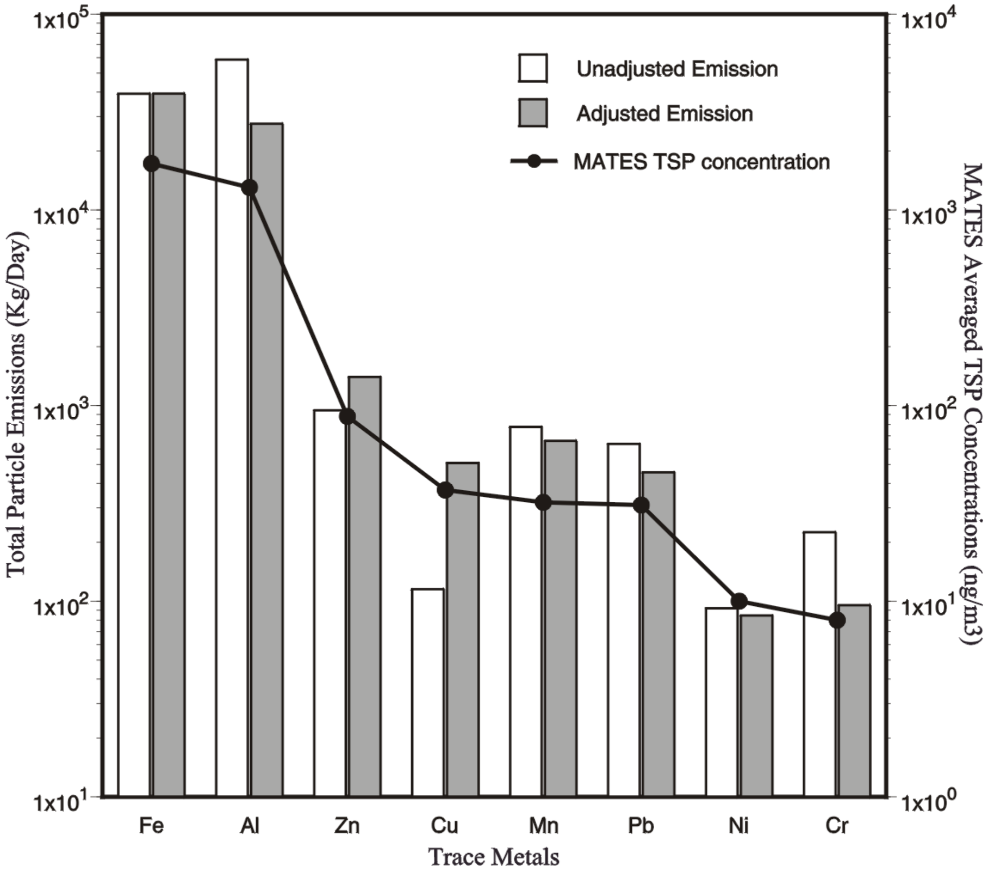

Figure 17: Comparisons of the relative abundance of unadjusted and adjusted trace metal emissions with the averaged trace metal abundance during MATES II

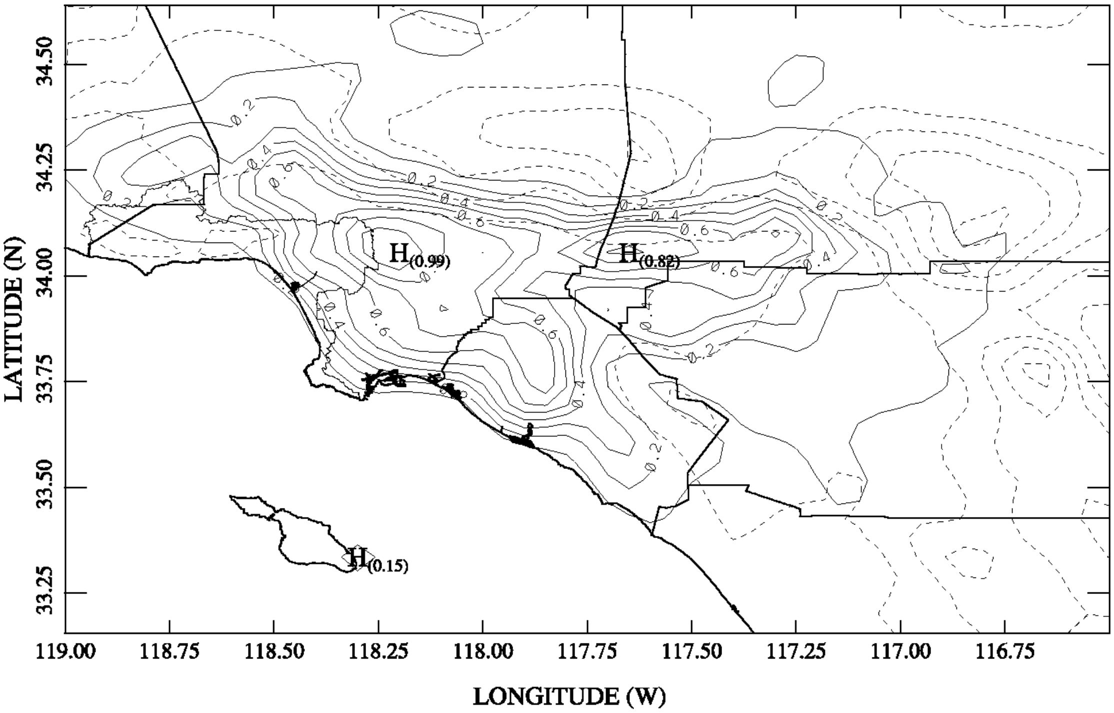

Figure 18a: 24-hour average deposition rate (g/ha-day) of the total mass of Zn for the summer case; the contour interval is 1.00×10^{-1} g/ha-day.

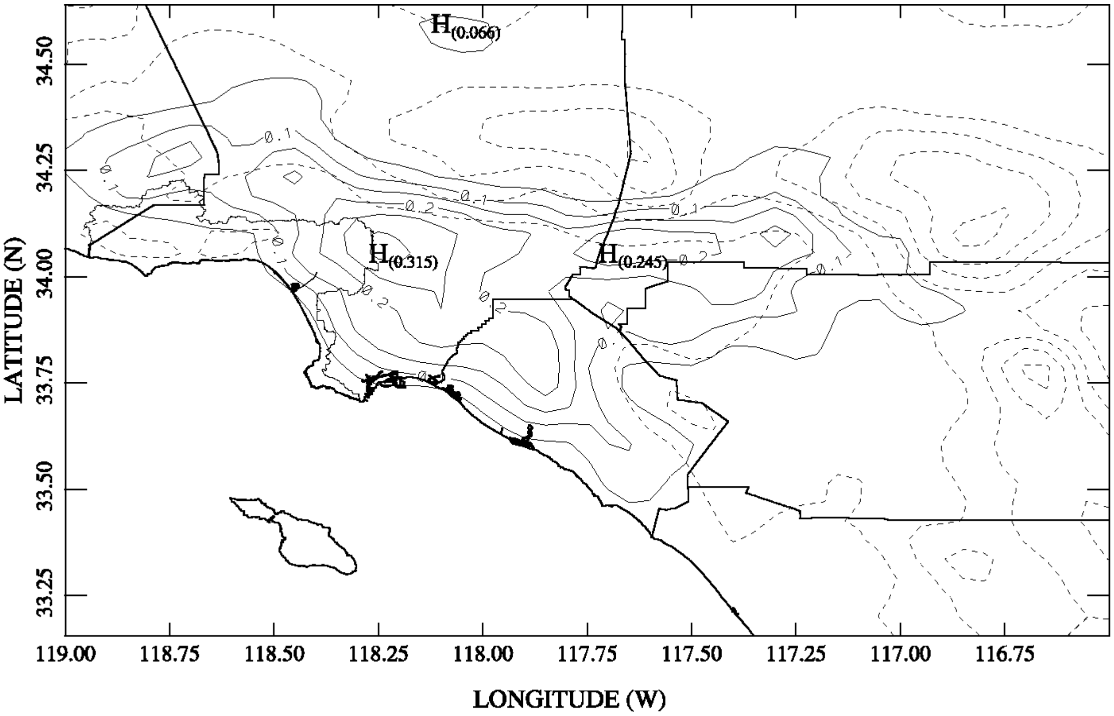

Figure 18b: 24-hour average deposition rate (g/ha-day) of the total mass of Pb for the summer case; the contour interval is 5.00×10^{-2} g/ha-day.

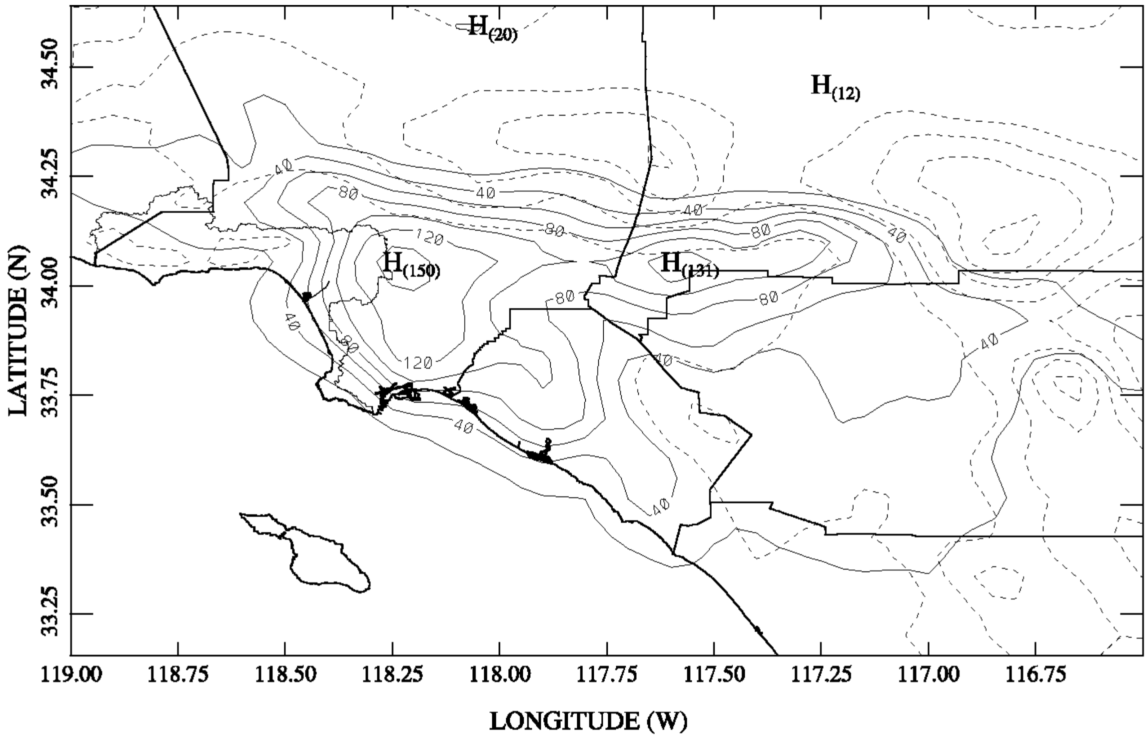

Figure 19a: 24-hour average concentration (ng/m^3) of the total mass of Zn for the winter case; the contour interval is 20.0 ng/m^3.

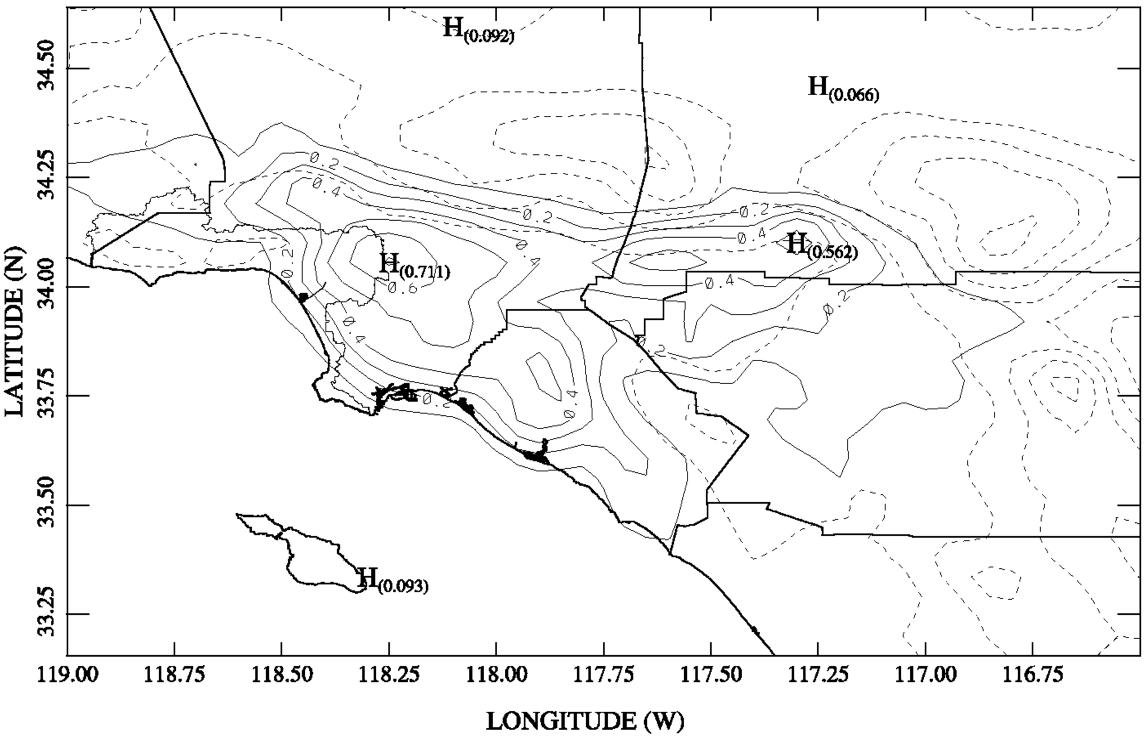

Figure 19b: 24-hour average deposition rate (g/ha-day) of the total mass of Zn for the winter case; the contour interval is 1.00×10^{-1} g/ha-day.

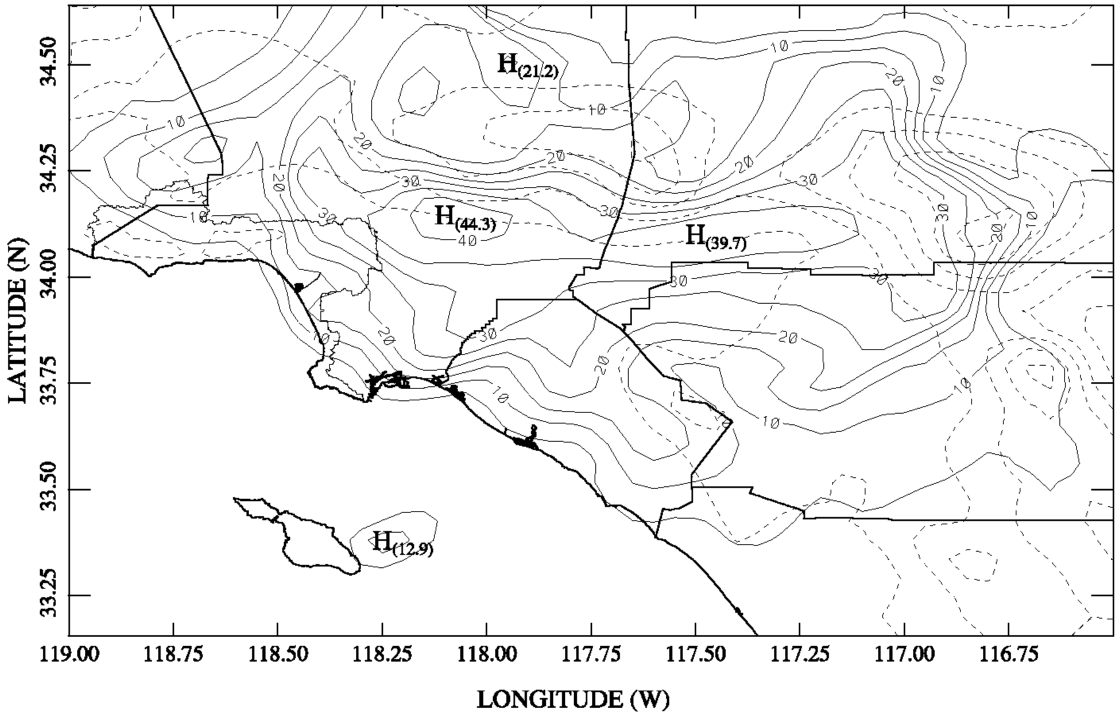

Figure 20a: Zn total mass concentration (ng/m^3) at 1600 PST for the summer case; the contour interval is 5 ng/m^3.

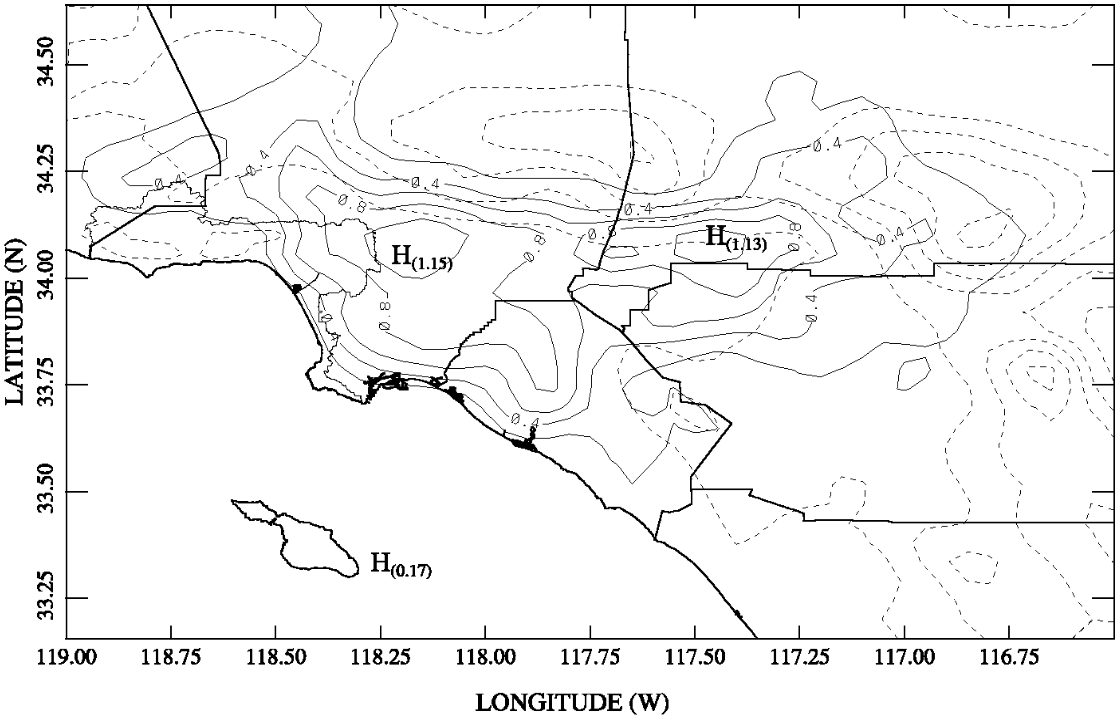

Figure 20b: Zn total mass deposition flux (g/ha-day) at 1600 PST in the summer case; the contour interval is 0.2 g/ha-day.

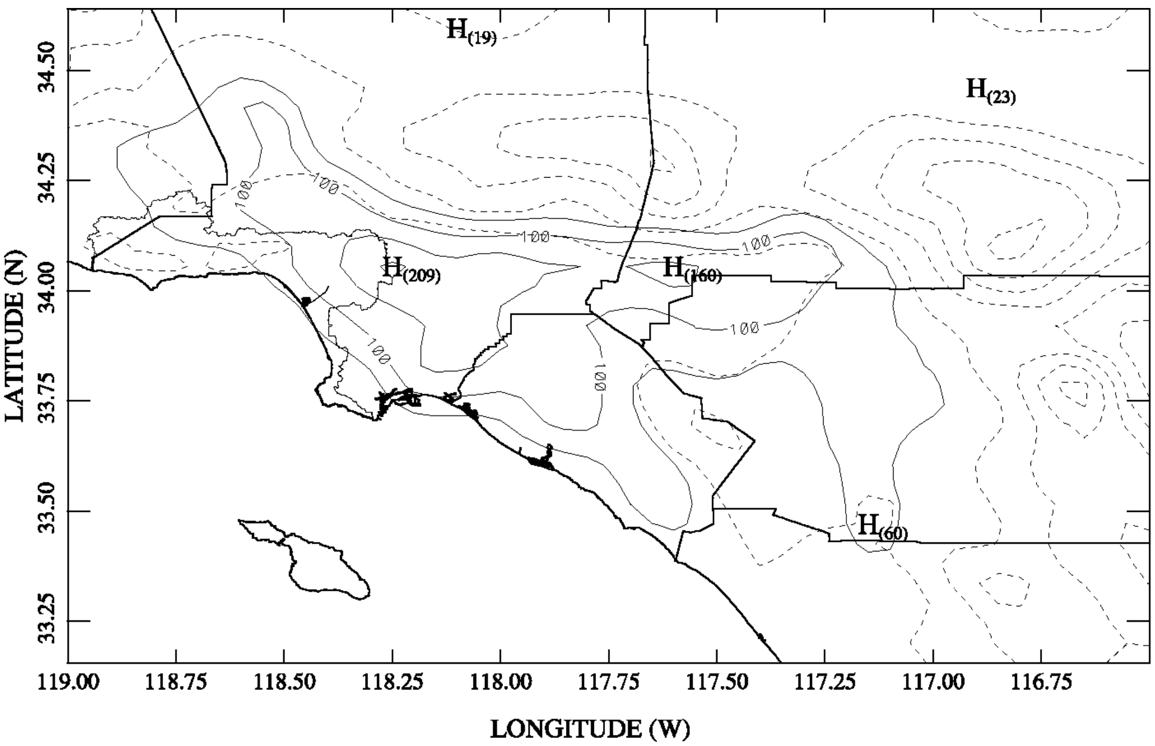

Figure 21a: Zinc total mass concentration (ng/m^3) at 0400 PST for the summer case; the contour interval is 50.0 ng/m^3.

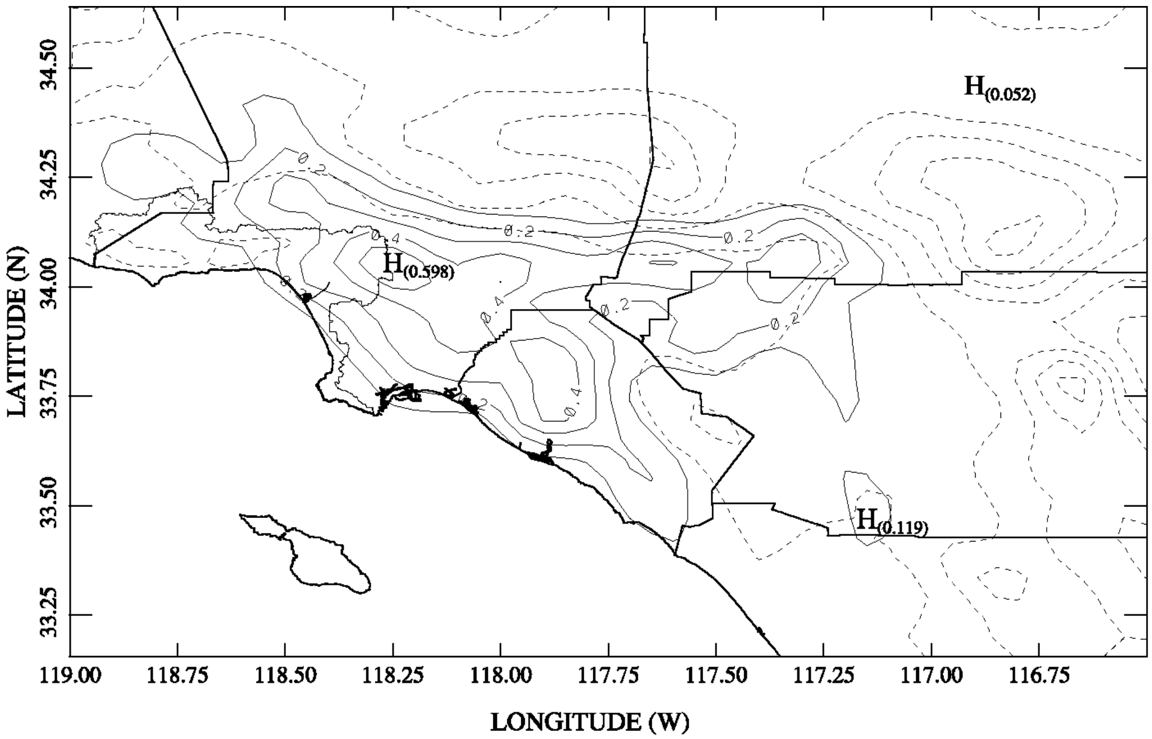

Figure 21b: Zinc total mass deposition flux (g/ha-day) at 0400 PST in the summer case; the contour interval is 0.1 g/ha-day.

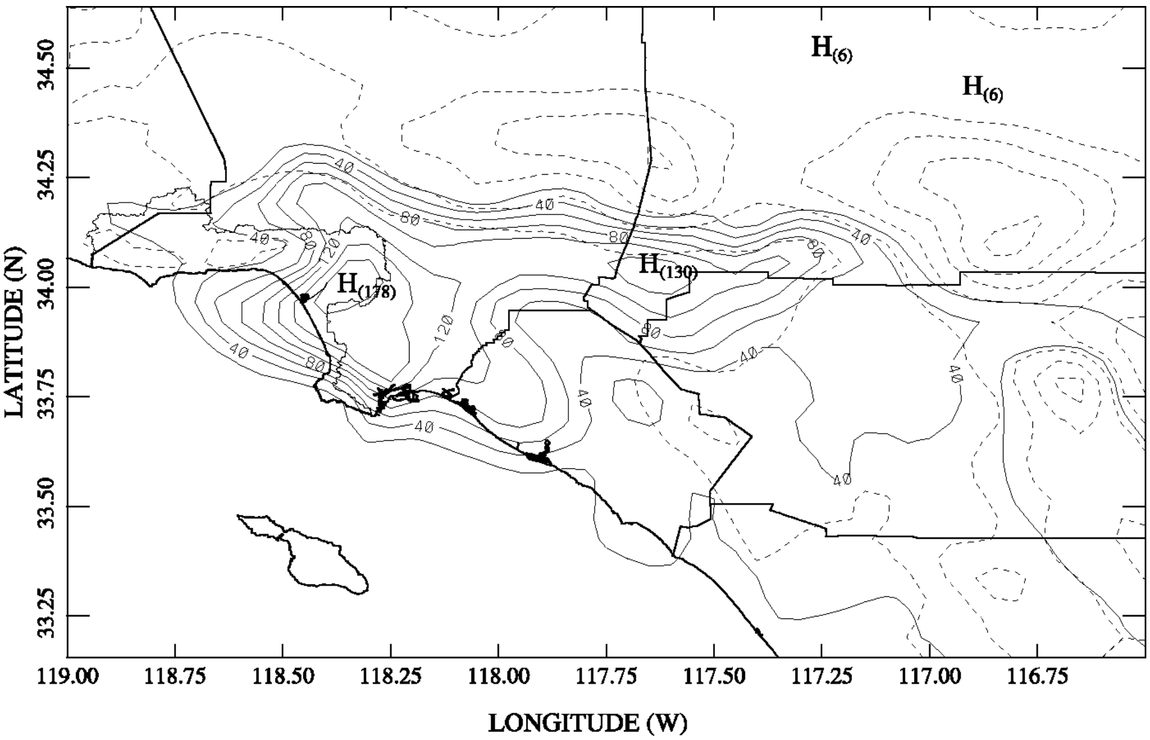

Figure 22a: Zinc total mass concentration (ng/m^3) at 0400 PST for the winter case; the contour interval is 20 mg/m^3.

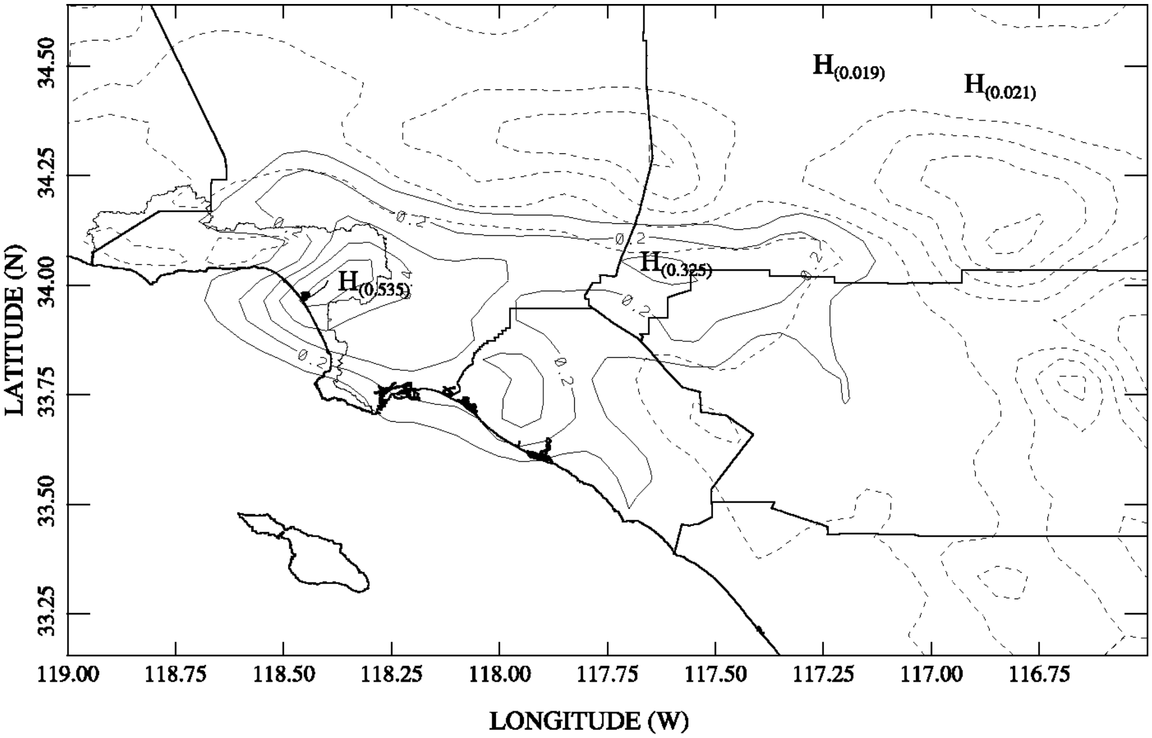

Figure 22b: Zinc total mass deposition flux (g/ha-day) at 0400 PSTfor the winter case; the contour interval is 0.1 g/ha-day.

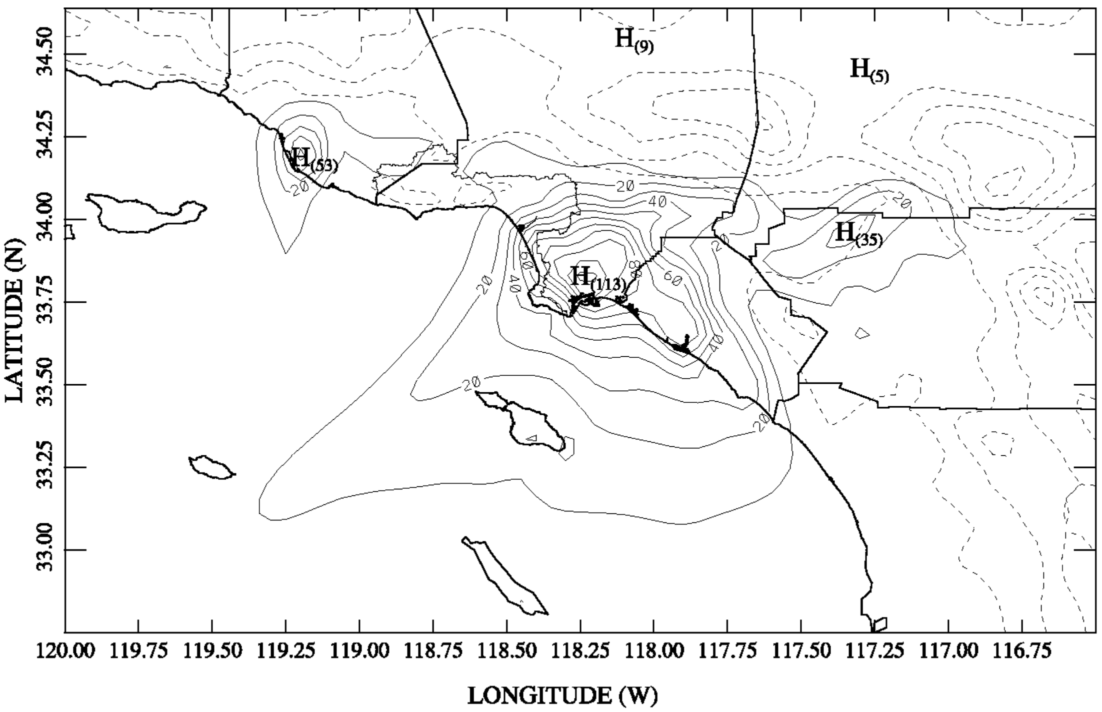

Figure 23a: 24-hour average concentration (ng/m^3) of the total mass of Zn for the Santa Ana case; the contour interval is 10.0 ng/m^3.

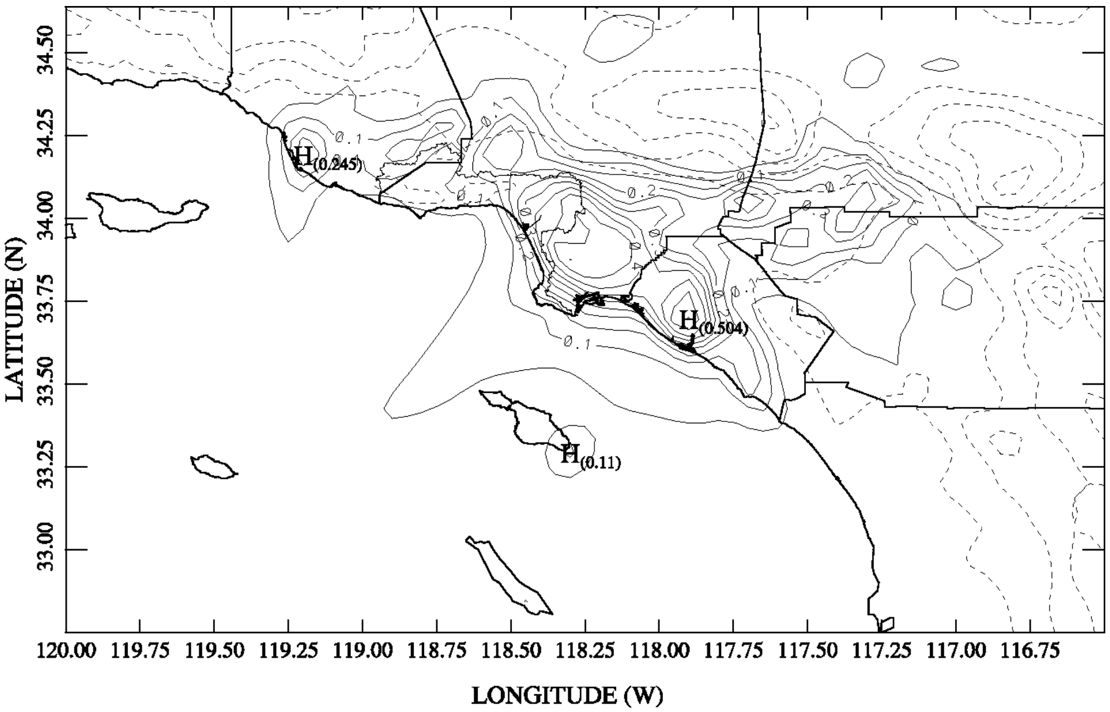

Figure 23b: 24-hour average deposition rate (g/ha-day) of the total mass of Zn for the Santa Ana case; the contour interval is 5.00×10^{-2} g/ha-day.

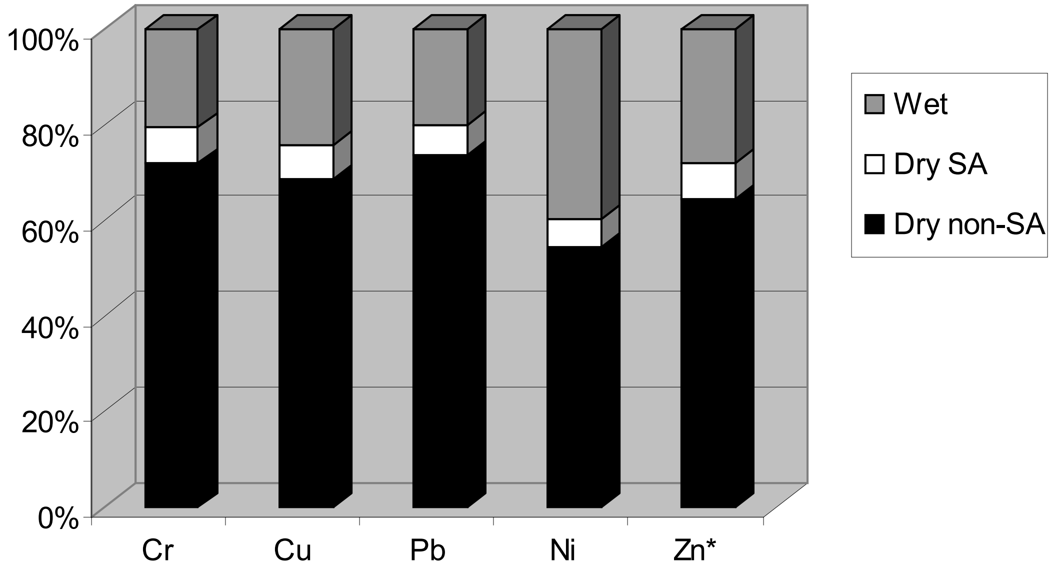

Figure 24: Relative contributions of dry non-Santa Ana deposition, dry Santa Ana deposition and wet deposition to the total loading of Santa Monica Bay, including in all cases both direct deposition and indirect runoff from the watershed.

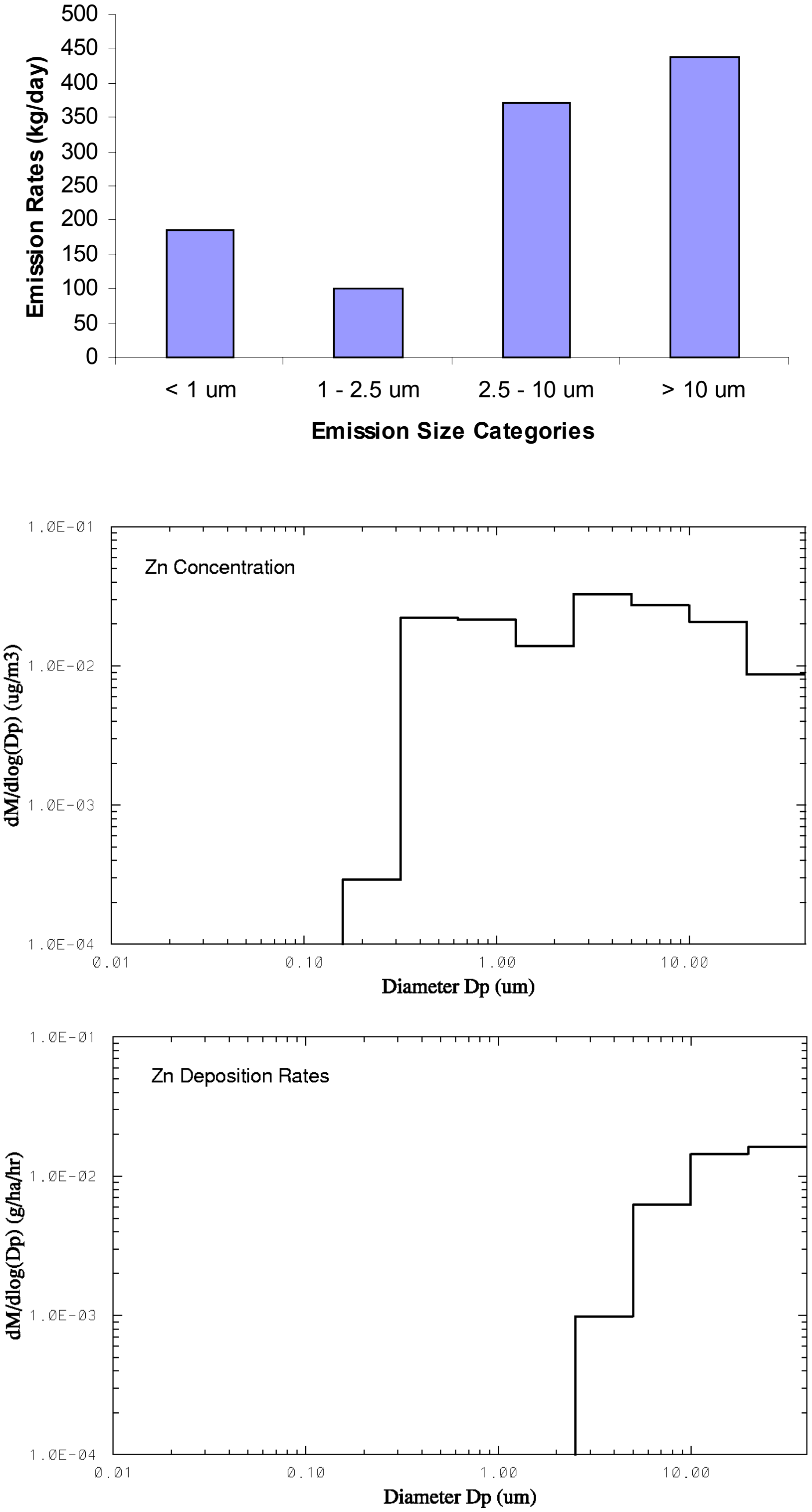

Figure 25: Distribution of Zn mass on aerosols in emissions (top) the airborne surface layer concentration (middle), and deposited particles (bottom).

APPENDIX I

Note: All data collected by this project and discussed in this data report may be obtained in MS Access database format or ASCII table format from the SCCWRP web site (www.sccwrp.org).

ATMOSPHERIC TRANSPORT AND DEPOSITION OF TOXIC CONTAMINANTS TO SANTA MONICA BAY, CA

• • • • •

Data Report

Prepared by

Southern California Coastal Water Research Project
7171 Fenwick Lane
Westminster, CA 92683
www.sccwrp.org

April 28, 2000

FOREWORD

This is a data report for the project designed to estimate loads of toxic constituents that deposit from atmospheric sources to Santa Monica and its surrounding watershed during 1999. The goal of this report was to provide the objectives, rationale, methods, quality assurance, information management, and raw data generated during the study. This report was not designed to provide all of the assessments identified by each of the research questions. The assessment report will follow after this data report and shall include many technical components including atmospheric transport and transformation modeling.

Part of the success of this study lies in its collaboration among three multi-disciplinary organizations. These organizations included the Santa Monica Bay Restoration Project (SMBRP), the Southern California Coastal Water Research Project (SCCWRP), and the University of California at Los Angeles Institute of the Environment (UCLA). By joining forces, these three organizations represented the necessary spectrum of specialties to address pollutant impacts in the Bay from aerial deposition including resource management, atmospheric scientists, water quality experts, and marine biologists.

Table of Contents

INTRODUCTION

There are a multitude of pollutant sources to Santa Monica Bay and it's surrounding watershed (SMBRP 1998). Some sources, such as treated wastewater, are well characterized (Raco-Rands 1997) and extensive effort has been spent assessing their impacts to the Bay (Dorsey et al 1995, Stull 1995). Other sources, however, are virtually unmonitored and the magnitude of their contribution to the Bay's overall pollutant load is unknown. One example of this type of source is aerial deposition. The Los Angeles metropolitan area exhibits amongst the worst air quality in the nation (EPA 1997). Aerosols in the ambient air of greater Los Angeles are known to contain concentrations of toxic constituents, as well as potentially eutrophying nutrients, for marine ecosystems (Prastinis 1994, Arey *et al* 1989, Kawamura and Kaplan 1986, Young *et al* 1976). Even so, little information currently exists for assessing the relative risk to the Bay from aerial deposition compared to other, better-characterized sources.

There are two main avenues of aerial deposition to Santa Monica Bay. The first avenue is direct deposition. Direct deposition occurs when aerosol particles deposit directly onto bay water surfaces. The second avenue is indirect deposition. Indirect deposition occurs when aerosol particles are deposited onto land surfaces within the watershed. These particles are then capable of being mobilized during subsequent rainstorms and transported to the Bay with stormwater runoff. Since the Los Angeles airshed is much larger than the Santa Monica Bay watershed, aerosols that are deposited directly and indirectly to the Bay could be generated from outside the watershed.

Research Questions

Understanding the transport and deposition of toxic contaminants to Santa Monica Bay is a large and complex proposition. Therefore, the study design focuses around three research questions. Each of the three questions were developed to assess mass emissions.

1) *What is the total annual load of toxic contaminants to Santa Monica Bay via atmospheric deposition, either directly or indirectly?*

   There are no regulatory criteria for loadings of toxic constituents via aerial deposition to the Bay. However, answering this question enables comparisons of inputs from atmospheric deposition to current inputs from other sources. This will provide resource managers charged with protecting the Bay the necessary information to evaluate the relative environmental risk from atmospheric deposition as a source of contaminants. If atmospheric deposition contributes a large portion of the total load for a specific pollutant, then greater efforts may need to be expended in order to control this source. If the contribution of that pollutant from atmospheric deposition is small, then less effort should be spent on aerial as a source of contamination and management efforts may be more efficiently directed elsewhere. Finally, if a management decision is made to reduce pollutants inputs from atmospheric deposition, the total annual load estimates generated during this study will provide the benchmark for assessing whether the management actions implemented were effective at reducing loads of pollutants to the Bay.

2. *What proportion of the annual load of toxic contaminants from atmospheric deposition is contributed during different seasons or specific meteorological events?*

   It is unclear whether annual loads from atmospheric sources are primarily large, but episodic in nature, or if they are a low level, but chronic contributor of pollutants to the Bay. An example of chronic contributions includes the daily offshore air flow pattern exhibited diurnally in the region. Examples of episodic events include seasonality (i.e. winter vs. summer), Santa Ana wind conditions, and rain storms. Studies in southern California and other areas around the nation indicate that episodic events can increase deposition rates significantly and may be extremely important components of the total annual load (Young and Chan 1977, Offenberg and Baker 1997). However, this assessment has not been accomplished within the Santa Monica Bay watershed. This understanding of when the greatest degree of inputs occurs is crucial to focusing future work including biological effect studies, source reduction strategies, or design of transport and deposition models.

3. *How do atmospheric concentrations of toxic contaminants vary spatially between Santa Monica Bay and other regions of Los Angeles?*

   There are two separate categories of sources that contribute to atmospheric deposition loads that are segregated upon their transport to the Bay. The first is from local sources within the watershed and the second category is from distant sources within the airshed, but outside the watershed that are subsequently transported to the Bay for deposition. The degree to which local sources contribute to the Bay's loading relative to distant sources will have a profound impact on how resource managers may approach control measures and implement management or regulatory actions. This is particularly true for other transport mechanisms including urban runoff.

METHODS

Study Site

The sampling design consisted of a Master Site located within the Santa Monica Bay watershed with many satellite sites with different sampling requirements (Figure 1). The master site was located on a rooftop at the University of California, Los Angeles (UCLA). This site has a long historical record of meteorological conditions (wind speed and direction, precipitation, barometric pressure, and humidity). The building is four stories above ground level (approx. 12 m) where airflow is not impeded by any nearby structure; the surrounding area is comprised of parking lots, trees and shrubs, and other buildings.

Nine sampling sites were located in Santa Monica Bay for seasurface microlayer measurements (Figure 1). These sites were designed in a grid fashion for assessing gradients across Bay water surfaces. They were not used for estimating deposition rates to Bay water surfaces.

Eight additional air sampling sites were utilized for this study (Figure 1). The sites were not maintained by the project team, but were sampled by the South Coast Air Quality Management District (AQMD). These sites collected air samples within the Los Angeles airshed, but outside of the Santa Monica Bay watershed. The locations included downtown Los Angeles, Anaheim, Diamond Bar, Rubidoux, Fontana, Ontario, Costa Mesa, and Long Beach. These sites provide an opportunity to extend the spatial scale of our study design. Our study team mimicked the sampling techniques and times to maintain consistency for combining data sets.

Sampling

A combination of approaches was used to sample aerosol concentrations and atmospheric deposition for making load estimates to land and water surfaces.

Wet deposition

Wet deposition was sampled directly using rainwater collectors developed by the National Atmospheric Deposition Program (NADP 1997). This technique utilizes a rain sensor that uncovers the sampler when precipitation is occurring, then covers the sampler when precipitation ceases to reduce evaporation and dry deposition contamination. All sampleable storms were targeted between January and May 1999

Figure 1. Map of the sampling sites in Santa Monica Bay.

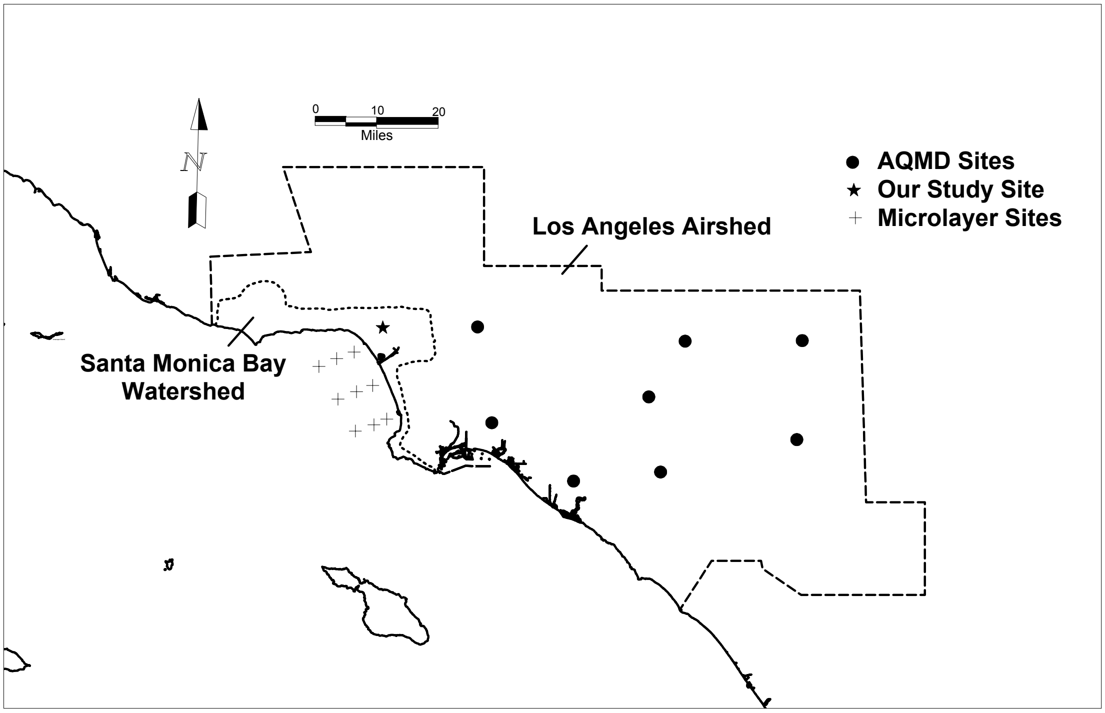

Aerosol concentrations

Dry deposition on land and water surfaces was estimated using measured air concentrations segregated by particle size. Theoretical deposition velocities for each particle size were calculated using local meteorological conditions. This technique has been adopted by both the NADP and the Integrated Air Deposition Network (Hillery *et al* 1998). Two types of air samplers were used. The first was a dichotomous air sampler that collects two size fractions; Particulate matter between 10 and 2.5 microns (PM_{10}) and particulate matter less than 2.5 microns ($PM_{2.5}$). In addition, a Multi-Orifice Uniform Diameter Impacter (MOUDI) sampler was used to collect aerosols in 12 different size fractions from >18 to < 0.06 microns.

Index periods were targeted for sampling during selected seasons. Dichotomous samples were collected every six days during winter (Jan-Feb, 1999), summer (Jul-Aug

1999) and fall (Sep-Oct 1999). MOUDI samples were collected once per month during these same index periods.

Surrogate surfaces

An aerodynamic surrogate surface developed by others (Zufall *et al.* 1998, Zufall and Davidson 1997) was deployed at our master site at UCLA. The surrogate surface was deployed simultaneously with the MOUDI sampler. The surface was designed to minimize turbulence and maintain laminar flow across its length to achieve consistent deposition results. The surrogate surface was covered with a Teflon filter and coated with oleic acid to minimize particle bounce.

Seasurface microlayer

A Teflon-coated rotating drum was used to collect samples of the seasurface microlayer (Cross et al 1987). Microlayer depths of approximately 50 microns are sampled using this system; the rotating drum is towed at slow speeds (1/4 knot) alongside a vessel with a non-contaminating hull and uses a zero emission electric motor. For comparison purposes, bulk seawater samples were collected at depths of 1 m using a peristaltic pump.

Chemical Analysis

Three types of sample analysis were conducted (Tables 1 and 2). The first sample analysis was total mass of particulates on each filter. The second type of analysis was determination of trace metals concentrations on aerosol particles, rainwater, and seasurface microlayer. The third type of analysis was determination of organic constituents on selected samples of aerosol particles.

Total Particulate Mass

The mass of aerosol particles was determined by weighing tared filters after sampling. All measurements were conducted using a calibrated microbalance and corrected for moisture content.

Trace Metal Analysis

Aerosol filter samples for trace metal analysis were prepared by strong acid digestion. Entire filters were placed into Teflon digestion vessels and 20 ml of ultrapure nitric acid (Optima, Fisher Scientific) was added. The acidified samples were digested in a CEM MSP1000 Microwave Oven by ramping to 100 psi over 15 min and then holding at 100 psi for 10 min. After cooling, the digestate was centrifuged to remove any remaining residue from the sample. The supernatant with sample digest was transferred to a 15 ml test tube prior to analysis.

Rainwater samples were prepared by adding ultrapure nitric acid, but microwave digestion was unnecessary. Microlayer and bulk seawater samples, however, were prepared using an iron-palladium (FePd) and ammonium pyrrolidine dithiocarbamate (APDC) technique to reduce seawater-related matrix interferences (Bloom and Crecilius 1984). The FePD and APDC chelate (extract) trace metals from the seawater matrix, thereby removing the interferences and concentrating the sample before analysis. The chelated precipitate is captured on a membrane filter, which is then digested using ultrapure nitric acid similar to the preparation procedures described for aerosol filters.

Inductively coupled plasma-mass spectroscopy (ICP-MS) was used to determine concentrations of inorganic constituents (aluminum, antimony, arsenic, beryllium, cadmium, chromium, copper, iron, lead, mercury, nickel, selenium, silver, and zinc) from sample digest solutions using a Hewlett Packard Model 4500 with Hewlett Packard Data Systems software and following protocols established by EPA Method 200.8 (EPA 1991). The internal standard solution included rhodium and thulium. Instrument blanks were run to identify sample carry-over. A spiked sample of known concentration was used as the laboratory control material.

Trace Organic Analysis

Samples for organic analysis were prepared using ultrapure dichloromethane and back-extracted to hexane using an Automated Solvent Exchange (ASE) technique following EPA Method SW846 3545 (EPA 1987). Extracted samples were cleaned-up using alumina-silica gel packed columns and elemental sulfur to reduce matrix-related interferences.

Gas chromatography-Mass Spectroscopy (CGMS) was used to determine concentrations in extracts of chlorinated hydrocarbon constituents (isomers and metabolites of DDT, 41 PCB congeners) and polynuclear aromatic hydrocarbon constituents (28 PAH). These techniques followed EPA methods SW-846 8081,8082, and 8270 with minor modifications (EPA 1987). A Hewlett-Packard 6890 GCMS equipped with a 30 m x 0.25 micron XLB column (J&W Scientific, Atlanta, GA) and Hewlett-Packard 7673 autosampler in full scan mode was used for these determinations.

TABLE 1. Maximum allowable reporting limits (RL) for target analytes by media type.

	Aerosol Particulates (Teflon Filters)[a]	Wet Deposition (Water)	Seasurface Microlayer (Seawater)
Trace Metals			
(ppm, mg/kg, mg/L)			
Cadmium	0.2	0.2	0.2
Chromium	16	16	16
Copper	7	7	7
Iron	500	500	500
Lead	9.3	9.3	9.3
Mercury	0.03	0.03	0.03
Nickel	4.2	4.2	4.2
Silver	0.2	0.2	0.2
Zinc	30	30	30
Polycyclic Aromatic Hydrocarbons (ppb, µg/kg)			
1-Methylnaphthalene	50	-	-
1-Methylphenanthrene	50	-	-
2,6-DimethylNaphthalene	50	-	-
2,3,5-Trimethylnaphthalene	50	-	-
2-Methylphenanthrene	50	-	-
Acenaphthene	50	-	-
Acenaphthylene	50	-	-
Anthracene	50	-	-
Benz[a]anthracene	50	-	-
Benzo[a]pyrene	50	-	-
Benzo[g,h,i]perylene	100	-	-
Benzo[k]fluoranthene	50	-	-
Biphenyl	50	-	-
Chrysene	50	-	-
Dibenz[a,h]anthracene	100	-	-
Fluoranthene	50	-	-
Fluorene	50	-	-
Methylanthracene	50	-	-
Indeno[1,2,3-c,d]pyrene	100	-	-
Naphthalene	50	-	-
Perylene	50	-	-
Phenanthrene	50	-	-
Pyrene	50	-	-

TABLE 1. continued

	Aerosol Particulates (Teflon Filters)[a]	Wet Deposition (Water)	Seasurface Microlayer (Seawater)
Polychlorinated Biphenyls			
(ppb, μg/kg)			
Congeners 18, 28, 37, 44, 49, 52, 66, 70, 74, 77, 81, 87, 99, 101, 105, 110, 114, 118, 119, 123, 126, 128, 138, 149, 151, 153, 156, 157, 158, 167, 168, 169, 170, 177, 180, 183, 187, 189, 194, 201, 206	7.5	-	-
Chlorinated Pesticides			
(ppb, μg/kg)			
o,p'-DDD	1	-	-
p,p'-DDD	1	-	-
o,p'-DDE	1	-	-
p,p'-DDE	1	-	-
o,p'-DDT	1	-	-
p,p'-DDT	1	-	-

[a] Aerosol concentrations (in mg/m^3) are calculated by multiplying the given concentration (mg/kg) by the total mass of the aerosol sample and volume of air sampled (kg/m^3).

TABLE 2. Laboratory Analysis Parameters

Parameter	Matrix	Units	Method	Storage and Hold Time
Microlayer Samples				
Trace metals	seawater	µg/l	Modified EPA 200.8	6 mos. acidified with HNO_3 @ 4C
Aerosol Samples				
Trace metals	Teflon Filters	ng/m^3	Modified EPA 200.8	6 mos @ -4C
Trace organics	Teflon Filters	ng/m^3	Modified SW846-8081 (Pesticides) SW846-Modified 8082 (PCB congeners) Modified SW846-8270 (PAHs)	2 mos @ -4C
Dry Deposition				
Trace metals	Teflon Filters	$ng/m^3/hr$	Modified EPA 200.8	6 mos @ -4C
Trace organics	Teflon Filters	$ng/m^3/hr$	Modified SW846-8081 (Pesticides) SW846-Modified 8082 (PCB congeners) SW846-8270 (PAHs)	2 mos @ -4C
Wet Deposition				
Trace metals	water	µg/l	Modified EPA 200.8	6 mos. acidified with HNO_3 @ 4C 28 d for mercury

QUALITY ASSURANCE AND QUALITY CONTROL

Quality assurance and quality control (QA/QC) was mandated during this project to ensure that the results were of sufficient quality to make assessments with known confidence. Therefore, data quality objectives (DQOs) were established to maintain quality assurance during sampling and laboratory analysis. These DQOs were benchmarks for achieving acceptable quality including precision, accuracy, representativeness, comparability, and completeness (Table 3). These DQOs, as well as other QAQC procedures and checks were identified in the project Quality Assurance Project Plan approved by the US EPA.

The DQOs were satisfactorily achieved for all of the parameters measured during this study (Table 3). Method blanks and calibration check samples consistently exceeded DQO expectations. For those trace metal calibration check samples that did not meet DQOs, less than 1% was attributable to the identified trace metals of interest (several more constituents are quantified than were required for this study). Accuracy of spiked samples and reference materials was exceedingly high. Precision of duplicate samples was within 100% of DQOs.

Sampling success was another critical component of QAQC during this project (Table 4). There was a total of 58 survey dates logged during the project. This resulted in 100% successful completion of microlayer and MOUDI sampling. There were only three storm events targeted for wet deposition sampling and eight were actually sampled. Due to the limited rainfall during this wet season, these rainstorms represented all but one event for the entire year. Only three aerosol sampling events were missed during the entire project. These were missed as a result of rain, which biases aerosol results, and not due to a QAQC deficiency. However, wet deposition data were collected during the missed rainy days. Six additional aerosol and two additional microlayer sampling events were conducted during November, 1998 to capture Santa Ana wind events.

Table 3. Quality assurance quality control limits and success at achieving the prescribed data quality objectives.

	Frequency	Control Limit	Total No.	No. Pass	Percent Pass
Method Blank					
	1/batch	< MDL for all analytes, or <5% of the measured sample concentration in samples for metals	495 Records 25 Batches	495	100
Calibration Check					
Metals	10%	± 10% true value for all metals	4679 Records	4066	86.9
PAH	start&end per batch	< 20% RPD for 80% of all analytes of interest	1287 Records	1200	93.2
CHC	start&end per batch	< 25% RPD for 80% of all analytes of interest	1364 Records	1310	96
Matrix Spike and Matrix Spike Duplicates					
Metals	10%	± 25% true value at <10x MDL,	172 Records	168	97.7
		± 20% true value at>10x MDL	0 records	-	-
		Dup analysis within 3σ of control limit	172 Records	172	100
PAH	1/batch	50 - 120% recovery for 80% of analytes at >10 MDL	2 Batches	2	100 Overall 86.6 % Recovery
CHC	1/batch	50 - 120% recovery for 80% of analytes at >10 MDL	2 Batches	2	100 Overall 85.3 % Recovery
Certified Reference Material or Laboratory Control Material					
Metals	1/batch	Within 3σ of control limit	25 Batches	25	100
PAH	1/batch	Within 3σ of control limit	2 Batches	2	100
CHC	1/batch	± 30% true value for 80% of all analytes of interest	2 Batches	2	100
Laboratory Duplicates					
Metals	1/batch	< 25% RPD	8 Batches	8	100
CHC	1/batch	< 30% RPD	1 Batch	1	100

Table 4. Sampling success during the project survey.

Sampling Dates	Aerosol Particulates (Teflon Filters)	Wet Deposition (Rain Water)	Seasurface Microlayer (Seawater)
October 20, 1998	X		
October 21, 1998			X
January 11, 1999			X
January 12, 1999	X		
January 13, 1999	X		
January 18, 1999	X		
January 24, 1999	X		
January 27, 1999		X	
January 30, 1999	X		
February 1, 1999		X	
February 5, 1999	X	X	
February 10, 1999		X	
February 18, 1999			X
February 20, 1999	X		
February 23, 1999	X		
February 25, 1999	X		
February 27, 1999	X		
March 1, 1999	X		
March 7, 1999	X		
March 10, 1999		X	
March 13, 1999	X		
March 16, 1999		X	
March 22, 1999		X	
March 26, 1999		X	
March 29, 1999	X		
July 5, 1999	X		
July 11, 1999	X		
July 12, 1999			X
July 13, 1999	X		
July 17, 1999	X		
July 23, 1999	X		
July 29, 1999	X		
July 30, 1999	X		
August 4, 1999	X		
August 10, 1999	X		
August 16, 1999	X		
August 18, 1999			X
August 20, 1999	X		
August 22, 1999	X		

Sampling Dates	Aerosol Particulates (Teflon Filters)	Wet Deposition (Rain Water)	Seasurface Microlayer (Seawater)
August 28, 1999	X		
September 4, 1999	X		
September 9, 1999	X		
September 15, 1999	X		
September 27, 1999	X		
October 3, 1999	X		
October 9, 1999	X		
October 18, 1999	X		
October 21, 1999			X
October 25, 1999	X		
October 27, 1999	X		
November 1, 1999	X		
November 2, 1999	X		
November 8, 1999	X		
November 9, 1999			X
November 12, 1999	X		
November 20, 1999	X		
November 26, 1999	X		
December 6, 1999	X		X

AERIAL DEPOSITION DATABASE STRUCTURE

A detailed information management system was designed to store all of the data types collected during this project. This information was managed using a relational database structure, a design that is most efficient for retrieving large volumes of data, particularly with a data set with many different types as encountered in this project. The design is compatible with several other environmental monitoring programs in Santa Monica Bay enabling easy export and retrieval of data into and out this project by others (SCBPP 1994).

The database structure for this project revolves around four basic types of data (Figure 2). These include information about stations (tblStations), information about sampling events (tblStationOccupation), information about each sample (tblFieldSamples), and information about sample results (tblChemistry). Each of the tables are linked through a single relational field called StationID. The relational field enables data users to query data from table to table. In each of the tables there are unique fields (i.e. results field for chemistry table) and there are restricted fields (i.e. yes/no, constrained lists, etc.). We have included ancillary tables, termed look-up lists (lulist_xx) that contain the constrained lists used for restricted fields.

Figure 2. Information management relational database design. Lines represent relational fields among data tables. Asterisks (*) represent look up lists for constrained fields.

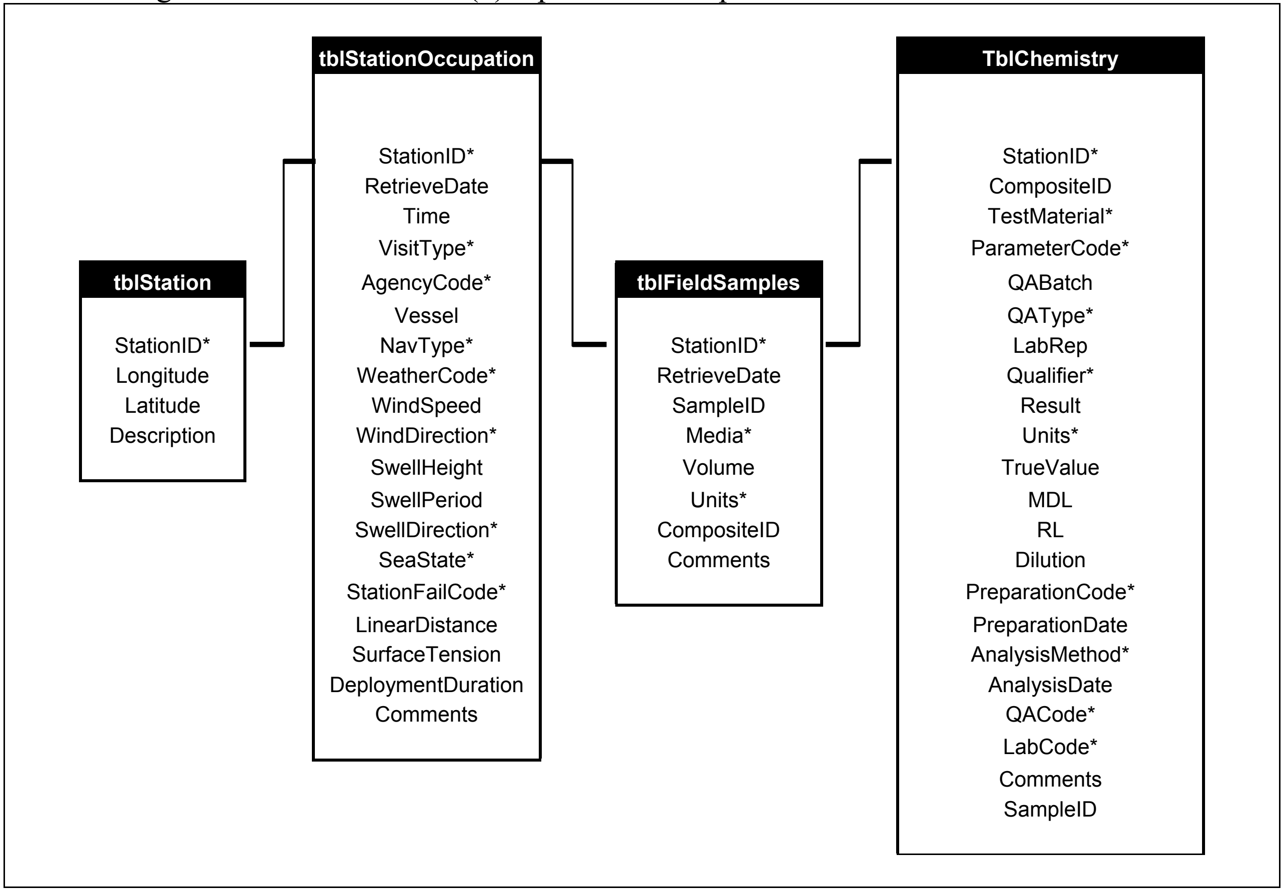

Station Table

The station table was central to data relations in the aerial deposition database (Table 5). Each record represented a description of a geographical location including a label, and latitude and longitude data reported in North American Datum (NAD) 83. A validation restriction in data type (y = yes, n = no) was placed on some of the fields to represent that data must be entered in this field.

Table 5. Station Table Structure.

Field Name	**Data Type** Required (Y/N)	**Description**
StationID	Text (Y)	A geographic location label from luList_03_Stations
Longitude	Date/Time (Y)	Decimal Degrees of Longitude (NAD 83)
Latitude	Date/Time (Y)	Decimal Degrees of Latitude (NAD 83)
Description	Text (Y)	The type of sample (Aerosol, Microlayer)

Station Occupation Table

The station occupation table was created to describe conditions during occupation of a station for sampling (Table 6). Each record contained a characterization of the station at the time of sampling in terms of the weather, sea state, sample type, vessel name, agency, and quality of the global positioning system (GPS) signal at the time of sampling. A record can also contain information about station sampling failures where the station was abandoned due to one of the acceptable reasons for station abandonment. The NavType field allowed the collecting agency to record the loss of the differential GPS signal. Additional comments may be included with up to 80 characters. Some of the fields may not be relevant to aerosol and wet sampling and need not be completed (i.e. LinearDistance, SurfaceTension and DeploymentDuration). The value (-99) is entered into the corresponding number fields, while NR is entered into the text fields to represent data that was not recorded.

Table 6. Station occupation table structure.

Field Name	**Data Type** Required (Y/N)	**Description**
StationID	Text (Y)	A geographic location label from luList_03_Stations
RetrieveDate	Date/Time (Y)	The date the sample was collected dd/mmm/yyyy
Time	Date/Time (Y)	The time the sample was collected expressed in 24 hour time
VisitType	Text (Y)	The type of sample (Aerosol, Microlayer). luList_VisitTypeCodes
AgencyCode	Text (Y)	A two letter agency code from luList_01_AgencyCodes
Vessel	Text (Y)	The Vessel Name
NavType	Text (Y)	DGPS for differential / GPS for non-differential
WeatherCode	Text (Y)	Predetermined weather codes from luList_08_Weather
WindSpeed	Number (Y)	Meters/second (-99) if not taken
WindDirection	Text (Y)	N,NE,E,SE,S,SW,W,NW NR = Not recorded
SwellHeight	Number (Y)	Meters (-99) if not taken
SwellPeriod	Number (Y)	Seconds (-99) if not taken
SwellDirection	Text (Y)	N,NE,E,SE,S,SW,W,NW NR = Not recorded
SeaState	Text (Y)	Description from calm, choppy, or rough NR = Not recorded
StationFailCode	Text (N)	Acceptable failure codes from luList_09_FailCodes
LinearDistance	Number (Y)	Microlayer only (-99) data still needs to be generated
SurfaceTension	Number (Y)	Dynes/cm microlayer only (-99) data still needs to be generated
DeploymentDuration	Number (Y)	Hours (-99) data still needs to be generated
Comments	Text (N)	Additional remarks

Field Samples Table

The field samples table was created to describe the samples that were collected at each station (Table 7). Each record contains a characterization of the sample collected in terms of the date, stationID, media type, volume, compositeID, and sample analysis at the time of sampling.

Samples were labeled by the following regime **19990111UCLAWETMN** (Figure 3). The first four digits correspond to the year the sample was taken in Y2K compliant format. The next four digits (5-8) equal the date when the sample was taken. In this case, January 11. The next four digits (9-12) are the stationID. Digits 13-16 represent the media type that was taken at that site (i.e. wet). The remaining two digits represent the sample analysis (i.e. metals) and the sample type (i.e. native) respectively.

Table 7. Field samples table structure.

Field Name	**Data Type** Required (Y/N)	**Description**
StationID	Text (Y)	A geographic location label from luList_03_Stations
RetrieveDate	Date/Time (Y)	The date the sample was collected dd/mmm/yyyy
SampleID	Text (Y)	Sample identification
Media	Text (Y)	The type of sample from luList_Media
Volume	Number (Y)	Air mass volume or amount of sample taken
Units	Text (Y)	ng, L, cubic meters
CompositeID	Text (N)	Composite01, Composite02 or Composite03
Comments	Text (N)	Additional remarks

Figure 3. Labeling scheme.

19990111UCLAWETMN

Date	StationID	Media Type	Analysis	Sample Type
11 Jan 1999	UCLA	WET Deposition	Metals	Native

Analysis	**Sample Type**
Metals	**B**lank
Nitrogen	**D**uplicate
Organics	**N**ative (Original)
	Rep

In this study, 362 samples were collected (Table 9). Two hundred and ninety-eight were analyzed for trace metals (i.e. cadmium, chromium, copper, lead, nickel, and zinc) and 59 were analyzed for organics (i.e. DDTs and PCBs). The remaining five samples were analyzed for nutrients (ammonia, nitrate, nitrite, phosphorous, and silicon). Composites were made for organics analysis on the following samples: all wet organic blanks (Composite01); all wet organic native samples (Composite02); and all dry deposition organic blanks (Composite03).

Table 8. Summary of sample inventory by media type.

	No. of Samples		
Media Type	**Trace Metals**	**Organics**	**Total**
DBL	28	--	28
DCO	31	--	31
DFI	31	--	31
SubTotal	90	--	90
MIC	73	--	73
BLK	8	--	8
BUL	8	--	8
SubTotal	89	--	89
DRY	9	7	16
DRY BLW	13	--	13
DRYMB	11	--	11
DRYOB	--	5	5
SubTotal	33	12	45
M01	5	2	7
M02	5	2	7
M03	5	2	7
M04	5	2	7
M05	5	2	7
M06	5	2	7
M07	5	2	7
M08	5	2	7
M09	5	2	7
M10	5	2	7
M11	5	2	7
MF	4	2	6
MMB	6	--	6
MOB	--	3	3
SubTotal	65	27	92
WET	10	9	19
WET BLW	11	11	22
SubTotal	21	20	41
Total	298	59	357
Nutrients			5

Chemistry Table

The chemistry table contained all of the laboratory result data from trace metals, organics and nutrient analysis (Table 8). Each record represented a result from a specific analysis for a particular parameter at a single station. Some of the fields may not need to be completed (CompositeID, Qualifier, TrueValue, and QACode). The "units" field is important because different compounds and analysis types produce values with various units associated with the method or result. To distinguish the dates of sample processing, preparation date and analysis date are included. The field QAType is used to distinguish QA and blank data from actual sample results.

Table 8. Chemistry table structure.

Field Name	**Data Type** Required (Y/N)	**Description**
StationID	Text (Y)	A geographic location label from luList_03_Stations
CompositeID	Text (N)	From the fish composite table
TestMaterial	Text (Y)	The material choices from luList_TestMaterial
ParameterCode	Text (Y)	The measured parameter from luList_18_ChemicalParameterCodes
QABatch	Text (Y)	The code for all of the samples processed in the same batch
QAType	Text (Y)	The type of result from luList_04_SampleTypes
LabRep	Number (Y)	Count
Qualifier	Text (N)	Any necessary qualifier from luList_13_QualifierCodes
Result	Number (Y)	The numerical result expressed in dry wt.
Units	Text (Y)	Units for result
TrueValue	Number (N)	QA samples only
MDL	Number (Y)	Method detection limit
RL	Number (Y)	Reporting limit
Dilution	Number (Y)	Dilution factor for composite
PreparationCode	Text (Y)	Preparation code from luList_34_ChemistryPreparationCodes
PreparationDate	Date/Time (Y)	the date the sample was extracted expressed as dd/mmm/yyyy
AnalysisMethod	Text (Y)	The analysis method from luList_33_AnalysisMethodCodes
AnalysisDate	Date/Time (Y)	The date the sample was processed by the instrument expressed as dd/mmm/yyyy
QACode	Text (N)	Any necessary qualifier from luList_13_QualiferCodes
LabCode	Text (Y)	The two digit agency code from luList_01_AgencyCodes
Comments	Text (N)	Additional remarks

FUTURE ACTIVITIES

There are two main activities that will occur following data reporting. The first activity is atmospheric transport and deposition modeling for making atmospheric deposition assessments. The second activity is additional sampling and analysis based upon the findings and data gaps identified during this study.

Atmospheric modeling is a tool that will aid in the assessment of atmospheric inputs. The modeling enables scientists to integrate data collected at various individual locations and extrapolate them to the entire region including Santa Monica Bay, its watershed, or the Los Angeles airshed. The modeling is also fundamental for making connections among sources and fates. The transport modeling will help to evaluate if sources outside the watershed are contributing to deposition in Santa Monica Bay. This activity will take advantage of the atmospheric transport and deposition model developed at UCLA. The UCLA surface meteorology and ozone generation (SMOG) model has modules for meteorology, pollutant sources and dispersion, photochemistry and aerosol microphysics, and radiative processes (Lu *et al* 1994, 1995). This model has been calibrated and verified using the Southern California Air Quality Study (SCAQ) (Lu *et al* 1996). In addition, the model will be able to incorporate newer data generated by the AQMD including its most recent inventory of toxic air emissions. Atmospheric modeling will occur over the next five months.

There were at least two main gaps in the present study that need to be addressed. The first data gap is measuring air concentrations over water surfaces. There are no historical data for aerosol concentrations over Santa Monica Bay and none have been collected during the present study. The lack of data for over-water measurements is a reflection of the logistical difficulty in obtaining these types of samples. A second data gap in the present study is the lack of trace organic concentrations, especially in the gaseous phase. Once again, these types of data are rare in the region because collecting this type of information is expensive and technically challenging. To address these data needs, a dedicated study has been proposed and accepted by the US EPA Great Waters Grant Program. Over-water measurements of aerosol and gaseous phase organic and inorganic constituents will be sampled in the next part of our study. These data will be extremely beneficial for further model calibration and validation, as well as providing the necessary data for making assessments of direct air-water exchange rates. Over-water sampling is expected to occur over the next seven months.

REFERENCES

Arey, J. R. Atkinson, B. Zielinska, and P. McElroy, 1989. Diurnal concentrations of volatile polycyclic aromatic hydrocarbons and nitroarenes during a photochemical air pollution episode in Glendora, CA. *Environmental Science and Technology* 23: 321-327

Bloom, N.S. and B.A. Crecelius. 1984. Determination of silver in seawater by coprecipitation with cobalt pyrrolidine dithiocarbamate and Zeeman graphite-furnace atomic absorption spectrometry. *Analytica Chimica Acta*. 156:139-145.

Clarke, J., E. Edgerton, and B. Martin. 1997. Dry deposition calculations for the Clean Air Status and Network. *Atmospheric Environment* 21:3667-3678.

Cross, J., J. Hardy, J. Hose, G. Hershelman, L. Antrium, R. Gossett, and E. Crecilius. 1987. Contaminant concentrations and toxicity of sea-surface microlayer near Los Angeles, California. *Marine Environmental Research* 23:307-323.

Dorsey, J., C. Phillips, A. Dalkey, and G. Deets, 1995. Changes in assemblages of infaunal organisms around wastewater outfalls in Santa Monica Bay, CA. *Bulletin Southern California Academy of Sciences* 94: 46 - 64.

Hillery, B., M. Simcik, I. Basu, R. Hoff, W. Strachan, D. Burniston, C. Chan, K. Brice, C. Sweet, and R. Hites. 1998. Atmospheric deposition of toxic pollutants to the Great Lakes as measured by the Integrated Atmospheric Deposition Network. *Environmental Science and Technology* 32:2216 - 2221.

Kawamura, K. and I. Kaplan. 1986. Biogenic and anthropogenic organic compounds in rain and snow samples collected in southern California. *Atmospheric Environment* 20:115-124

Lu, R., R. Turco, and M. Jacobsen. 1994. Air pollution transport in a coastal environment: Part I: two-dimensional simulation of sea-breeze and mountain effects. *Journal of Atmospheric Science* 51:2285-2308.

Lu, R., R. Turco, and M. Jacobsen. 1995. Air pollution transport in a coastal environment: Part II: three-dimensional simulation over the Los Angeles region. *Journal of Geophysical Research* 29:1499-1518.

Lu, R. and R. Turco. 1996. Ozone distributions over the Los Angeles Basin: Three dimensional simulations with the SMOG Model. *Atmospheric Environment* 30: 4155-4176

NADP. 1997. National Atmospheric Deposition Program/National Trends Network wet deposition in the United States 1996. Illinois State Water Survey, Champaign, IL.

Offenberg, J. and J. Baker, 1997. Polychlorinated biphenyls in Chicago precipitation: Enhanced wet deposition to near-shore Lake Michigan. *Environmental Science and Technology* 31: 1534 - 1538.

Prastinis, S. 1994. Motor vehicle contributions to fine carbonaceous aerosol in Los Angeles. *Aerosol Science and Technology* 21:360-366.

Raco-Rands, V., 1997. Characteristics of effluents from large municipal wastewater facilities in 1995. Pp. 3 - 16 *In*: Weisberg, S.(ed.), Southern California Coastal Water Research Project Annual Report 1995. Southern California Coastal Water Research Project, Westminster, CA

SMBRP, 1998. State of the Bay Report. Santa Monica Bay Restoration Project, Monterey Park, CA.

SCBPP, 1994. Information Management Plan for the Southern California Bight Pilot Project. Southern California Coastal Water Research Project, Westminster, CA

Stull, J., 1995. Two decades of marine biological monitoring, Palos Verdes, CA. *Bulletin Southern California Academy of Sciences* 94: 21 - 45.

US EPA. 1983. Chemical methods for the examination of water and wastes. U.S. Environmental Protection Agency, Environmental Monitoring and Support Laboratory, Cincinnati, OH. EPA-600/4-79-020.

US EPA. 1991. Methods for the determination of metals in environmental samples. U.S. Environmental Protection Agency, Office of Research and Development, Washington, D.C. EPA/600/4-91/010.

US EPA. 1997. National air pollutant emission trends, 1990-1996. U.S. Environmental Protection agency, Office of Air Planning and Research, Research Triangle Park, NC. EPA-454/R-97-011

Young, D., McDermott, and T. Heesen, 1976. Aerial fallout of DDT in southern California. *Bulletin of Environmental Contamination and Toxicology* 16: 604 - 611

Young, D. and T. Chan, 1977. Fire fallout of metals off California. *Marine Pollution Bulletin* 8: 109 - 112

Zufall, M., C. Davidson, P. Gaffrey, and J. Ondov. 1998. Airborne concentrations and dry deposition fluxes of particulate species to surrogate surfaces deployed in southern Lake Michigan. *Environmental Science and Technology* 32: 1623-1628.

Zufall, M. and C. Davidson. 1997. Dry deposition of particles to water surfaces. Pp. 1-16 *In*: Baker, J. (ed.) Atmospheric deposition of contaminants to the Great Lakes and coastal waters. SETAC Press, Pensacola, FL.

APPENDIX A

• • • • •

Look Up Lists

Look-Up Lists

The following lookup lists are in alphabetical order and correspond to the constrained fields cited in the atmospheric deposition database table structures (Tables 5-9).

luList_03_Stations.

StationID	Longitude	Latitude	Description
0000			Laboratory Blank
M210	-118.421	33.8782	Microlayer 210
M220	-118.468	33.8539	Microlayer 220
M230	-118.541	33.8158	Microlayer 230
M310	-118.453	33.9365	Microlayer 310
M320	-118.504	33.919	Microlayer 320
M330	-118.586	33.8928	Microlayer 330
M410	-118.509	34.0059	Microlayer 410
M420	-118.558	33.9873	Microlayer 420
M430	-118.637	33.9565	Microlayer 430
UCLA	-118.45	34.0666	On top of Buelter Hall at UCLA

luList_4_SampleType

Sample Code	Sample Type
B	Laboratory Blank
BDUP	Blank Duplicate
BS	Blank Spike
Composite01	Composited Wet Rinse Water
Composite02	Composited DI Water
Composite03	Composited Rain Water
DUP	Duplicate
M	Matrix spike and matrix spike duplicate
QA	
R	Laboratory Control Material (LCM) or Certified Reference Material (CRM)

LuList_8_Weather Codes

WeatherCode
Blowing Sand
Clear
Continuous layers of Clouds
Drizzle
Fog
NR
Overcast
Partly Cloudy
Rain
Thunderstorm

luList_9_FailureCodes

FailCode	FailureReason
A	Canted
B	Washed
C	Poor Closure
D	Disturbed Surface
E	< 5 cm pentreation
F	>5 & < 8 cm penetration
G	Fouled Net
H	Torn Net
I	No contact w/ bottom
J	Improper distance/Time
K	Abandoned
L	Rocky Bottom
M	Kelp Bed
N	Obstructions
None	No Failure
O	<3m (bay)
P	<6M (Ocean)

FailCode	FailureReason
Q	> 200m
R	No Access
S	Lost Sample
T	Abandoned before sampling
U	Equipment Malfunction
V	Unfavorable Weather

luList_13_QualifierCodes

Qualifier	Description
<	less than
>	greater than
A	Count base on calculation of Aliquot
NA	Not Analyzed
ND	Not Detected
NS	Not Sampled
P	Present, not counted

luList_18_ChemicalParameterList

ODES CODE	COMMON NAME
1-METHNAP	1-Methylnapthalene
1-MPHENAH	1-Methylphenanthrene
167-3MNAP	1,6,7-Trimethylnaphthalene
2-METHNAP	2-Methylnapthalene
236-3MNAP	2,3,6-Trimethylnaphthalene
26-2MNAP	2,6-Dimethylnaphthalene
2BANTH	Dibenz[a,h]anthracene
ACENAPE	Acenaphthene
ACENAPTYLE	Acenaphthylene
Aldrin	Aldrin

ODES CODE	COMMON NAME
ALUMINUM	Aluminum
ANTHRACENE	Anthracene
ANTIMONY	Antimony
ARSENIC	Arsenic
BAA	Benz[a]anthracene
BAP	Benzo[a]pyrene
BARIUM	Barium
BBF	Benzo[b]fluoranthene
BEP	Benzo[e]pyrene
BERYLLIUM	Beryllium
BGHIP	Benzo[g,h,i]perylene
BHC-alpha	BHC-alpha
BHC-beta	BHC-beta
BHC-delta	BHC-delta
BHC-gamma	BHC-gamma
BIPHENYL	Biphenyl
BKF	Benzo[k]fluoranthene
C10LAB-2	2-phenyldecane
C10LAB-3	3-phenyldecane
C10LAB-4	4-phenyldecane
C10LAB-5	5-phenyldecane
C11LAB-2	2-phenylundecane
C11LAB-3	3-phenylundecane
C11LAB-4	4-phenylundecane
C11LAB-5	5-phenylundecane
C11LAB-6	6-phenylundecane
C12LAB-2	2-phenyldodecane
C12LAB-3	3-phenyldodecane
C12LAB-4	4-phenyldodecane
C12LAB-5	5-phenyldodecane
C12LAB-6	6-phenyldodecane
C13LAB-2	2-phenyltridecane
C13LAB-3	3-phenyltridecane
C13LAB-4	4-phenyltridecane
C13LAB-5	5-phenyltridecane
C13LAB-7/6	7&6-phenyltridecane
C14LAB-2	2-phenyltetradecane

ODES CODE	COMMON NAME
C14LAB-3	3-phenyltetradecane
C14LAB-4	4-phenyltetradecane
C14LAB-5	5-phenyltetradecane
C14LAB-6	6-phenyltetradecane
C14LAB-7	7-phenyltetradecane
CADMIUM	Cadmium
CHLORDANE-a	aChlordane
CHLORDANE-g	gChlordane
CHROMIUM-T	Chromium
CHRYSENE	Chrysene
COBALT	Cobalt
COPPER	Copper
d10-Acenaphthene	
d10-Phenanthrene	
d12-Chrysene	
d12-Perylene	
d8-Naphthalene	
Dieldrin	
Endosulfan Sulfate	
Endosulfan-I	
Endosulfan-II	
Endrin	
Endrin Aldehyde	
FLUORANTHN	Fluoranthene
FLUORENE	Fluorene
Heptachlor	
Heptachlor Epoxide	
ICDP	Indeno(1,2,3-c,d)pyrene
IRON	Iron
LEAD	Lead
LIPID	Lipid
MANGANESE	Manganese
MERCURY	Mercury
Methoxychlor	Methoxychlor
Mirex	Mirex
MOLYBDENUM	Molybdenum
NAPTHALENE	Naphthalene

ODES CODE	COMMON NAME
NICKEL	Nickel
Nitrate	
Nitrite	
OP DDD	2,4'-DDD
OP DDE	2,4'-DDE
OP DDT	2,4'-DDT
PCB101	PCB 101
PCB105	PCB 105
PCB110	PCB 110
PCB114	PCB 114
PCB118	PCB 118
PCB119	PCB 119
PCB123	PCB 123
PCB126	PCB 126
PCB128	PCB 128
PCB138	PCB 138
PCB149	PCB 149
PCB151	PCB 151
PCB153	PCB 153
PCB156	PCB 156
PCB157	PCB 157
PCB158	PCB 158
PCB167	PCB 167
PCB168	PCB 168
PCB169	PCB 169
PCB170	PCB 170
PCB177	PCB 177
PCB18	PCB 18
PCB180	PCB 180
PCB183	PCB 183
PCB187	PCB 187
PCB189	PCB 189
PCB194	PCB 194
PCB200	PCB200
PCB201	PCB 201
PCB206	PCB 206
PCB209	PCB209

ODES CODE	COMMON NAME
PCB28	PCB 28
PCB37	PCB 37
PCB44	PCB 44
PCB49	PCB 49
PCB52	PCB 52
PCB65	PCB65
PCB66	PCB 66
PCB70	PCB 70
PCB74	PCB 74
PCB77	PCB 77
PCB81	PCB 81
PCB87	PCB 87
PCB99	PCB 99
PERYLENE	Perylene
PHENANTHRN	Phenanthrene
PHOSPHORUS	Phosphorus
PP DDD	4,4'-DDD
PP DDE	4,4'-DDE
PP DDT	4,4'-DDT
PYRENE	Pyrene
SELENIUM	Selenium
Silican	
SILVER	Silver
SOLIDS, TOTAL	
TCMX	TCMX
THALLIUM	Thallium
TIN	Tin
TITANIUM	Titanium
TOC	TOC
Total Detectable DDTs	Total Detectable DDTs
Total Detectable PAHs	Total Detectable PAHs
Total Detectable PCBs	Total Detectable PCBs
Toxaphene	Toxaphene
VANADIUM	Vanadium
ZINC	Zinc

luList_19_QATypeCodes

QACode	QADescription
A	Acceptable Data
BMDL	Below MDL
BRL	Below Reporting Level
D	Lab Contamination
E	Estimated Value
FR	Field Replicate
MS	Matrix Spike
MSD	Matrix Spike Duplicate
Q	Questionable Data
RLS	Reporting Level Spike
SRM1941	SRM 1941

luList_33_AnalysisMethodCodes

MethodCode	Method
160.3M	Columbia Analytical Code
CHN	EA1108 CHN Elemental Analyzer
CVAA	Cold Vapor Atomic Absorption Analysis
FAA	Flame Atomic Absorption Spectrometer
FIAS	Flow Injection Analysis System
GCECD	CG/ECD
GCMS	GS/MS
GFAA	Graphite Furnace Atomic Absorption Analysis
HAA	Hydride Atomic Absorption Analysis
ICPAES	Inductively Coupled Plasma Atomic Emmision Spectrometer
ICPEAS	
ICPMS	Inductively Coupled Plasma Mass Spectrometer
IONGCMS	Ion Trap GC/MS
Missing	

luList_34_ChemistryPreparationCodes

PrepCode	Preparation Method
ASE	Accelerated Solvent Extraction
EPA 7471A	
EPA245.5	Mercury in Sediment (Cold Vapor with Permanganate Digestion)
EPA3050A	Strong Acid Hot Plate Method (EPA3050A)
EPA3050B	Strong Acid Hot Plate or Microwave Method (EPA3050B)
EPA3051	Strong Acid Microwave Method (EPA 3051)
EPA3055	Strong Acid Hot Plate Method (EPA 3055)
EPA3500	
FePD	
MASE	Microwave Assisted Solvent Extraction
Missing	Missing Value
ROLLER	Roller Table Extraction
SFE	Supercritical Fluid Extraction
SONIC	Ultrasonic Extraction
SOXHLET	Soxhlet Solvent Extraction

luList_MediaType

MediaType	MediaDescription
A	A blank composite
B	Blank DRY
BLK	Microlayer Blank DI Water
BUL	Bulk Seawater
C	Wet Composite
CRG	Laboratory Blank
DBL	Dichotomous Blank
DCO	Dichotomous Coarse
DFI	Dichotomous Fine
DRY	Dry Depostion Plate
DRY BLW	Blank DI Water DRY
DRYMB	Dry Filter Metal Blank
DRYOB	Dry Filter Organic Blank
M01	Moudi Filter Number 1
M02	Moudi Filter Number 2
M03	Moudi Filter Number 3

MediaType	MediaDescription
M04	Moudi Filter Number 4
M05	Moudi Filter Number 5
M06	Moudi Filter Number 6
M07	Moudi Filter Number 7
M08	Moudi Filter Number 8
M09	Moudi Filter Number 9
M10	Moudi Filter Number 10
M11	Moudi Filter Number 11
MF	Moudi After Filter Number 12
MIC	Microlayer
MMB	Moudi Filter Metals Blank
MOB	Moudi Filter Organics Blank
RB	Blank Rain Water
WET	Wet Deposition Bucket
WET BLW	Blank DI Water WET
WETN	Nutrients (Rain Water)

luList_TestMaterialType

Type
DI Water
Dichotomous Filtered Air
Dry Filtered Air
Microlayer
Moudi Filtered Air
Rain Water
Sea Water
Sediment
Tissue

lulist_VisitTypeCodes

Type	Description
AEROSOL	Moudi or Dichotomous
DRY	Dry Depostion
MIC	Microlayer
WET	Wet Depostion

APPENDIX II

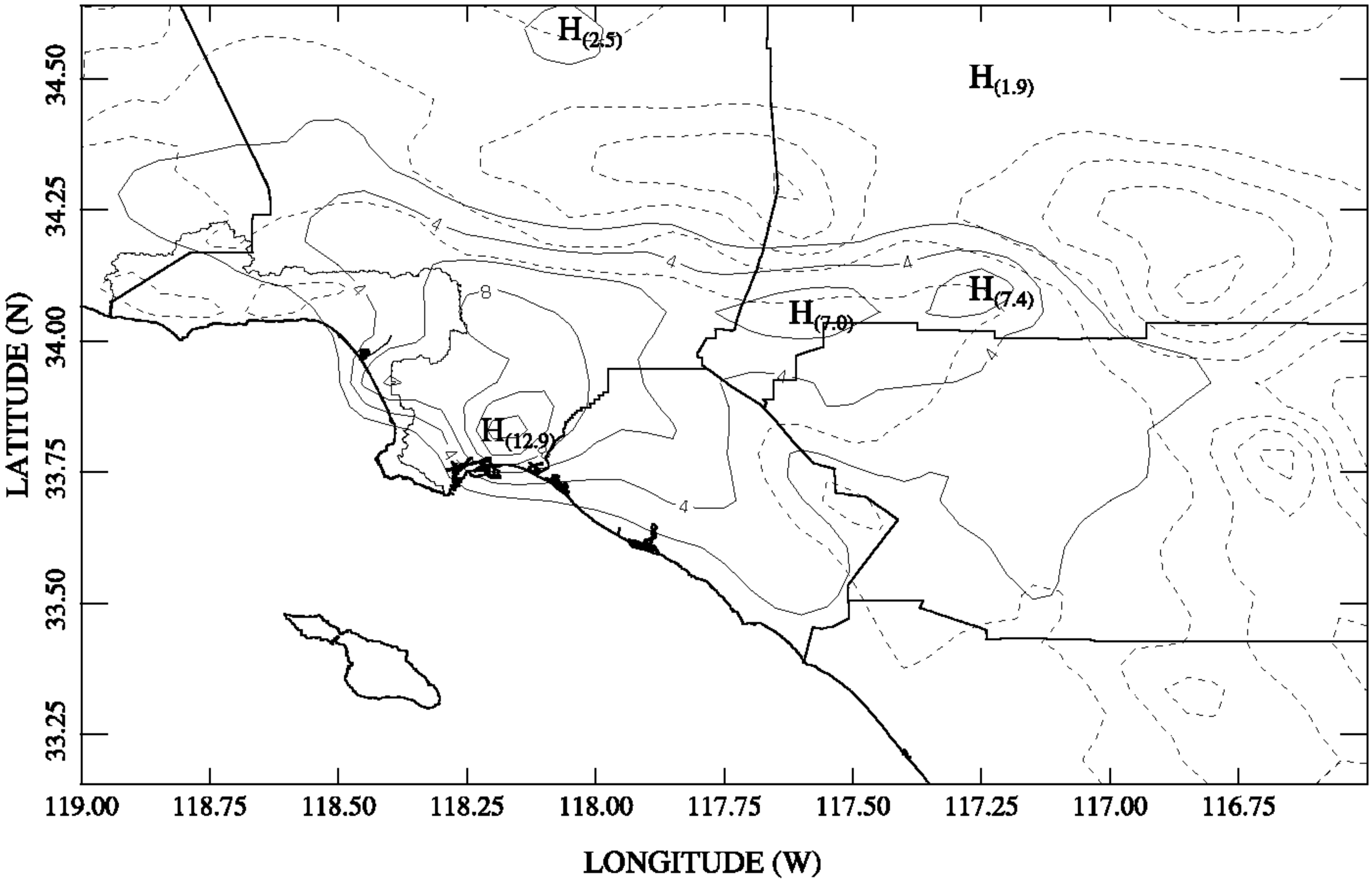

Figure A1: 24-hour average concentration (ng/m^3) of the total mass of Cr for the summer case; the contour interval is 2.0 ng/m^3; the area average concentration is 1.55 ng/m^3.

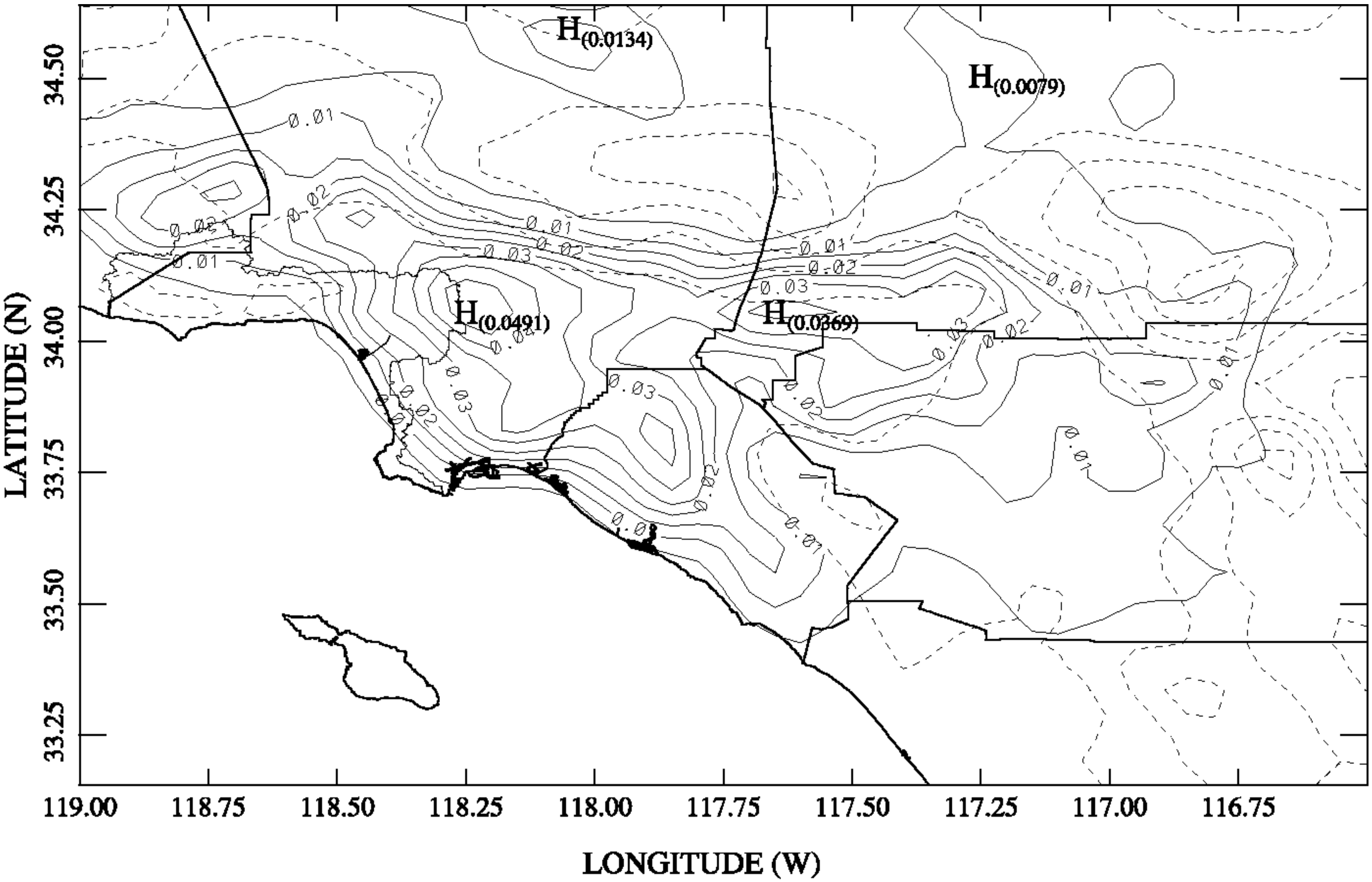

Figure A2: 24-hour average deposition rate (g/ha-day) of the total mass of Cr for the summer case; the contour interval is 5.00×10^{-3} g/ha-day; the total deposition on the domain is 33.6 kg/day.

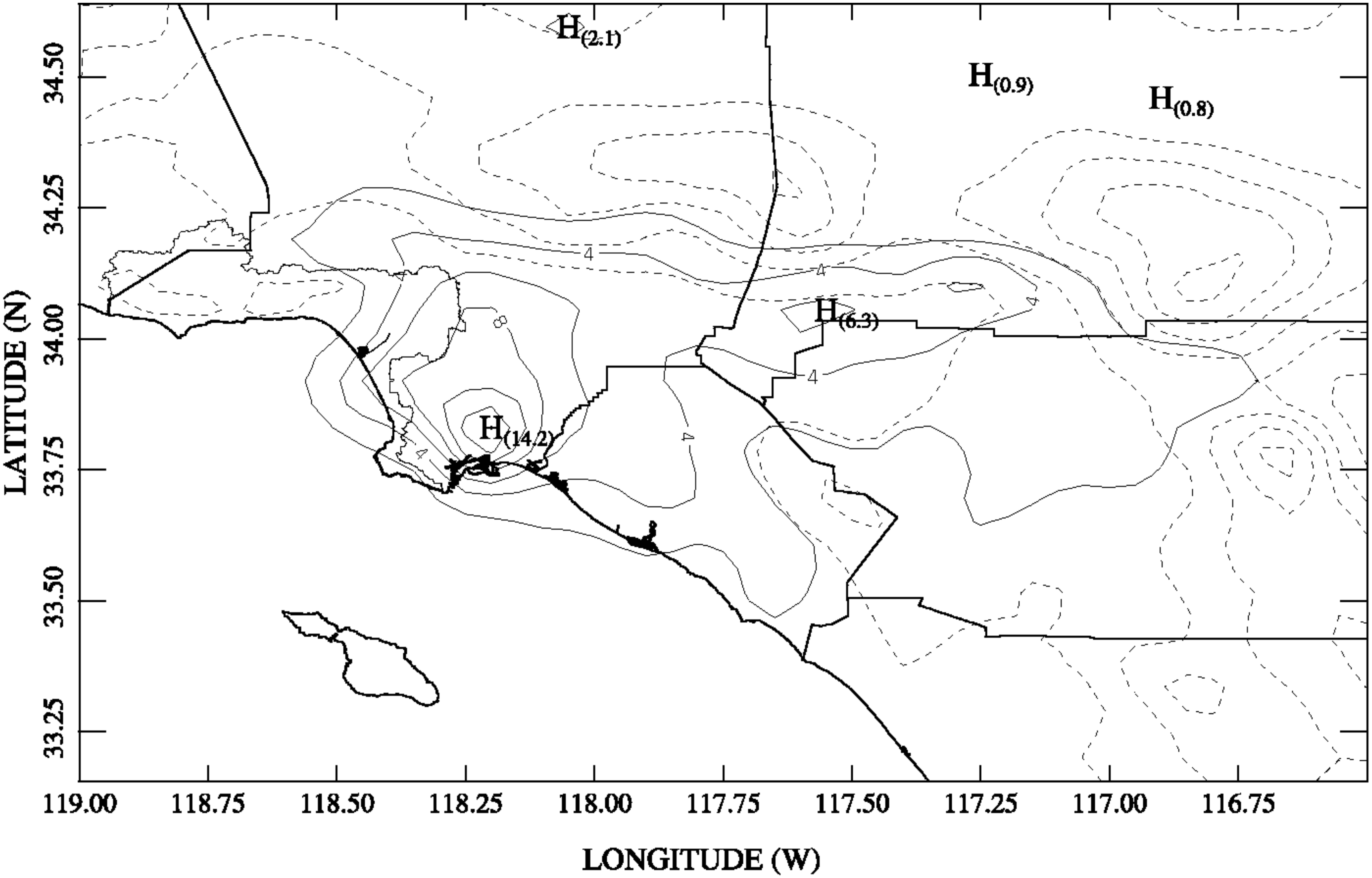

Figure A3: 24-hour average concentration (ng/m^3) of the total mass of Cr for the winter case; the contour interval is 2.0 ng/m^3; the area average concentration is 1.44 ng/m^3.

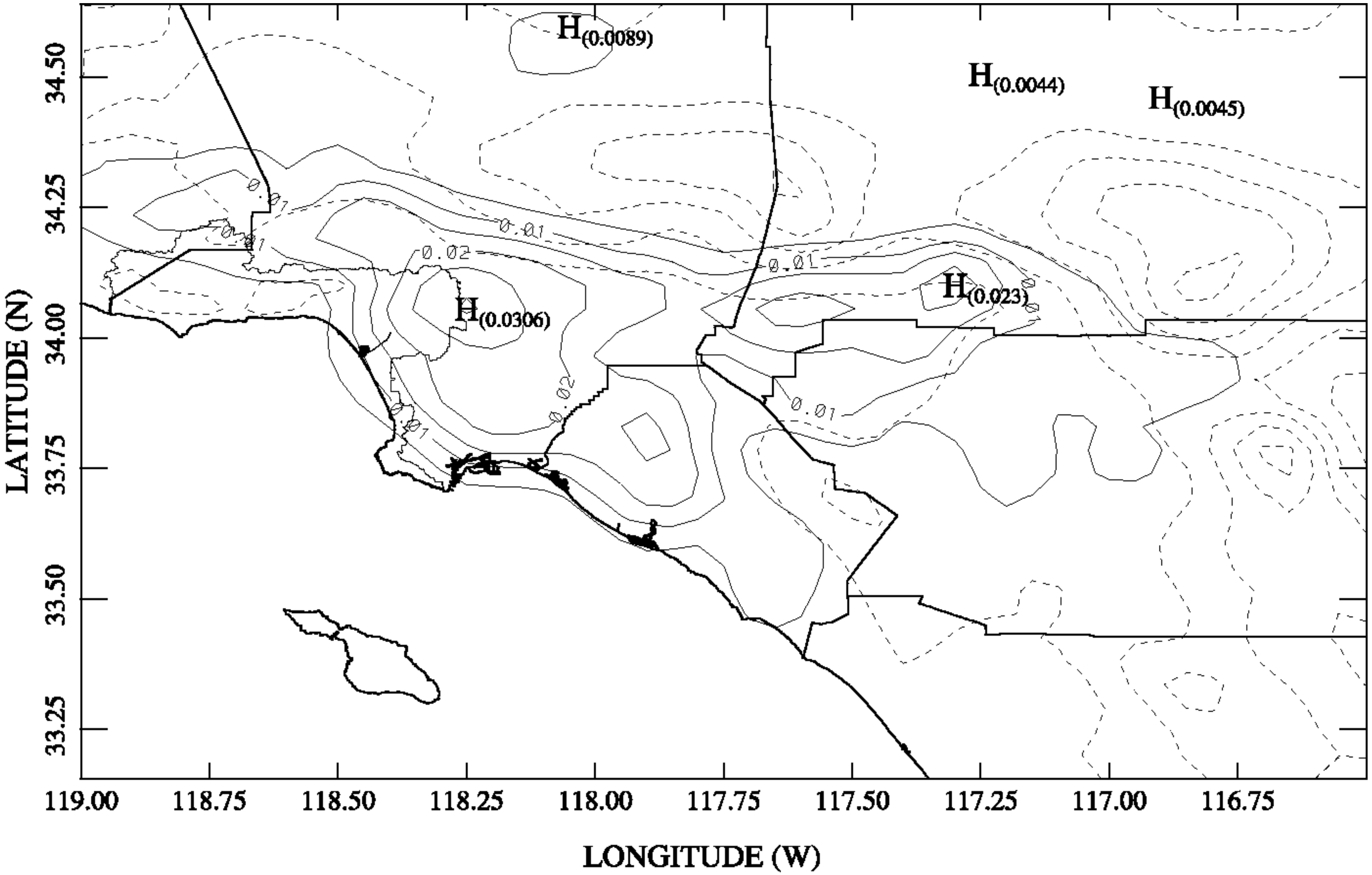

Figure A4: 24-hour average deposition rate (g/ha-day) of the total mass of Cr for the winter case; the contour interval is 5.00×10^{-3} g/ha-day; the total deposition on the domain is 19.2 kg/day.

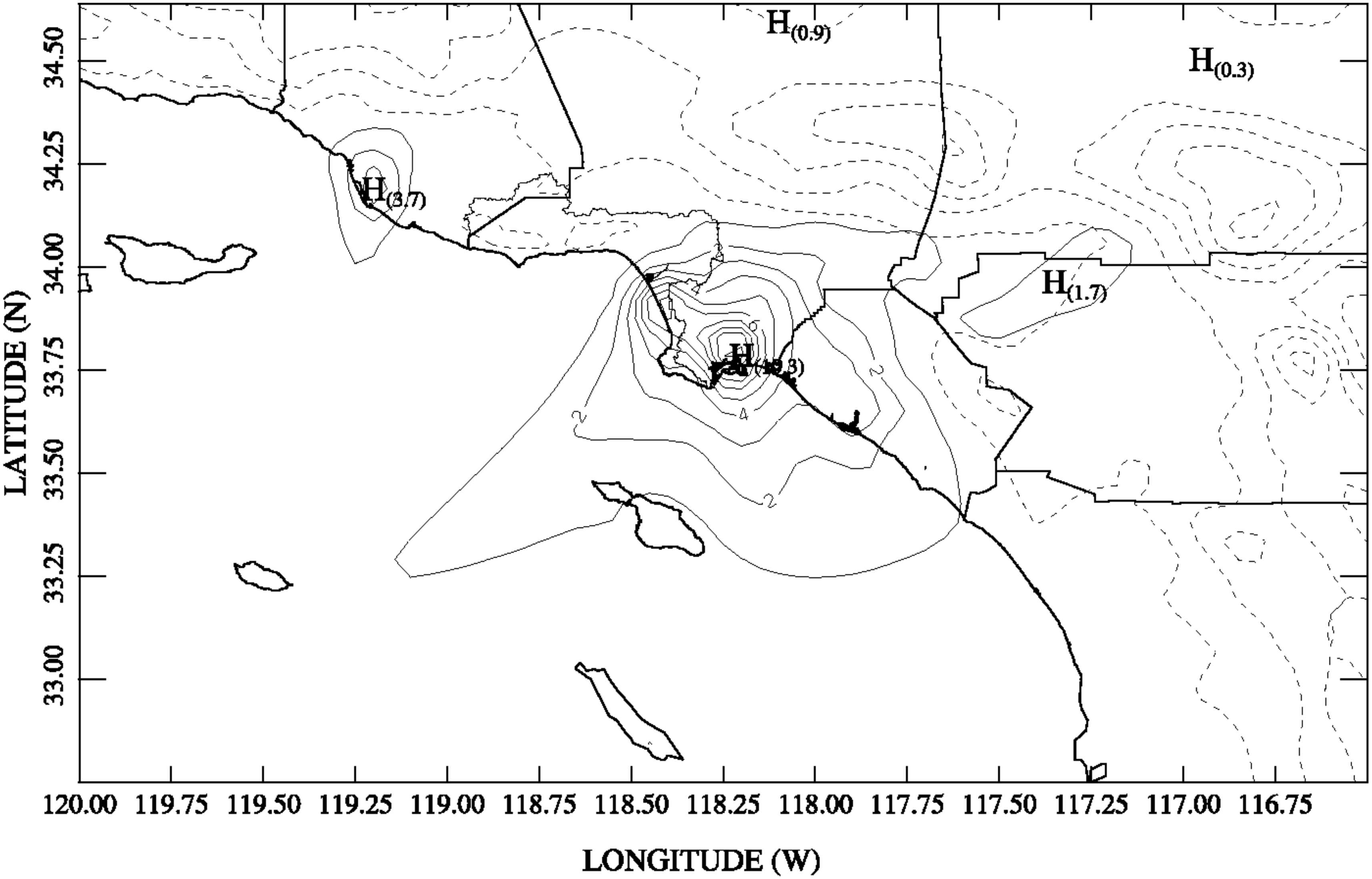

Figure A5: 24-hour average concentration (ng/m^3) of the total mass of Cr for the Santa Ana case; the contour interval is 1.0 ng/m^3; the area average concentration is 0.56 ng/m^3.

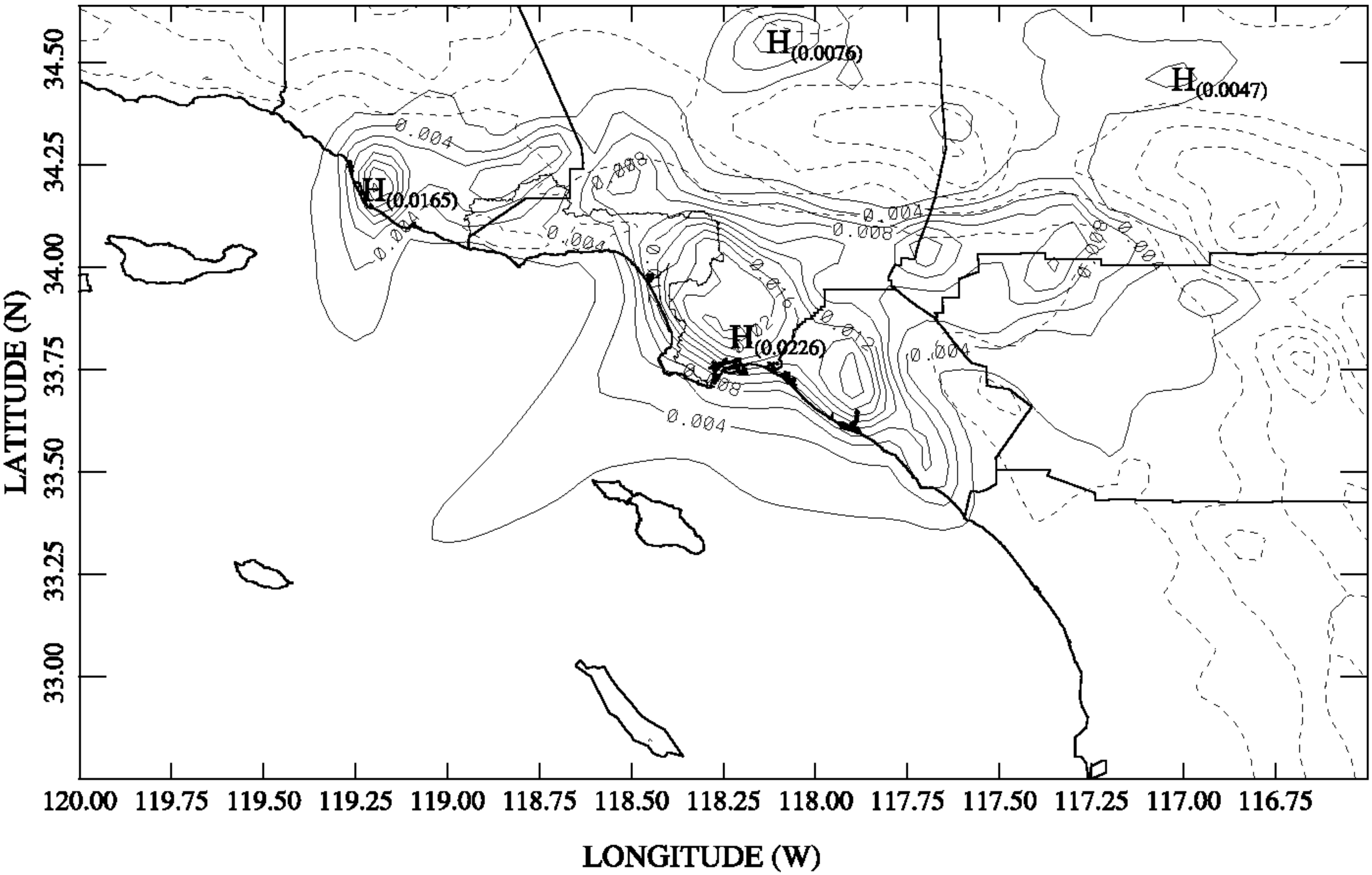

Figure A6: 24-hour average deposition rate (g/ha-day) of the total mass of Cr for the Santa Ana case; the contour interval is 2.00×10^{-3} g/ha-day; the total deposition on the domain is 17.2 kg/day.

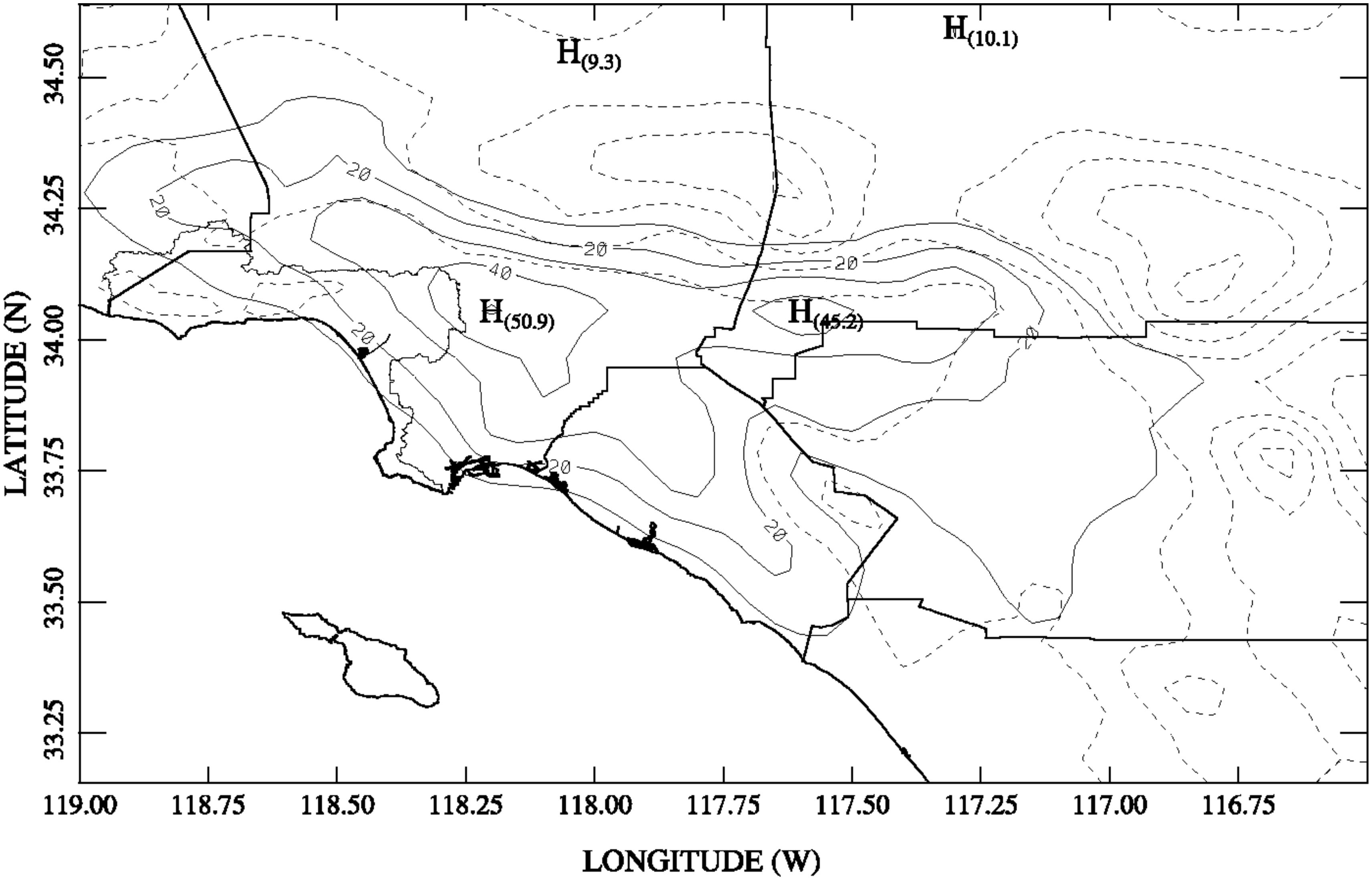

Figure A7: 24-hour average concentration (ng/m^3) of the total mass of Cu for the summer case; the contour interval is 10.0 ng/m^3; the area average concentration is 8.35 ng/m^3.

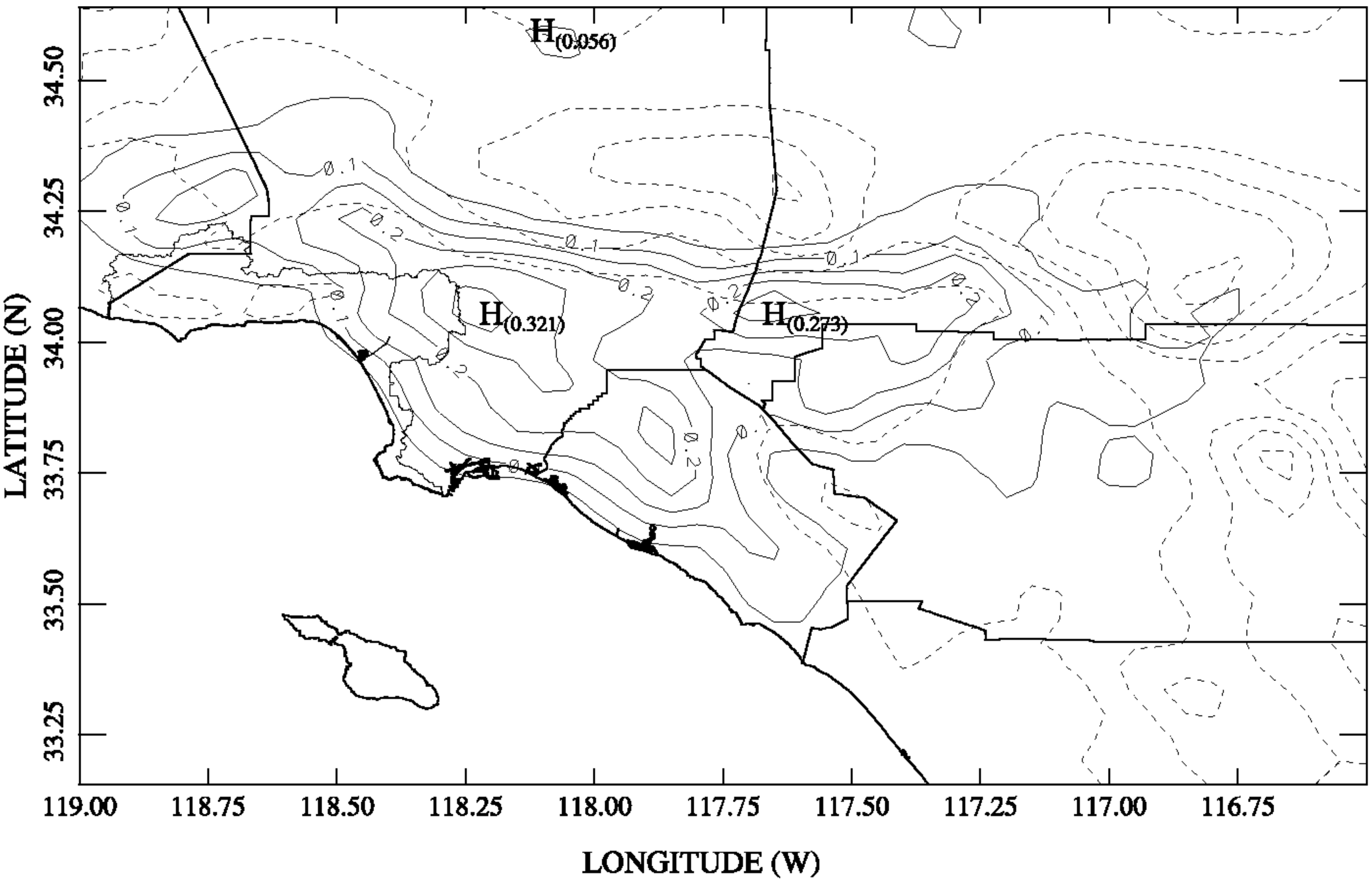

Figure A8: 24-hour average deposition rate (g/ha-day) of the total mass of Cu for the summer case; the contour interval is 5.00×10^{-2} g/ha-day; the total deposition on the domain is 210.8 kg/day.

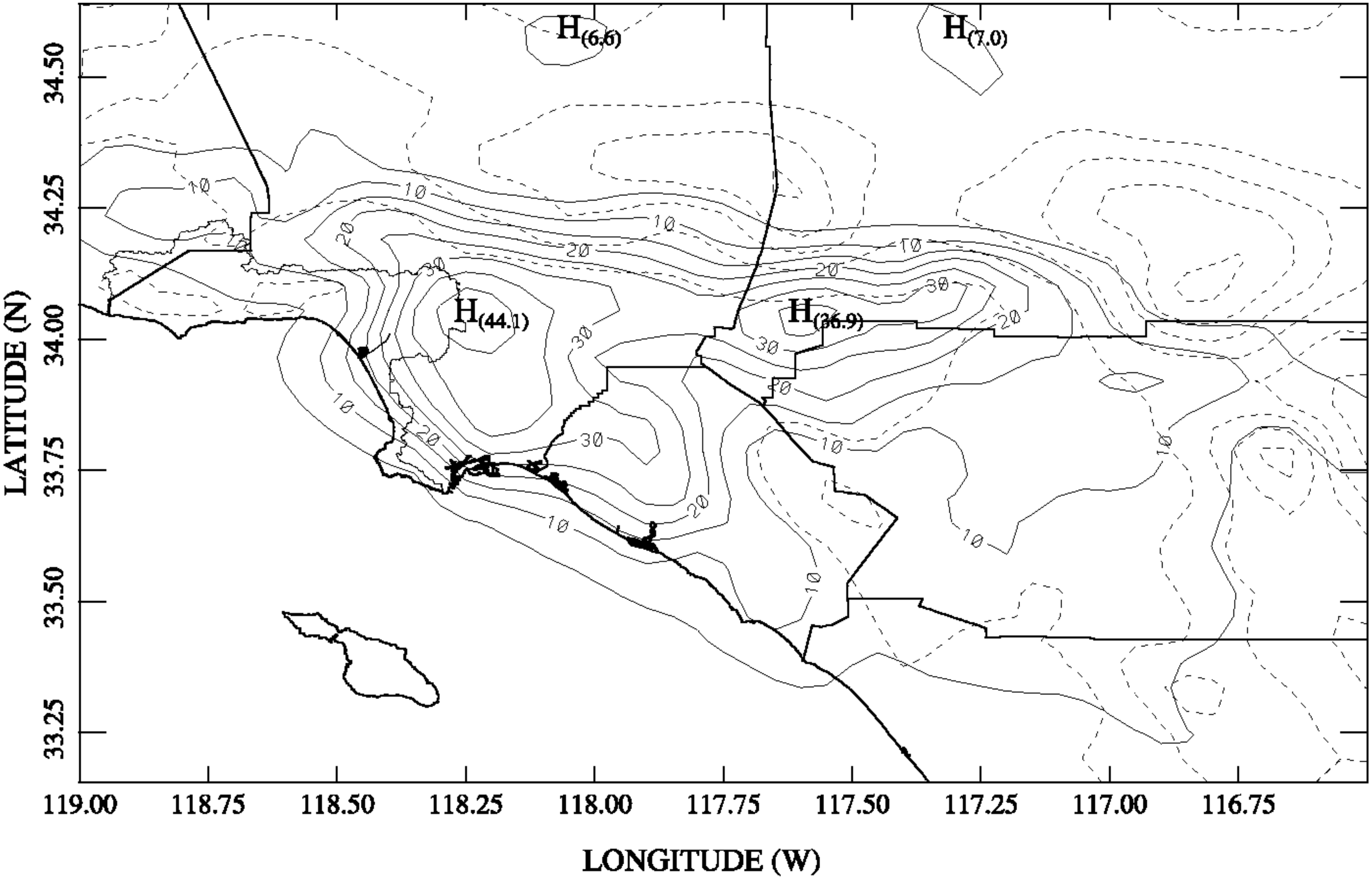

Figure A9: 24-hour average concentration (ng/m^3) of the total mass of Cu for the winter case; the contour interval is 5.0 ng/m^3; the area average concentration is 7.18 ng/m^3.

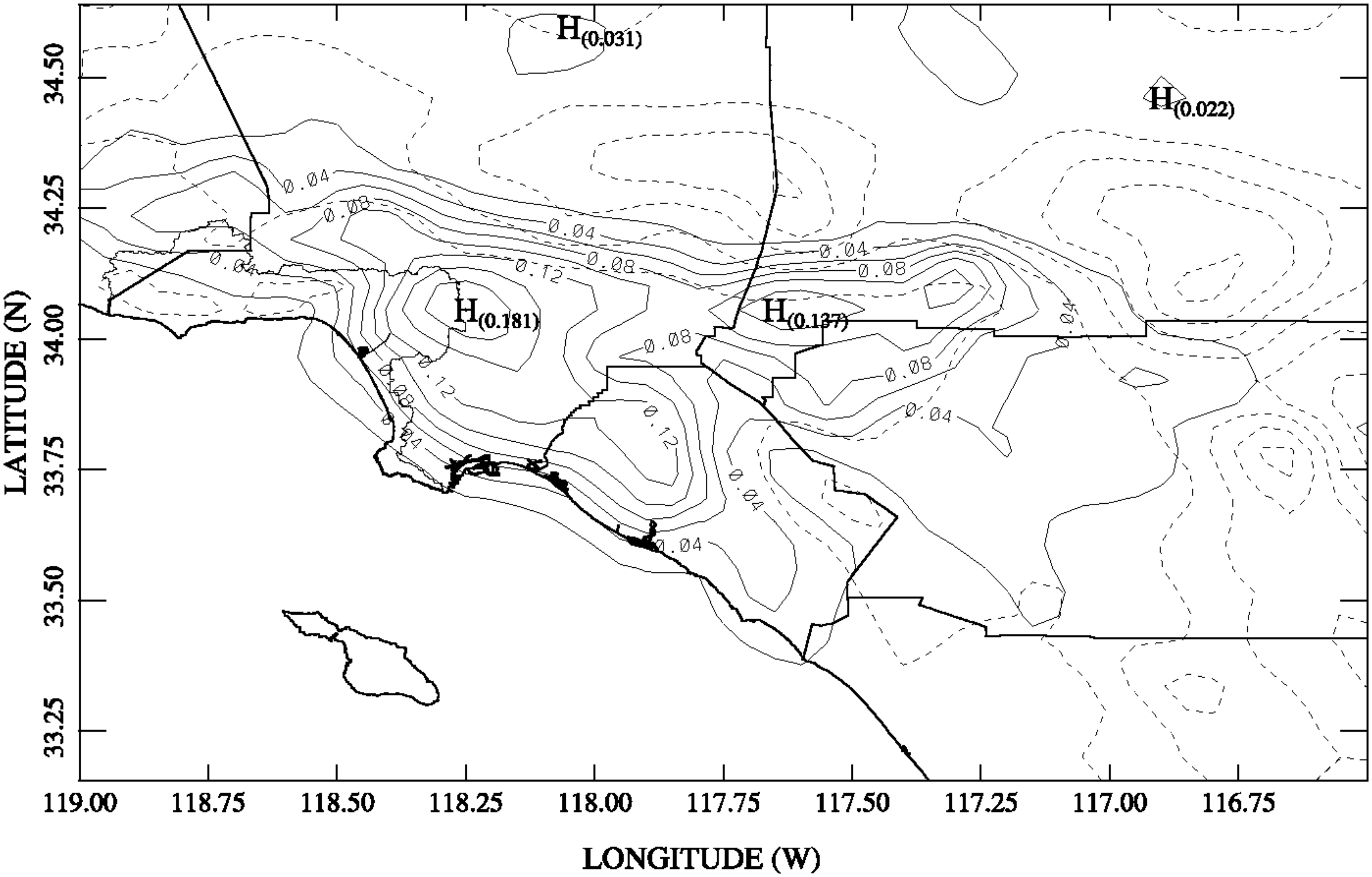

Figure A10: 24-hour average deposition rate (g/ha-day) of the total mass of Cr for the winter case; the contour interval is 2.00×10^{-2} g/ha-day; the total deposition on the domain is 113.1 kg/day.

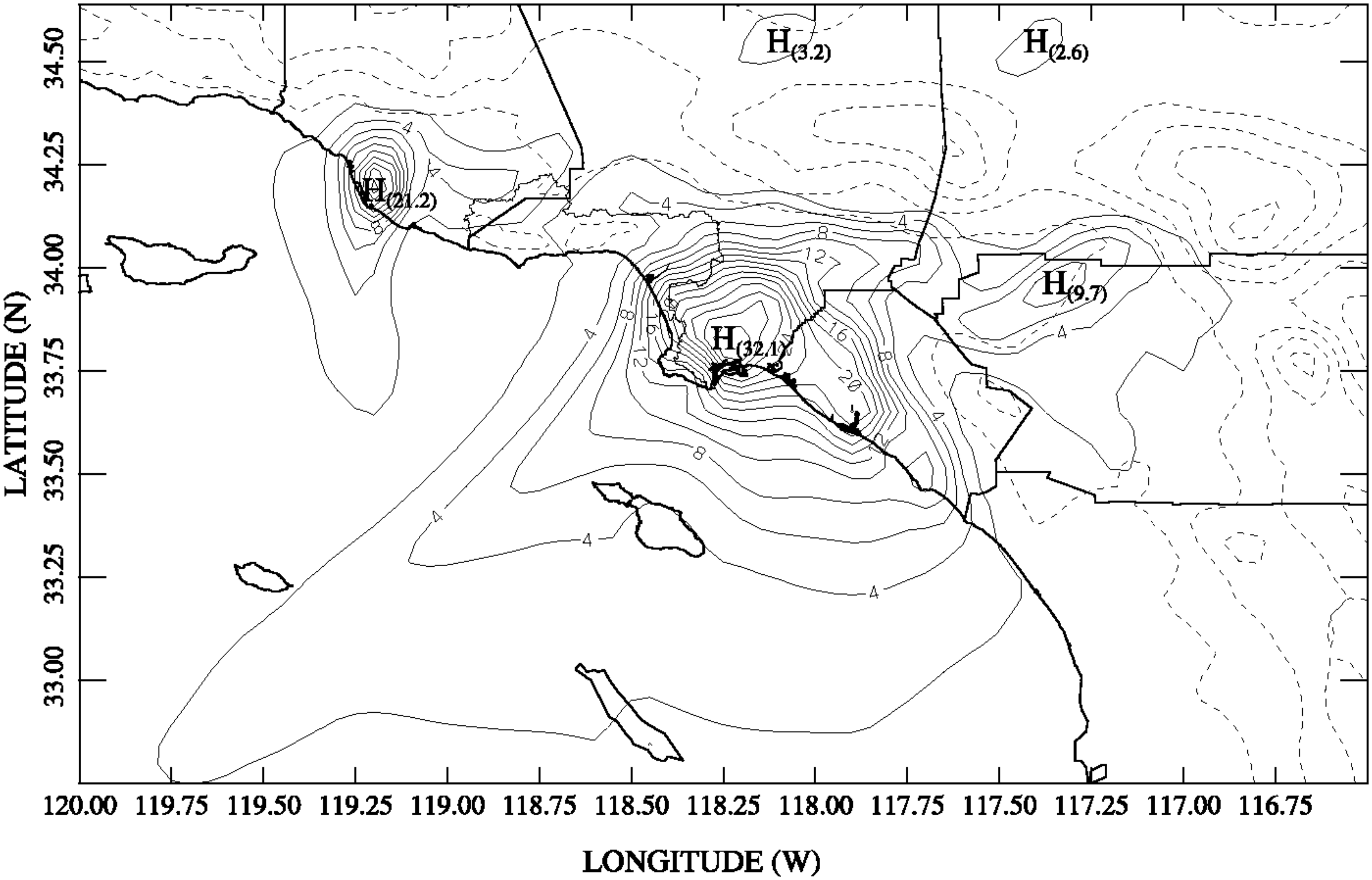

Figure A11: 24-hour average concentration (ng/m^3) of the total mass of Cr for the Santa Ana case; the contour interval is 2.0 ng/m^3; the area average concentration is 2.66 ng/m^3.

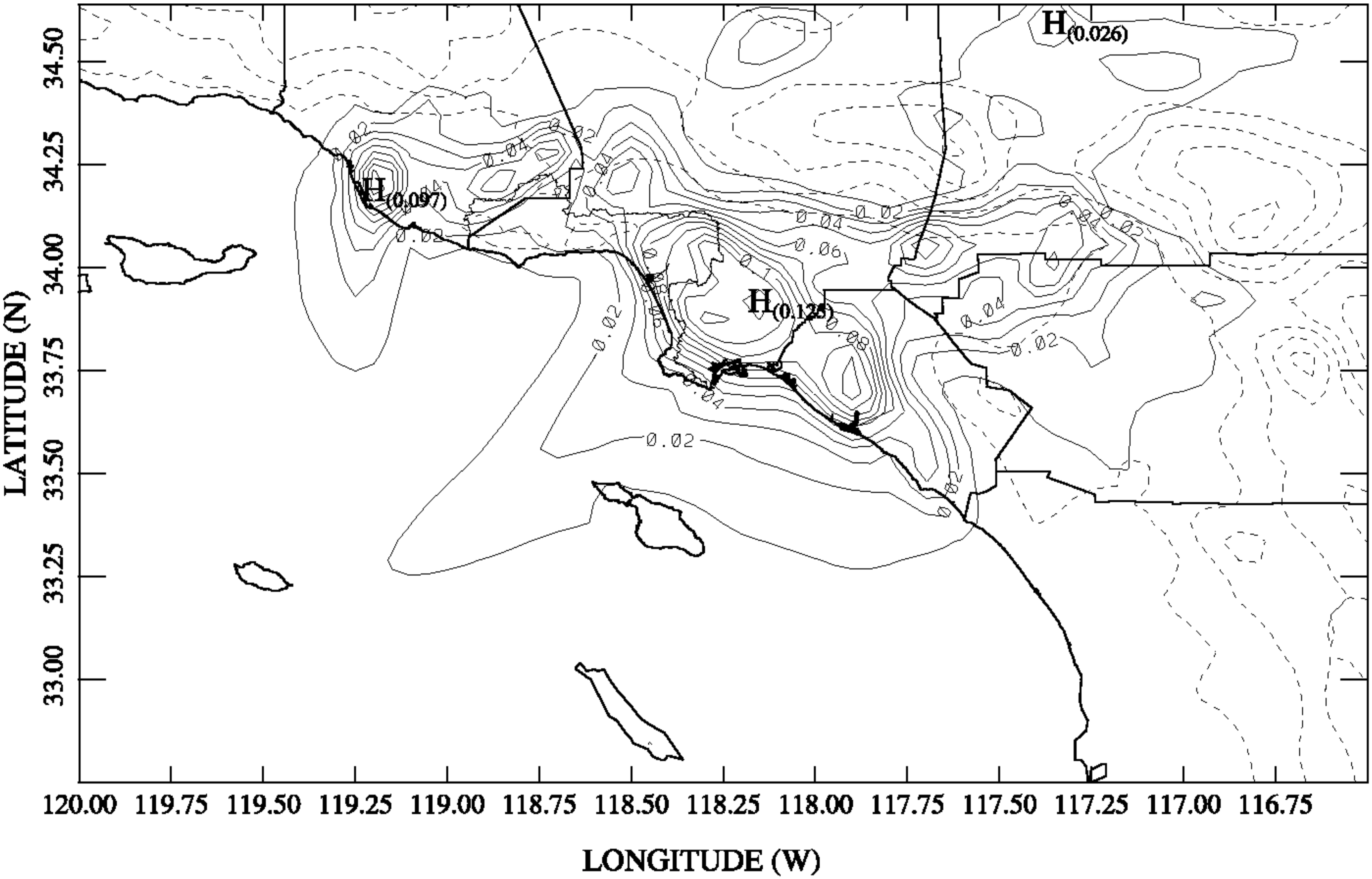

Figure A12: 24-hour average deposition rate (g/ha-day) of the total mass of Cu for the Santa Ana case; the contour interval is 1.00×10^{-2} g/ha-day; the total deposition on the domain is 104.6 kg/day.

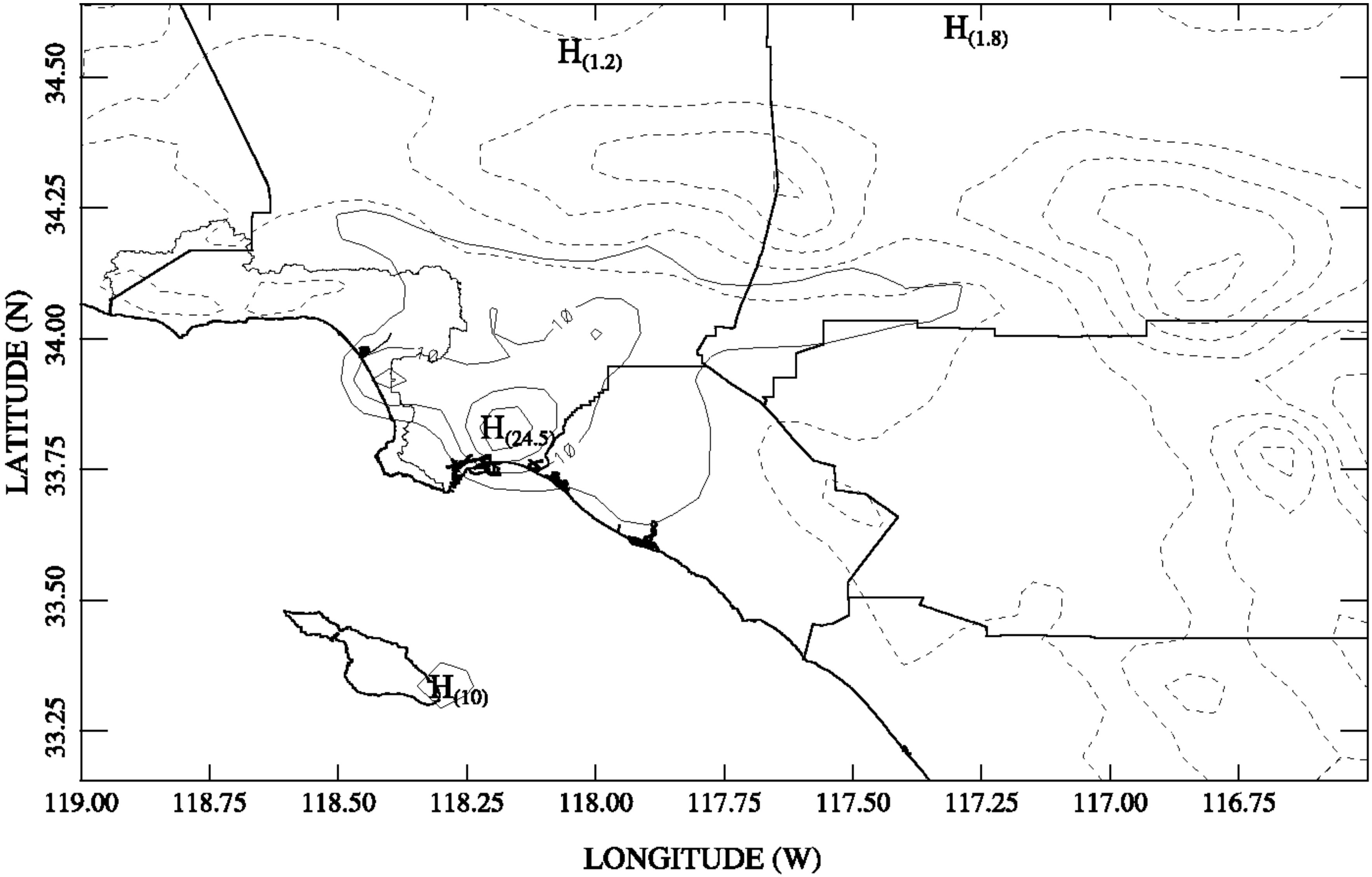

Figure A13: 24-hour average concentration (ng/m^3) of the total mass of Ni for the summer case; the contour interval is 5.0 ng/m^3; the area average concentration is 1.68 ng/m^3.

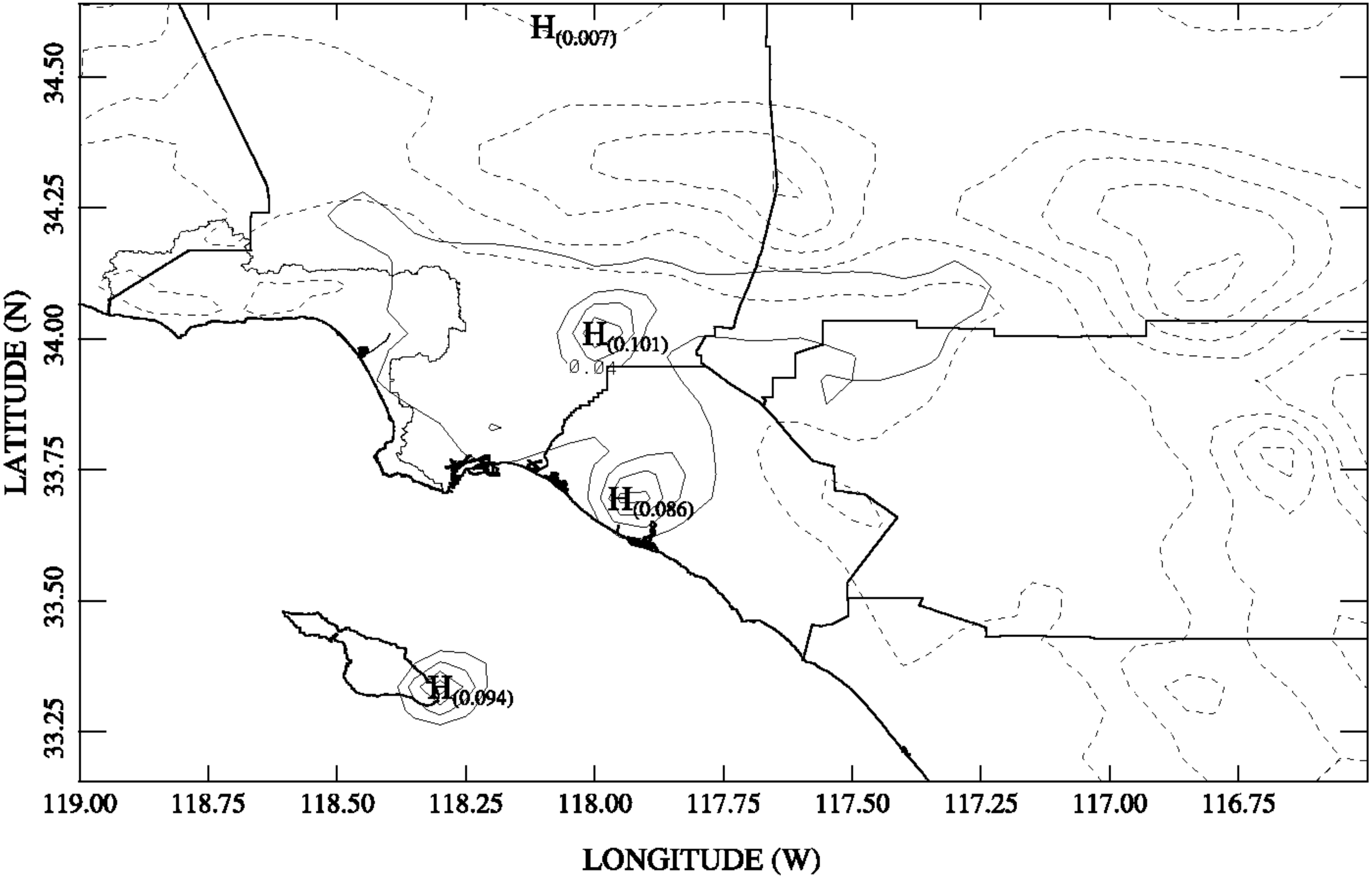

Figure A14: 24-hour average deposition rate (g/ha-day) of the total mass of Ni for the summer case; the contour interval is 2.00×10^{-2} g/ha-day; the total deposition on the domain is 29.9 kg/day.

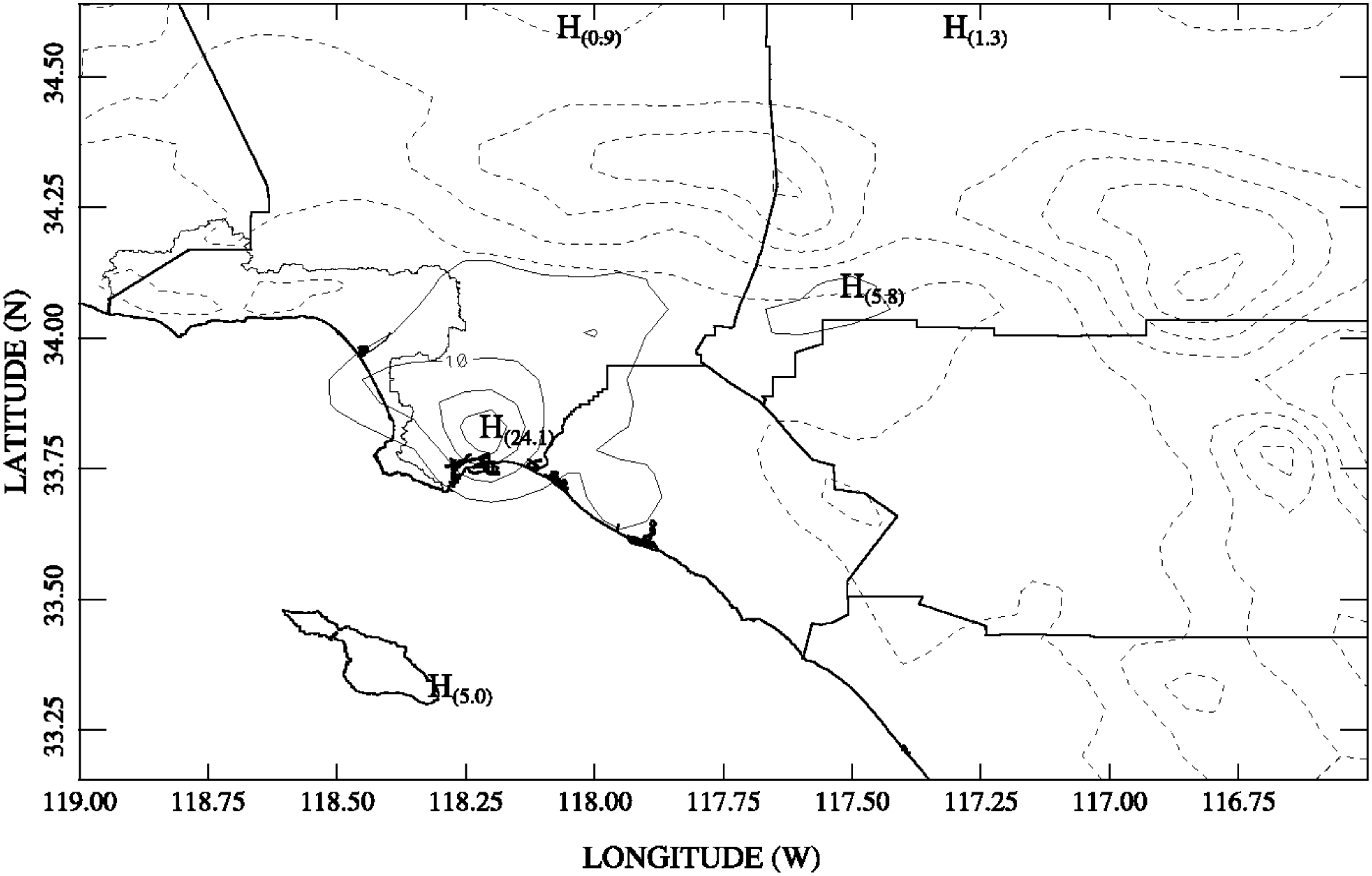

Figure A15: 24-hour average concentration (ng/m^3) of the total mass of Ni for the winter case; the contour interval is 5.0 ng/m^3; the area average concentration is 1.51 ng/m^3.

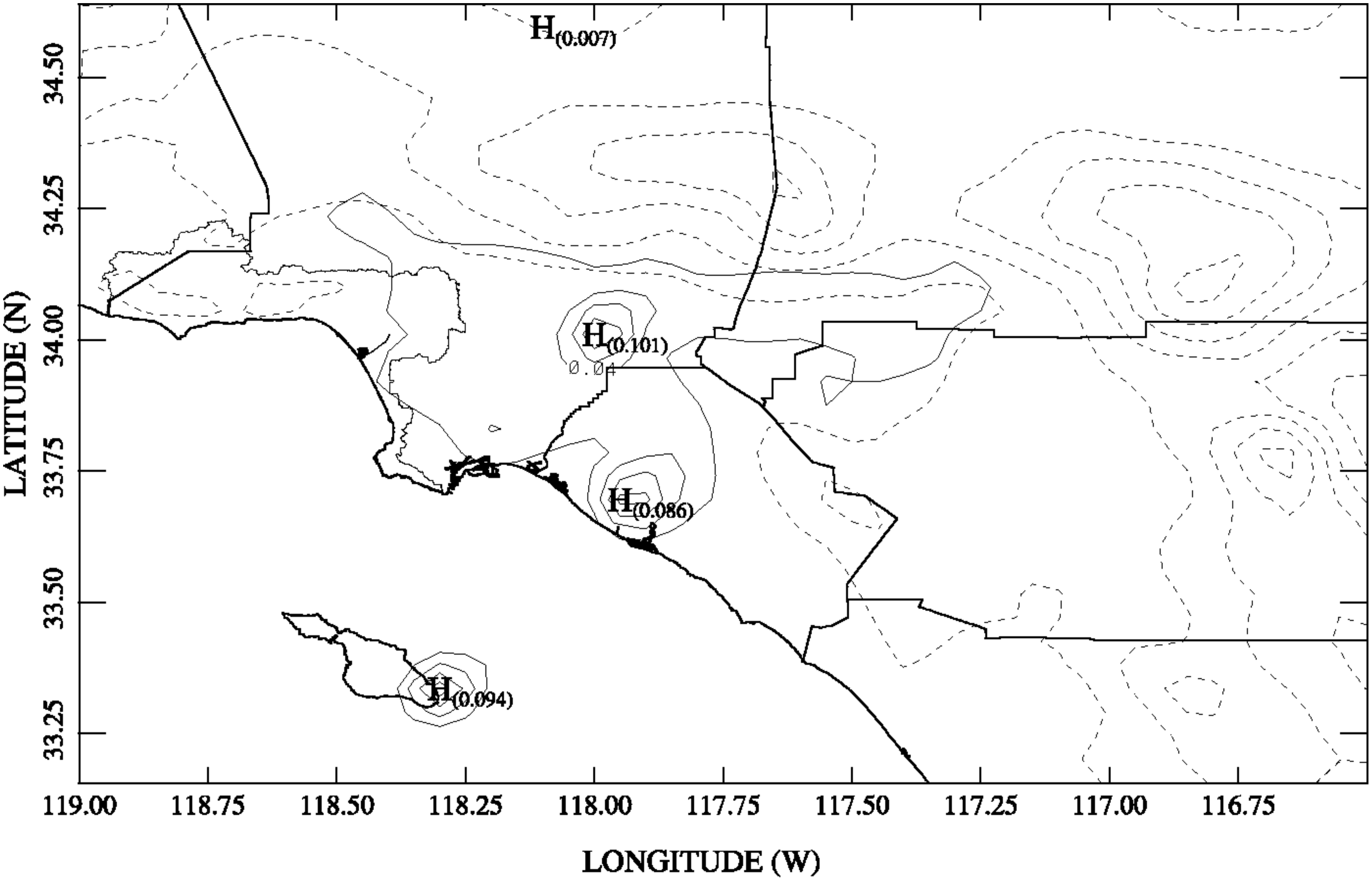

Figure A16: 24-hour average deposition rate (g/ha-day) of the total mass of Ni for the winter case; the contour interval is 2.00×10^{-2} g/ha-day; the total deposition on the domain is 16.4 kg/day.

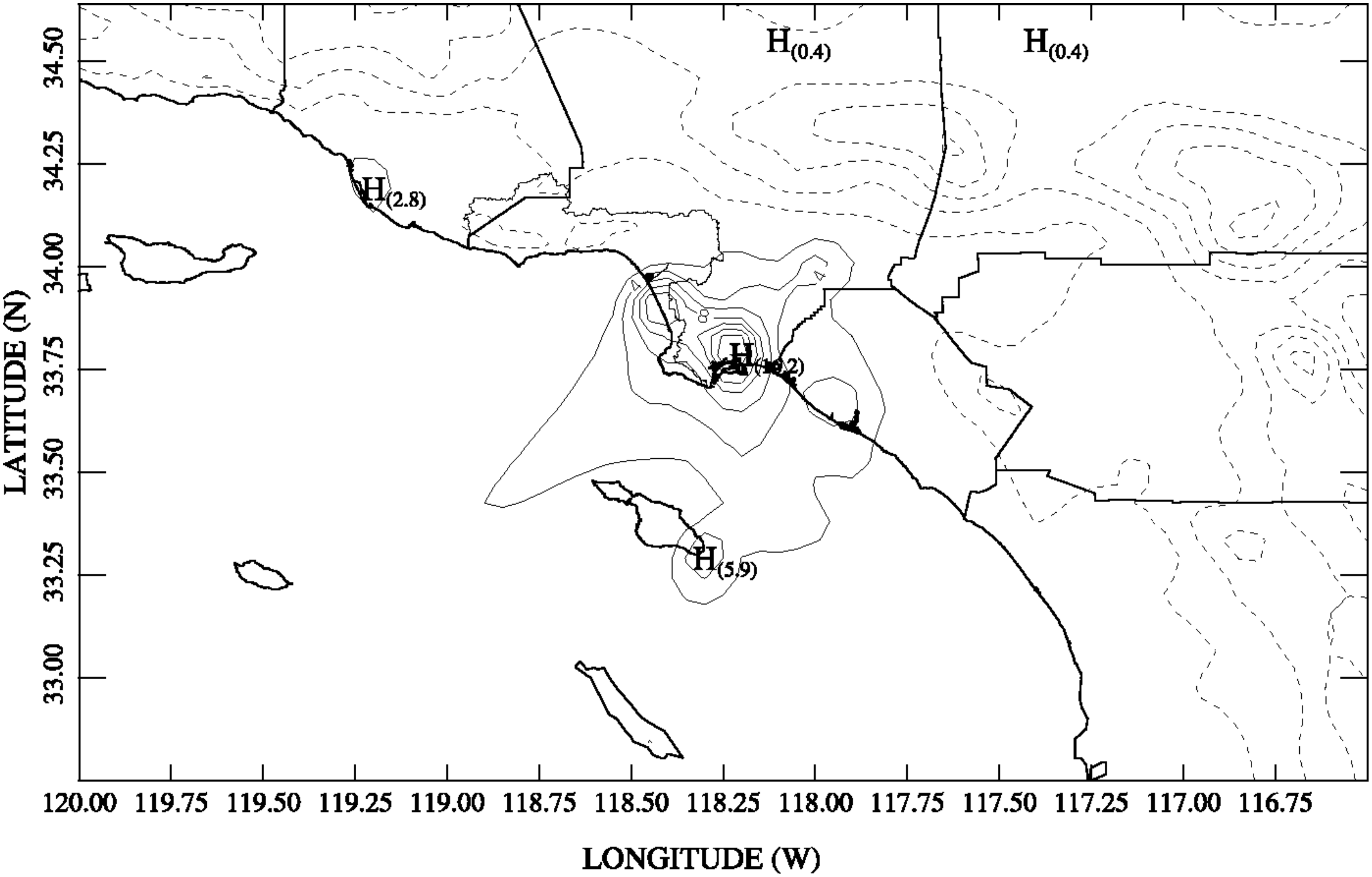

Figure A17: 24-hour average concentration (ng/m^3) of the total mass of Ni for the Santa Ana case; the contour interval is 2.0 ng/m^3; the area average concentration is 0.63 ng/m^3.

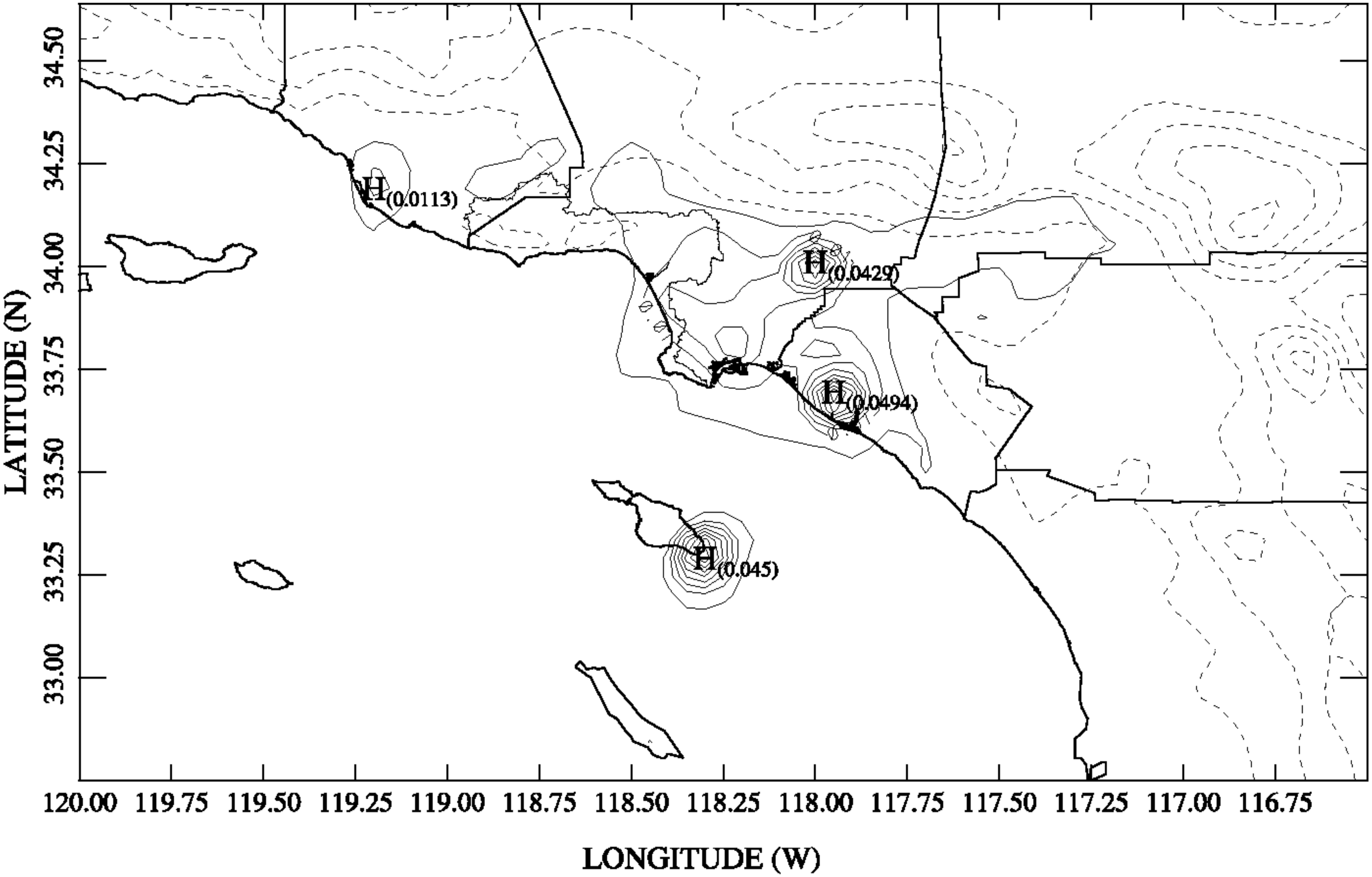

Figure A18: 24-hour average deposition rate (g/ha-day) of the total mass of Ni for the Santa Ana case; the contour interval is 5.00×10^{-3} g/ha-day; the total deposition on the domain is 15.5 kg/day.

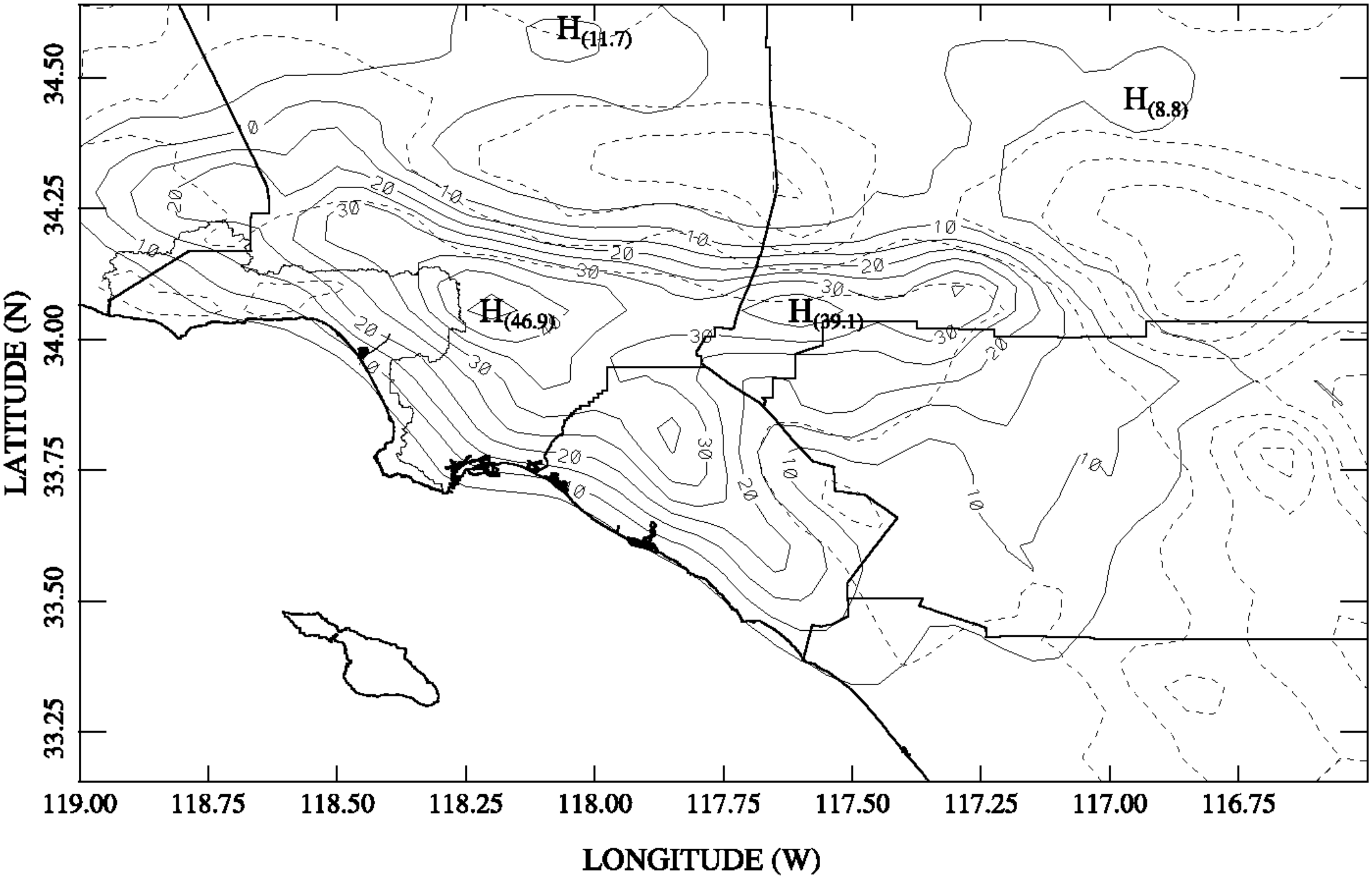

Figure A19: 24-hour average concentration (ng/m^3) of the total mass of Pb for the summer case; the contour interval is 5.0 ng/m^3; the area average concentration is 7.48 ng/m^3.

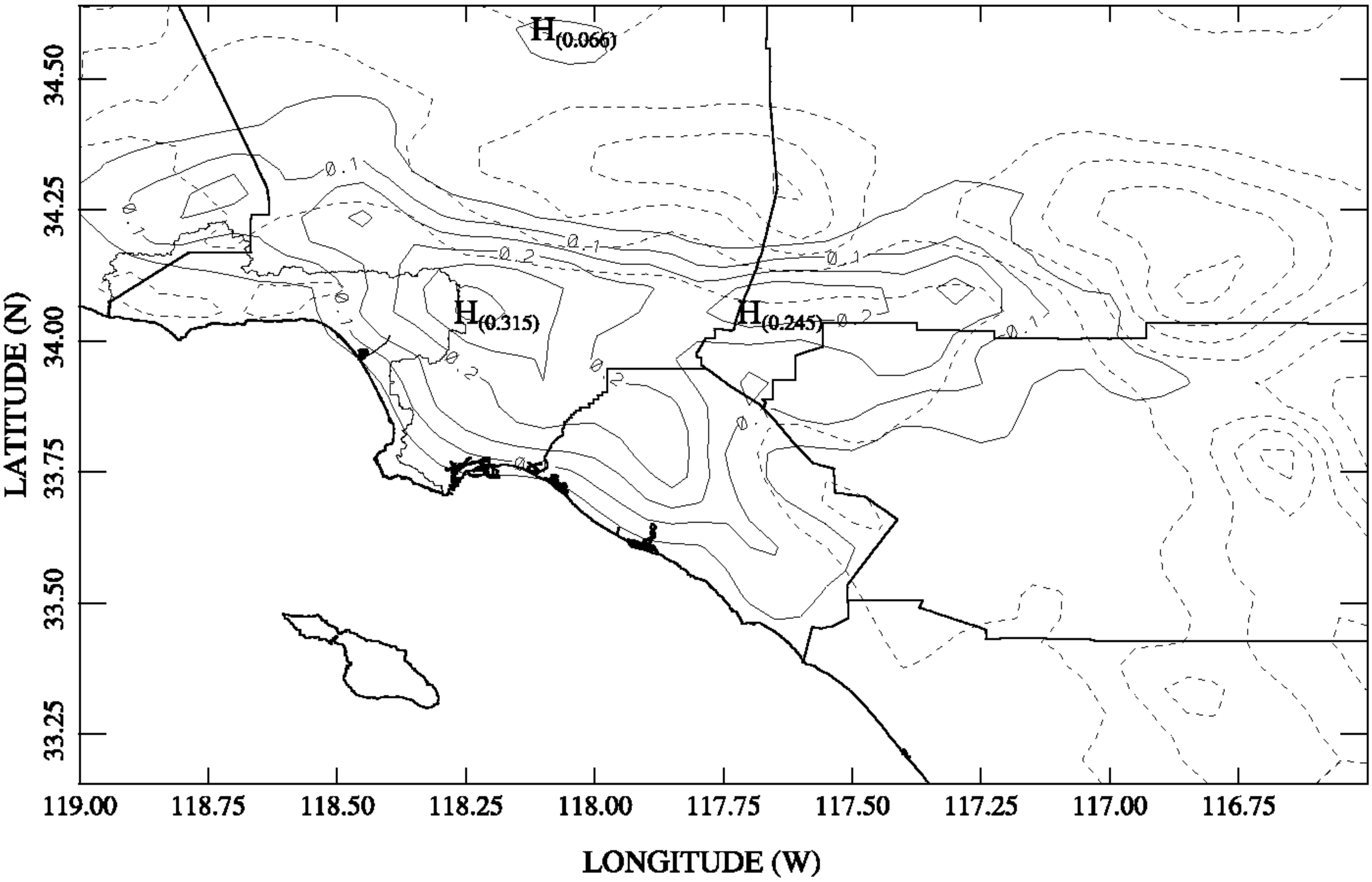

Figure A20: 24-hour average deposition rate (g/ha-day) of the total mass of Pb for the summer case; the contour interval is 5.00×10^{-2} g/ha-day; the total deposition on the domain is 195.8 kg/day.

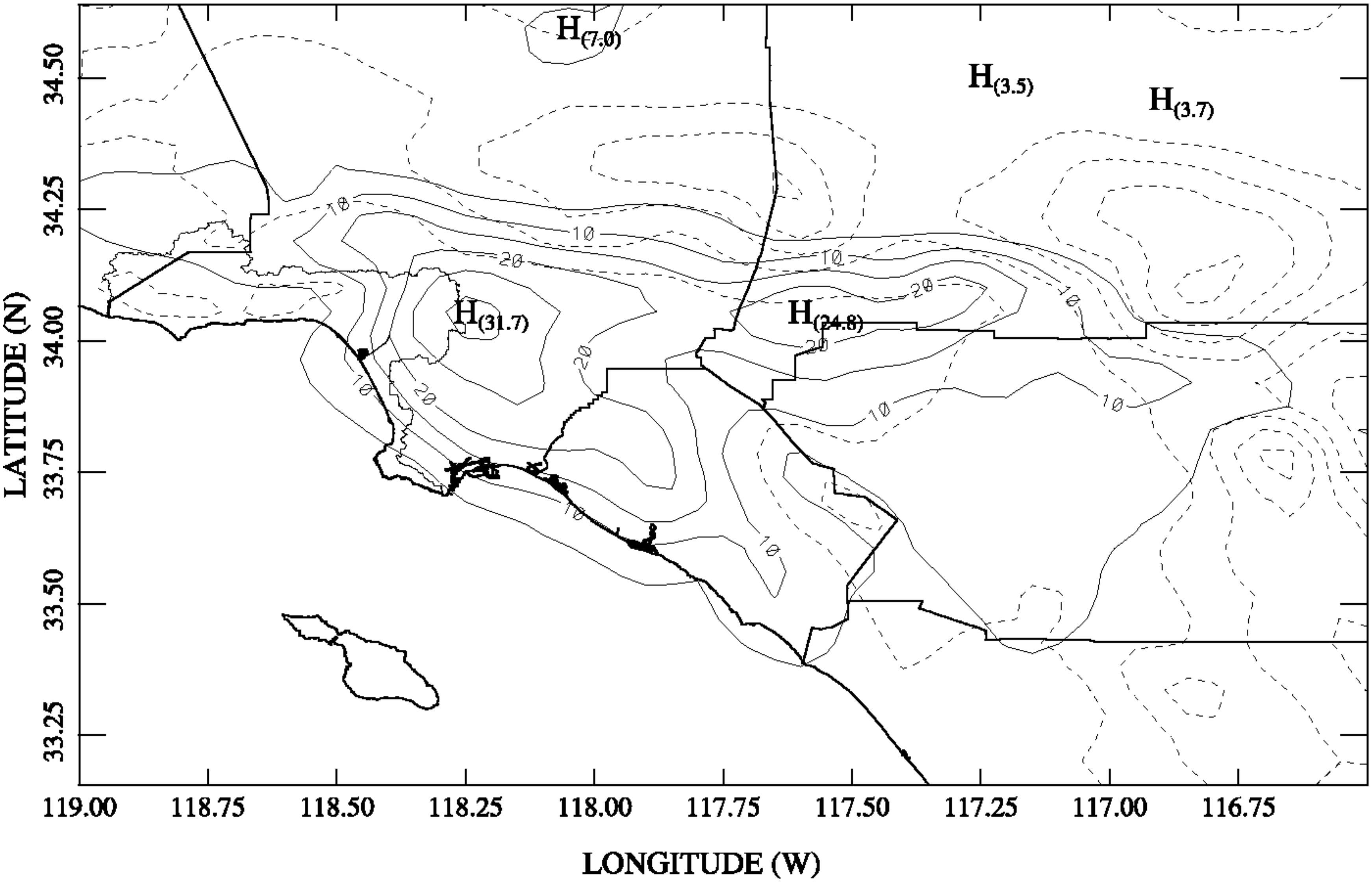

Figure A21: 24-hour average concentration (ng/m^3) of the total mass of Pb for the winter case; the contour interval is 5.0 ng/m^3; the area average concentration is 5.04 ng/m^3.

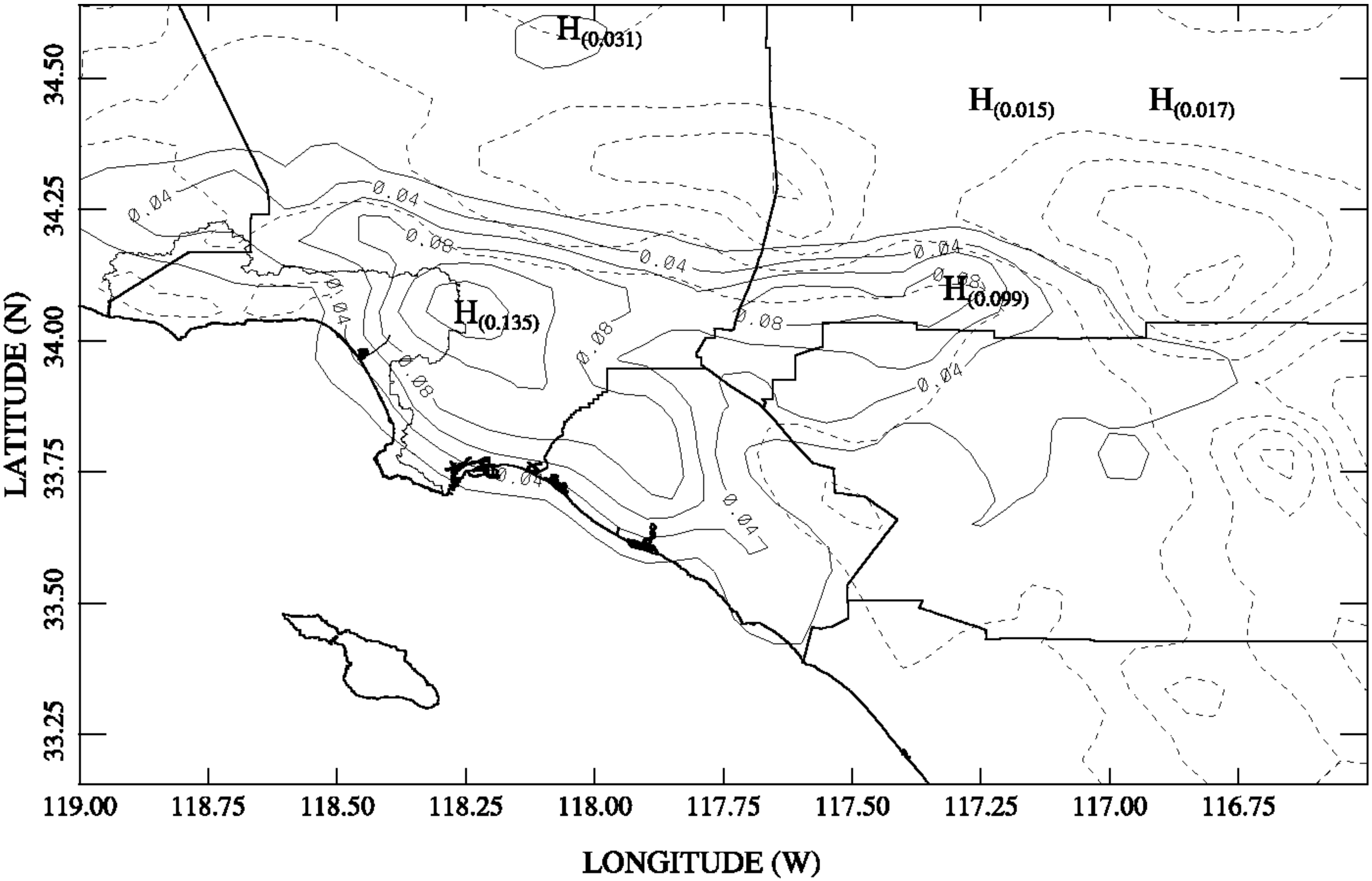

Figure A22: 24-hour average deposition rate (g/ha-day) of the total mass of Pb for the winter case; the contour interval is 2.00×10^{-2} g/ha-day; the total deposition on the domain is 81.8 kg/day.

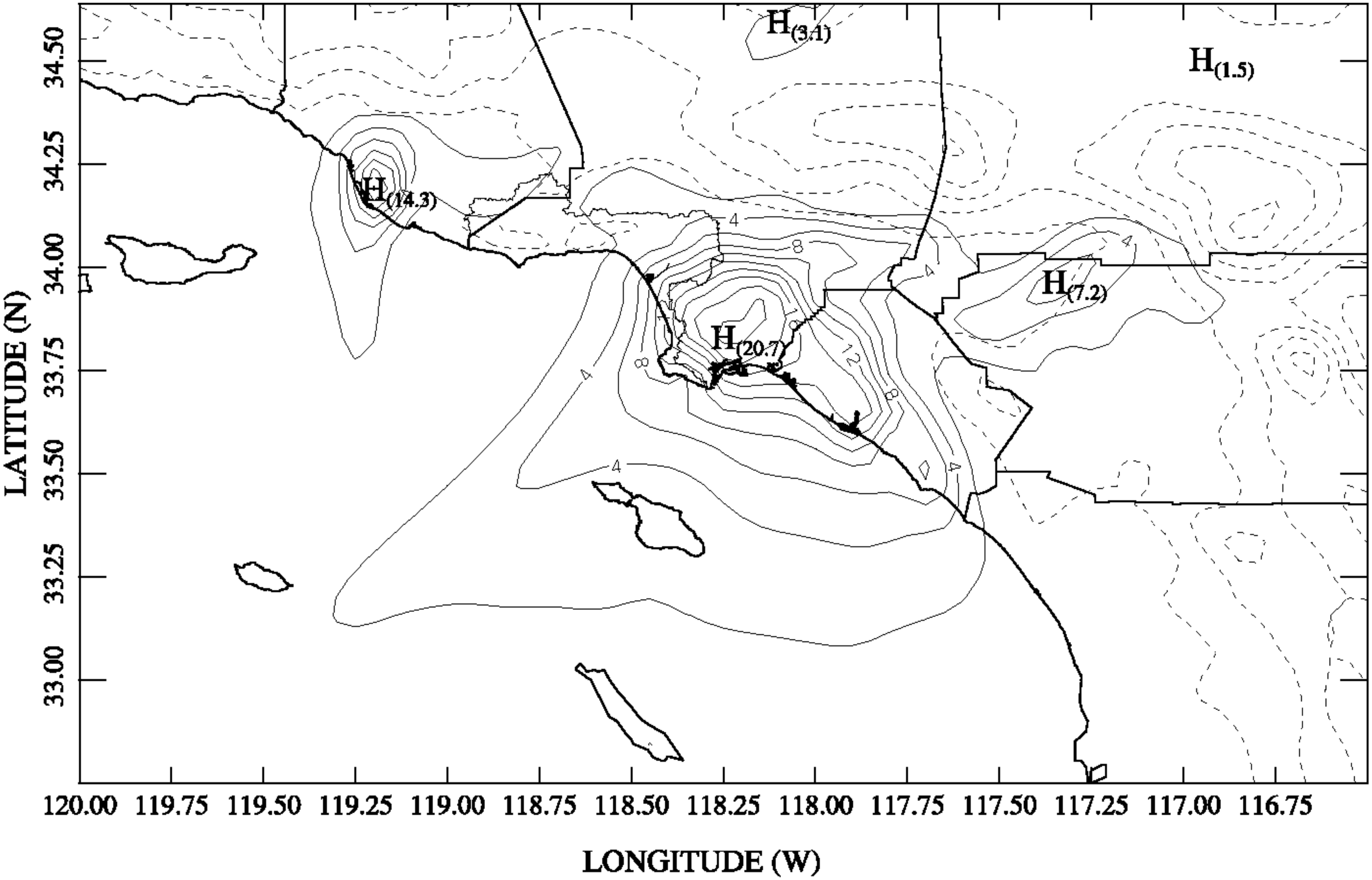

Figure A23: 24-hour average concentration (ng/m^3) of the total mass of Pb for the Santa Ana case; the contour interval is 2.0 ng/m^3; the area average concentration is 1.83 ng/m^3.

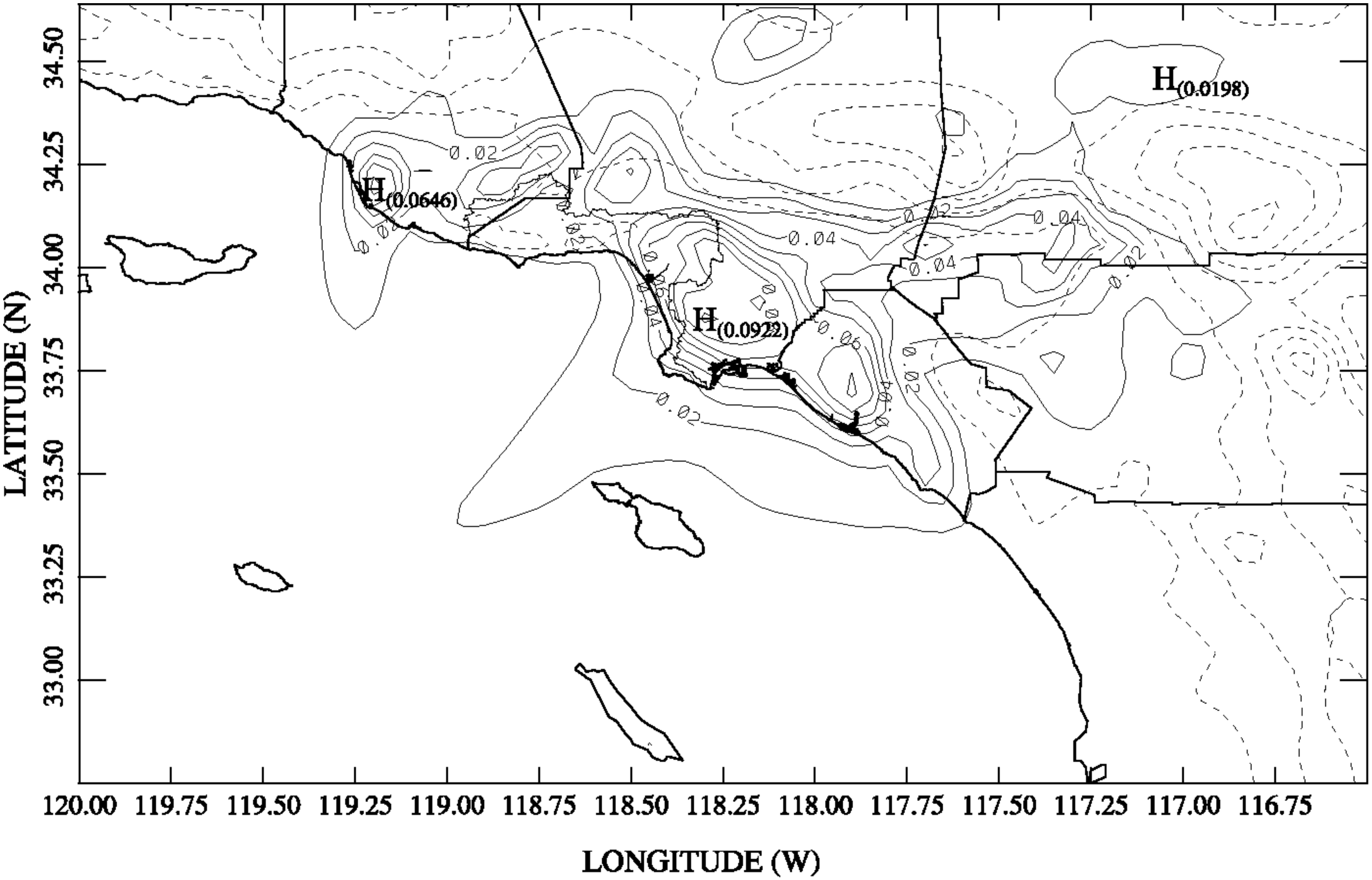

Figure A24: 24-hour average deposition rate (g/ha-day) of the total mass of Pb for the Santa Ana case; the contour interval is 1.00×10^{-2} g/ha-day; the total deposition on the domain is 74.5 kg/day.

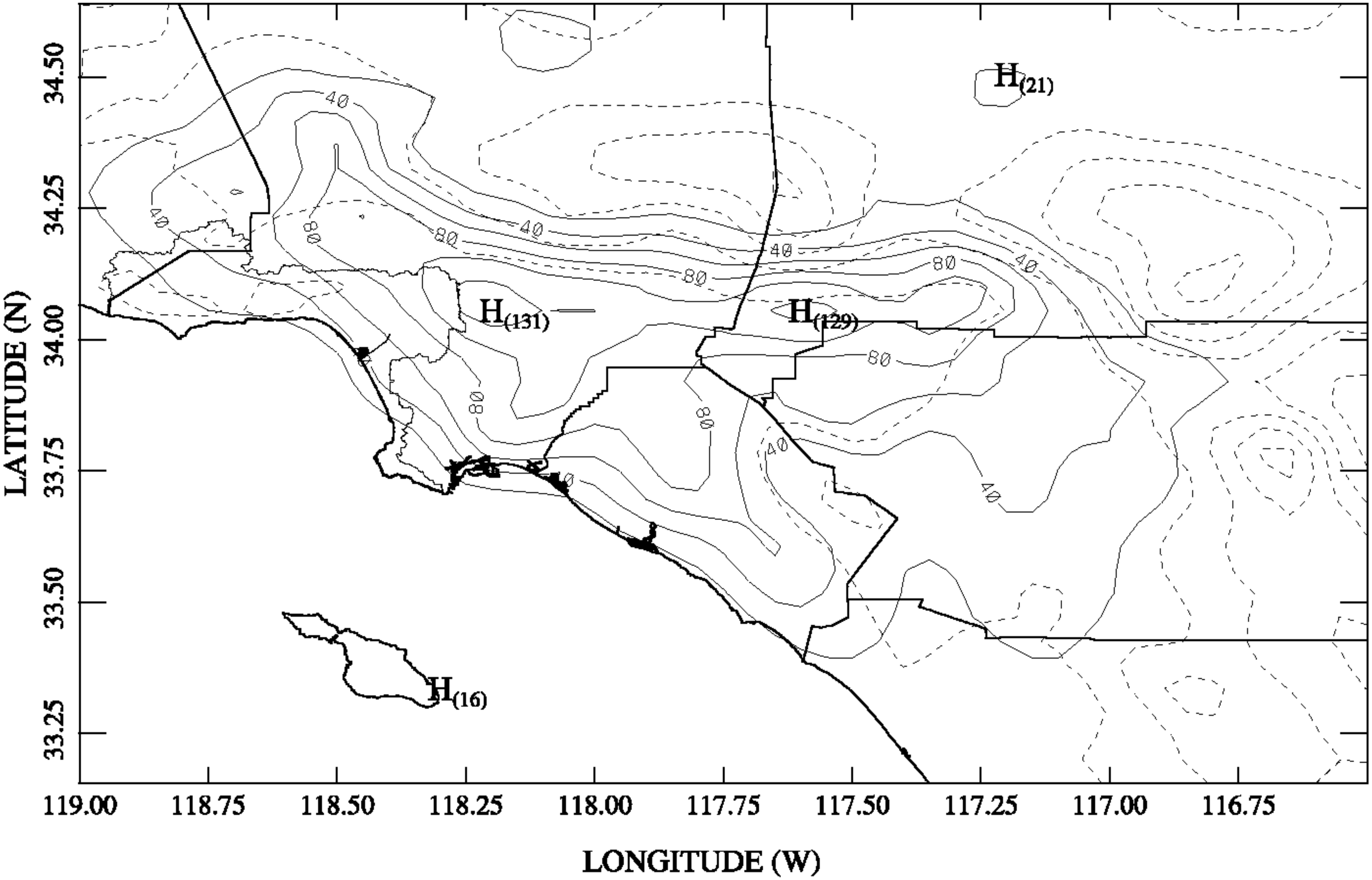

Figure A25: 24-hour average concentration (ng/m^3) of the total mass of Zn for the summer case; the contour interval is 20.0 ng/m^3; the area average concentration is 23.3 ng/m^3.

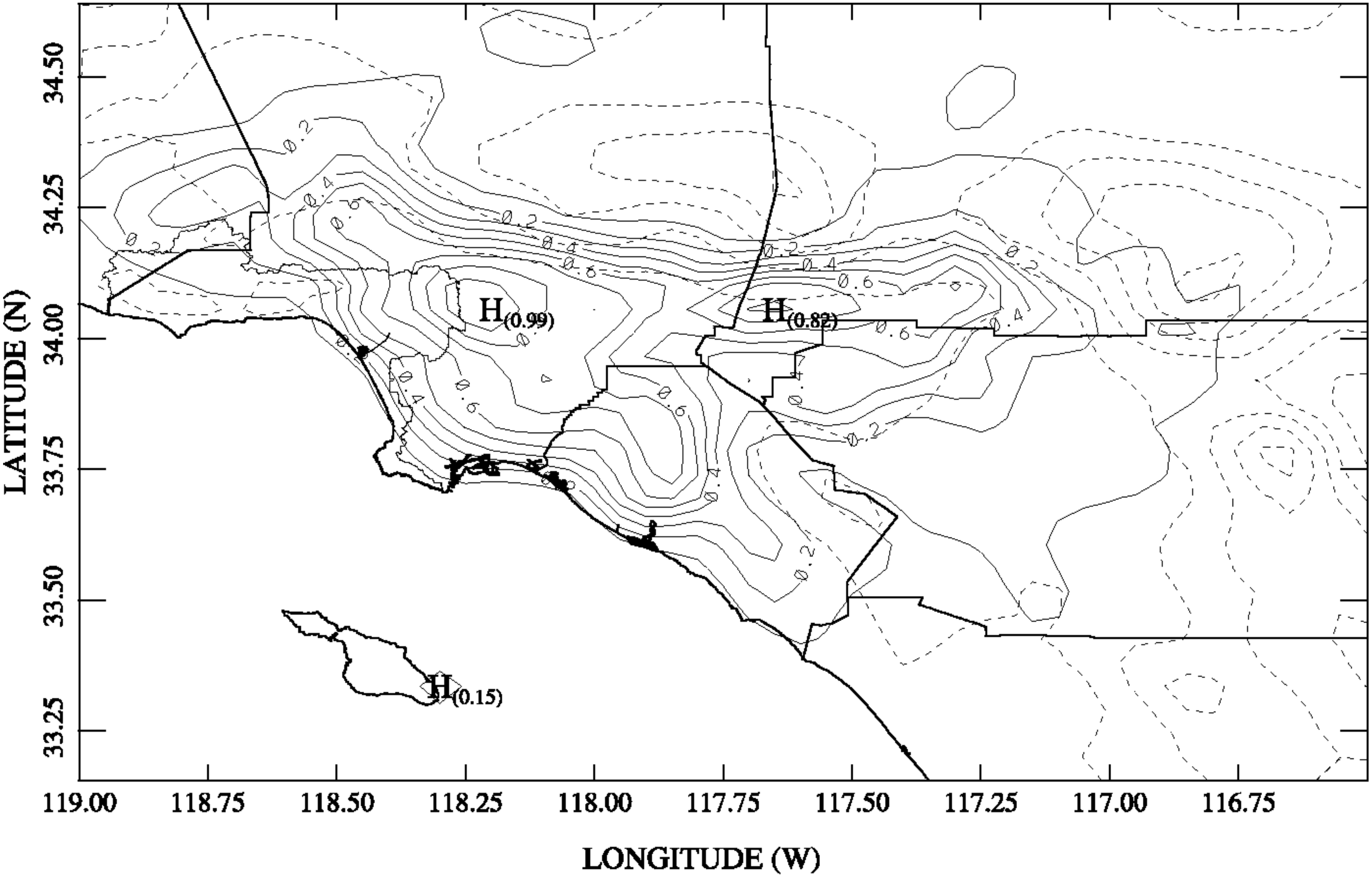

Figure A26: 24-hour average deposition rate (g/ha-day) of the total mass of Zn for the summer case; the contour interval is 1.00×10^{-1} g/ha-day; the total deposition on the domain is 605.8 kg/day.

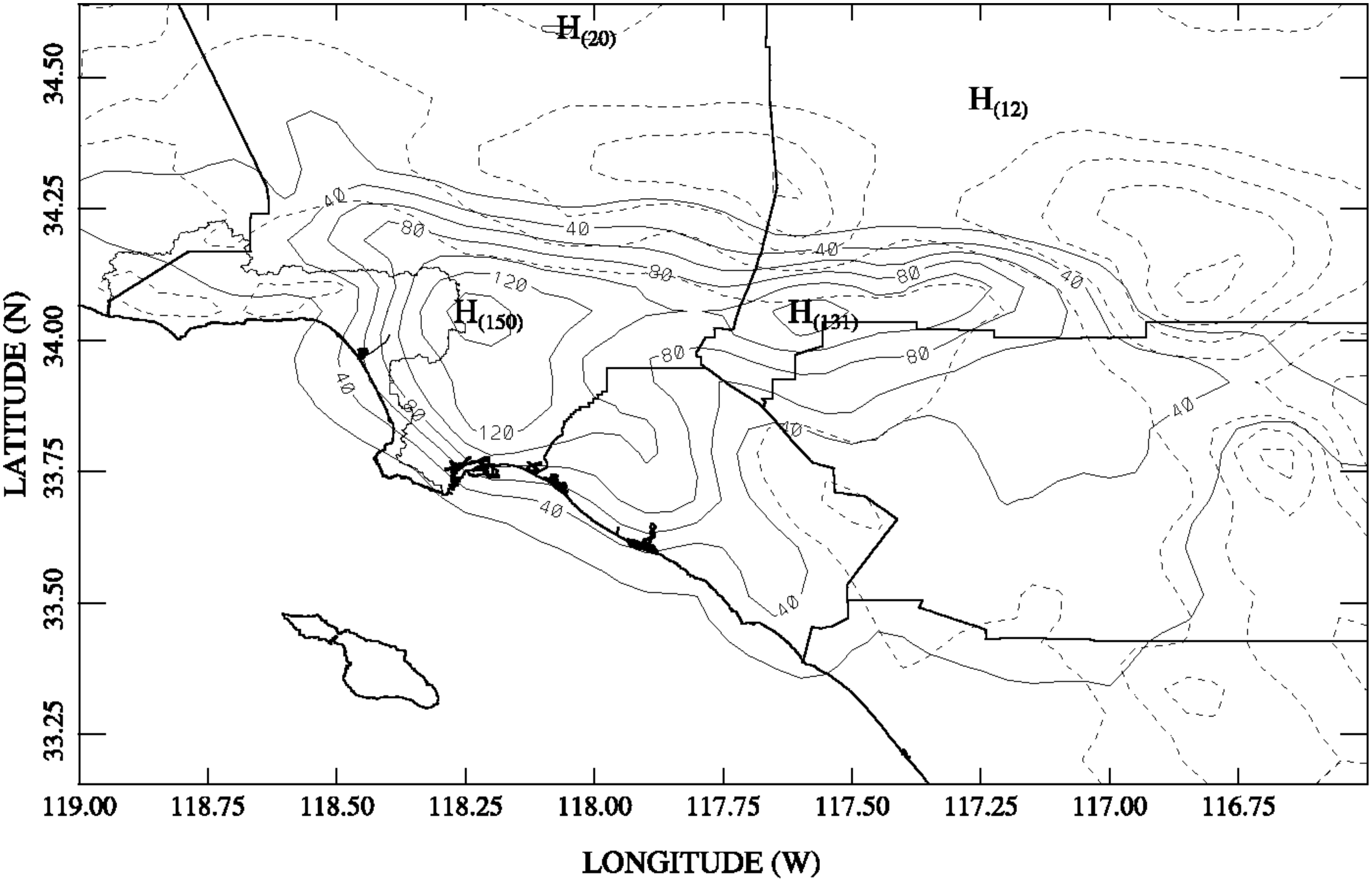

Figure A27: 24-hour average concentration (ng/m^3) of the total mass of Zn for the winter case; the contour interval is 20.0 ng/m^3; the area average concentration is 24.5 ng/m^3.

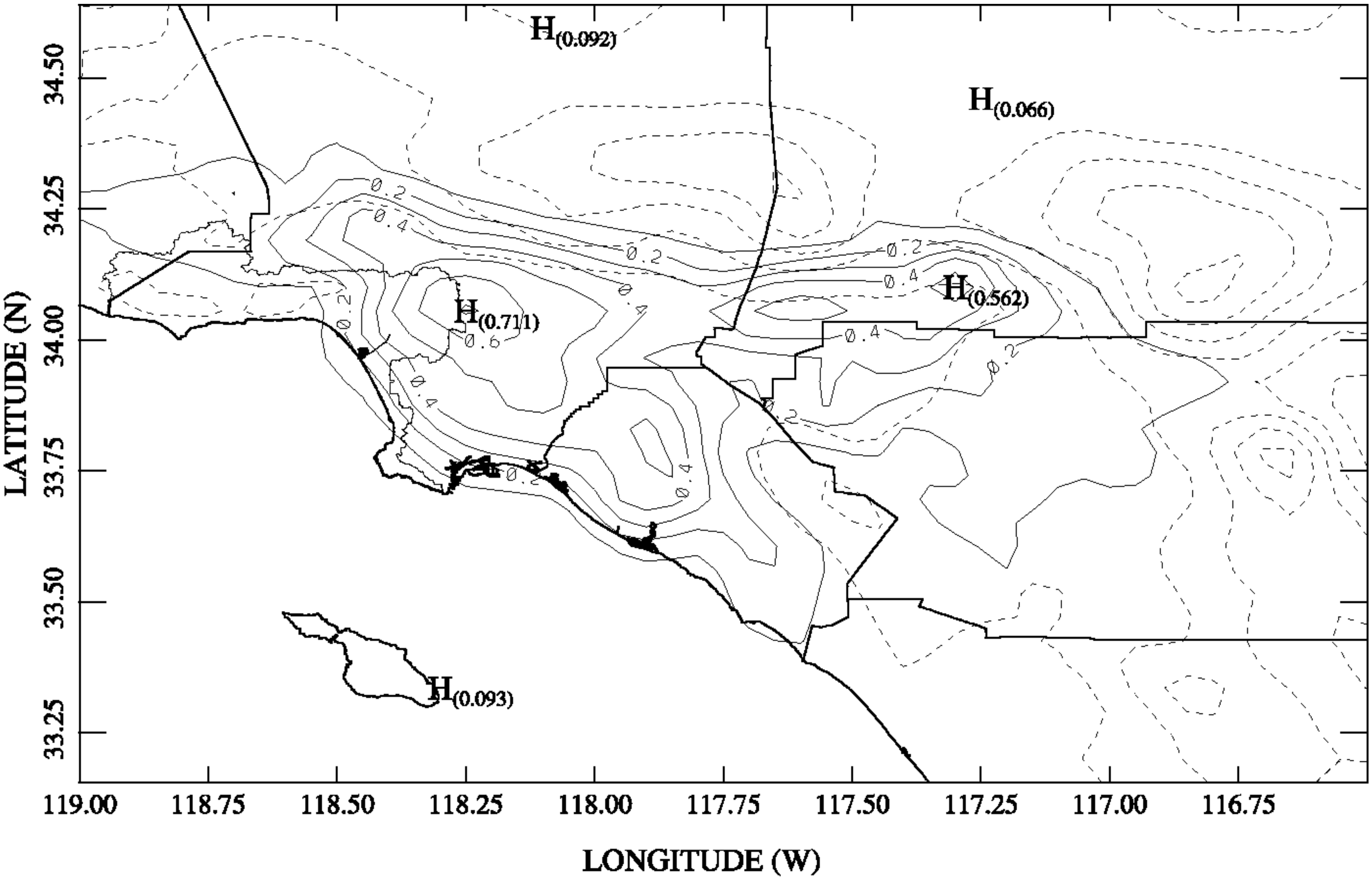

Figure A28: 24-hour average deposition rate (g/ha-day) of the total mass of Zn for the winter case; the contour interval is 1.00×10^{-1} g/ha-day; the total deposition on the domain is 415.1 kg/day.

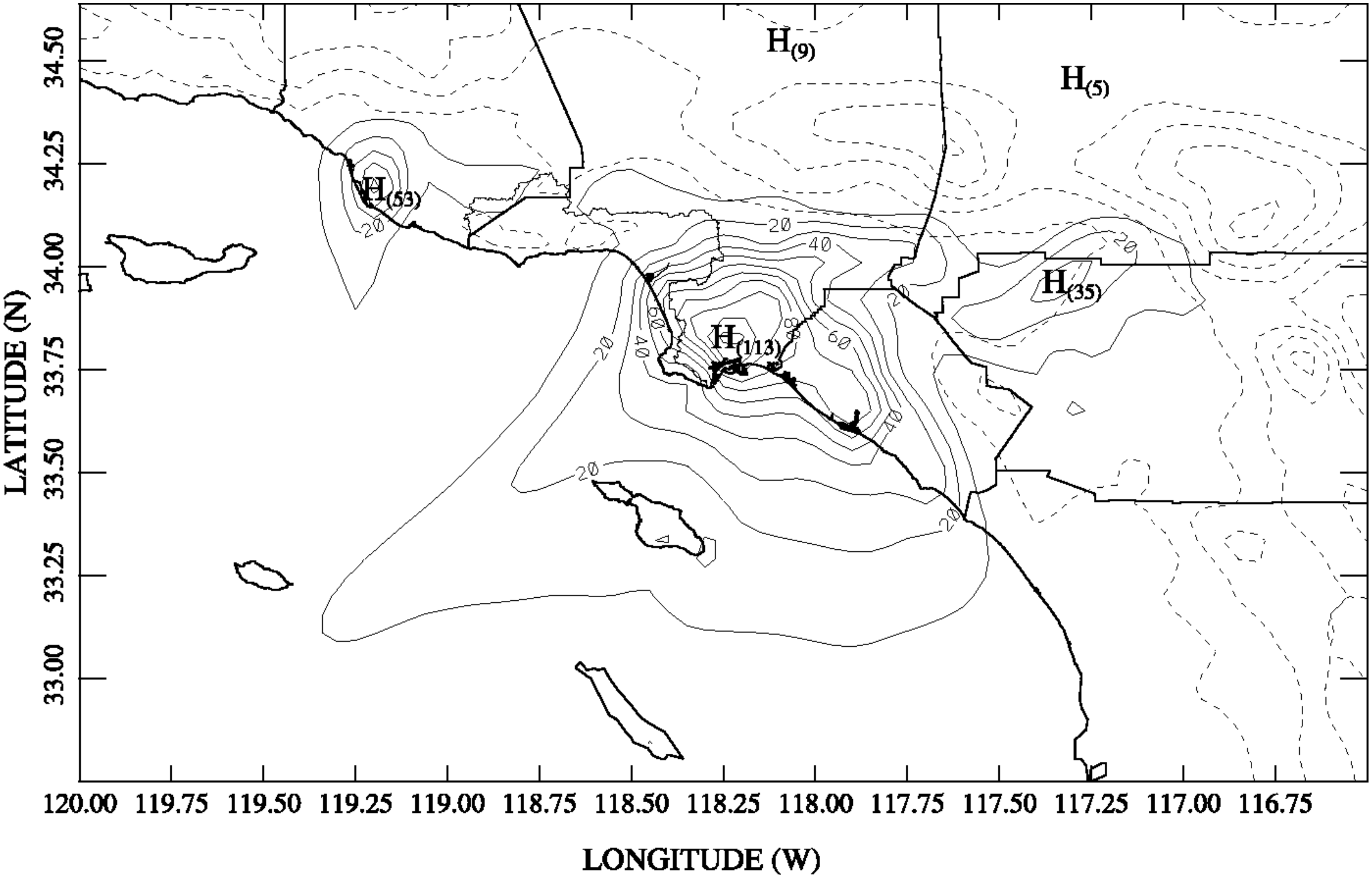

Figure A29: 24-hour average concentration (ng/m^3) of the total mass of Zn for the Santa Ana case; the contour interval is 10.0 ng/m^3; the area average concentration is 8.98 ng/m^3.

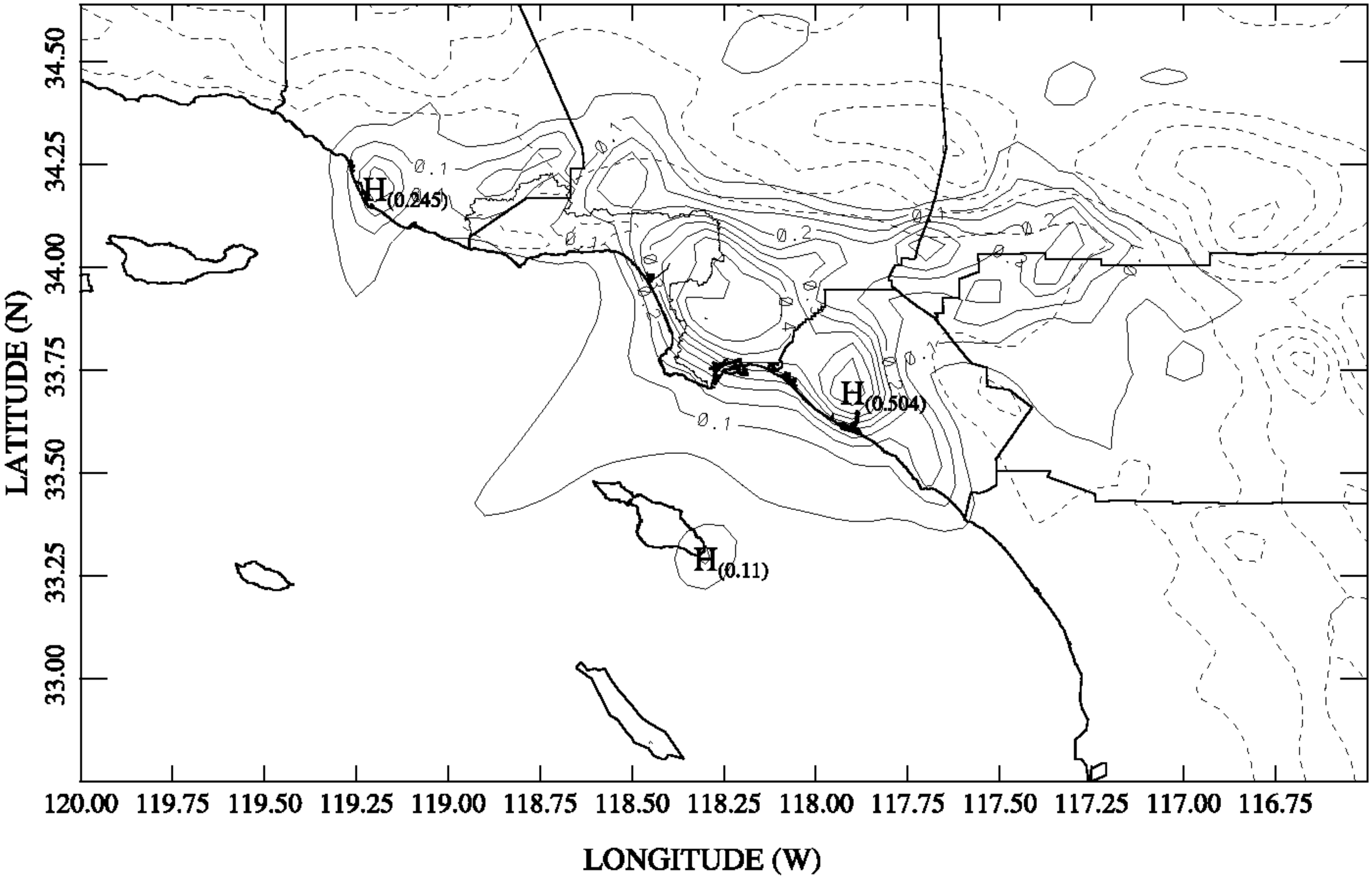

Figure A30: 24-hour average deposition rate (g/ha-day) of the total mass of Zn for the Santa Ana case; the contour interval is 5.00×10^{-2} g/ha-day; the total deposition on the domain is 361.2 kg/day.